



**THE UNIVERSITY  
OF BIRMINGHAM**

**CONTROLLED RELEASE OF ISOTHIAZOLINE  
BIOCIDES FROM INDUSTRIAL MINERALS**

By

**YAO KANGA**

A thesis submitted to the  
University of Birmingham  
For the degree of  
**ENGINEERING DOCTORATE**

School of Chemical Engineering  
College of Engineering  
University of Birmingham  
September 2010

UNIVERSITY OF  
BIRMINGHAM

**University of Birmingham Research Archive**

**e-theses repository**

This unpublished thesis/dissertation is copyright of the author and/or third parties. The intellectual property rights of the author or third parties in respect of this work are as defined by The Copyright Designs and Patents Act 1988 or as modified by any successor legislation.

Any use made of information contained in this thesis/dissertation must be in accordance with that legislation and must be properly acknowledged. Further distribution or reproduction in any format is prohibited without the permission of the copyright holder.

## **ABSTRACT**

This project investigated how various minerals of different surface areas and morphologies can be used to adsorb isothiazoline biocides for controlled-release and antimicrobial purposes.

The absorption of the biocides on the mineral powders was achieved by way of using a bench high shear mill (dry process), or combining them to hydrated minerals (wet process). The characterisation of the minerals was achieved by XRF (chemical composition), XRD (crystal composition), SEM (morphology), B.E.T nitrogen (surface area), and Light Scattering (particle size distribution). HPLC was used to determine the concentration of the biocide in solution, and the Flow Microcalorimeter used to measure the bond strength between the biocide molecules and the minerals. The minerals were added to an exterior paint made according to an Imerys in-house formulation. Various modifications of this initial coating formulation were made in order to compare the biocide 2-Octyl-4-isothiazolin-3-one (OIT) release profiles from impregnated and non-impregnated minerals.

Montmorillonite clay was the best performing mineral in all experiments (adsorption and desorption both from the minerals and paints films, strength of bond analysis, and bioassay). All other minerals tested carried the biocide with varying degree of success. Optical and mechanical tests performed on paint films containing various minerals suggested there were no significant differences between the films. Rheology tests demonstrated that newly developed formulations were easy to apply to a surface.

# ACKNOWLEDGEMENTS

I would like to thank my Lord Jesus Christ for all he has done for me during my time at Imerys, in my numerous journeys around the country and elsewhere, and keeping my family safe during all the years I was absent.

I want to express my gratitude to Dr. Richard Greenwood, Dr. Neil Rowson (School of Chemical Engineering, University of Birmingham), to Dr. David Skuse, Mr. Jarrod Hart (Imerys Minerals), to Dr. Maneesh Singh (DNV, Norway), and to Dr. Cesar Agra-Guittierez for their enthusiasm, dedication and patient supervision.

Special acknowledgement is made to my wife Gill and my daughter Adjouah for their encouragement, love and understanding during the years I was absent from home

I would like to thank EPSRC for the funding they provided for this project. Special thanks also to all laboratory friends and colleagues and other EngD students for sharing important intellectual discussions. Last but not least to Dr. Roy Goodman for his help with the sodium silicate work, Isobelle Oulton for her help on the HPLC and the setting up of the Microbiology experiments, Michele Henry and all those in the paint laboratory who help with all aspects of the paint work.

Yao Kanga  
Watford, Hertfordshire,  
September 2010

# LIST OF CONTENTS

ABSTRACT.....	2
ACKNOWLEDGEMENTS .....	3
LIST OF CONTENTS .....	I
FIGURE INDEX.....	IV
LIST OF TABLES .....	VIII
LIST OF TERMS.....	IX
 1 CHAPTER ONE – INTRODUCTION .....	 1
1.1 Imerys Minerals .....	2
1.1.1 History and Development .....	2
1.1.2 Group development from 2000 to 2010 .....	3
1.1.3 Group development by activity .....	3
1.2 Company market size.....	6
1.2.1 Minerals for Ceramics, Refractories, Abrasives & Foundry.....	7
1.2.2 Performance & Filtration Minerals .....	7
1.2.3 Pigments for Paper .....	8
1.2.4 Materials & Monolithics.....	9
1.3 Overview of clay processing technologies at Imerys .....	10
1.3.1 Steps in hydrous process flow at Sandersville, Georgia, USA .....	11
1.3.2 Steps in calcined process flow at Sandersville, Georgia, USA .....	13
1.4 Overview and objectives of the project .....	14
 2 CHAPTER TWO – LITERATURE SURVEY .....	 23
2.1 Introduction.....	24
2.1.1 Overview of controlled release technologies .....	24
2.1.2 Overview of drug release mechanisms from polymeric devices.....	26
2.1.3 Diffusion controlled release from non-degradable systems.....	26
2.1.4 Solvent activation controlled release.....	29
2.1.5 Biodegradable systems .....	30
2.1.6 Empirical equation for describing drug release .....	33
2.2 Introduction to mechanisms involved in bacterial colonisation (fouling) of surfaces in the paint industry .....	33
2.3 Biocides in the coating industry.....	35
2.4 Roles of Minerals .....	38
2.5 Biocides and minerals in antifouling coatings .....	38

3	CHAPTER THREE – MINERAL CHARACTERISATION .....	43
3.1	Introduction.....	44
3.2	Minerals used and characterisation methods .....	44
3.2.1	Crystallography analysis by XRD method.....	46
3.2.2	Chemical composition analysis by X-ray fluorescence method .....	47
3.2.3	Powders' morphology detection by Scanning Electron Microscopy (SEM) .....	48
3.2.4	Particle size analysis by Light Scattering (using the Malvern Mastersizer) .....	50
3.2.5	Surface area measurement by B.E.T. (Brunauer Emmett and Teller) .....	52
3.3	Biocide selection and measurement.....	55
3.3.1	Biocide selection .....	55
3.3.2	Degradation of isothiazolines .....	57
3.3.3	Concentration measurement by HPLC.....	59
3.3.4	Concentration measurement by UV-Vis .....	61
3.4	Strength of biocide adsorption onto minerals .....	67
3.4.1	General principles of Flow Microcalorimetry (FMC) .....	67
3.4.2	Possible FMC results .....	68
4	CHAPTER FOUR – RESULTS OF MINERAL CHARACTERISATION.....	69
4.1	Mineral characterisation studies .....	70
4.2	Mineral size distribution analysis by the Mastersizer.....	70
4.2.1	Materials and Methods.....	74
4.2.2	Results.....	75
4.3	Mineral characterisation by X-ray Fluorescence (XRF).....	79
4.3.1	Materials and Method .....	79
4.3.2	Results.....	80
4.4	Material characterisation by X-ray Diffraction (XRD) .....	84
4.4.1	Material and method .....	84
4.4.2	Results.....	84
4.5	Morphology assessment by Scanning Electron Microscopy (SEM) .....	86
4.5.1	Material and method .....	87
4.5.2	Results.....	88
4.6	Discussion .....	90
5	CHAPTER FIVE – ADSORPTION ISOTHERM STUDIES .....	95
5.1	Flow Microcalorimetry (FMC) .....	96
5.1.1	Materials and Methods.....	96
5.1.2	Results.....	98
5.2	Adsorption Isotherms.....	103
5.2.1	Material and Method.....	103
5.2.2	HPLC settings .....	104
5.2.3	Methods of adsorption .....	105
5.2.4	Adsorption isotherm studies.....	106
5.2.5	Results for OIT Adsorption on the selected minerals .....	109
5.2.6	Adsorption of CIT/MIT on carriers .....	113
5.3	Discussion .....	120

6	CHAPTER SIX – OIT DESORPTION STUDIES .....	123
6.1	Materials and Methods.....	124
6.1.1	Typical paint formulation .....	125
6.1.2	Method of desorption measurement .....	126
6.2	Results of the desorption experiments .....	128
6.3	Discussion .....	135
7	CHAPTER SEVEN – BIOASSAY STUDIES .....	139
7.1	Materials and Methods.....	140
7.1.1	Biocide adsorption onto the minerals.....	140
7.1.2	Paint preparation .....	142
7.1.3	“Renault”, or paint ageing test .....	142
7.1.4	Bioassay (OIT potency test).....	143
7.1.5	Determination of OIT loading of paint films .....	146
7.2	Results .....	146
7.3	Discussion .....	159
8	CHAPTER EIGHT – INDUSTRIAL PERCEPTIVE OF THE PROJECT .....	162
8.1	Industrial aims of the project .....	163
8.2	Technology used .....	164
8.2.1	Mineral “impregnation” of biocide .....	164
8.2.2	Paint making and ageing test.....	166
8.2.3	Bioassay measurements .....	166
8.3	Paint mechanical and optical test measurements .....	167
8.3.1	Colour measurement (The CIE “Lab” and XYZ Colour Space) .....	167
8.3.2	Gloss Measurement .....	171
8.3.3	Contrast Ratio (Opacity) Measurement.....	175
8.3.4	Scrub Resistance .....	178
8.3.5	Stain Resistance .....	181
8.3.6	Rheology tests.....	183
8.4	Conclusion .....	188
9	CHAPTER NINE – CONCLUSION AND FUTURE WORK.....	190
10	REFERENCES .....	197
11	APPENDICES .....	205
12	CONFERENCES ATTENDED AND PAPERS PUBLISHED .....	223

# FIGURE INDEX

Figure 1.1: 2009 sales by business group (in Billions of Euro).....	9
Figure 1.2: Hydrous process flow at Imerys Georgia, USA (courtesy of Imerys Minerals) ...	11
Figure 1.3: Calcined process flow (paper grade) at Imerys Georgia, USA (courtesy of Imerys Minerals) .....	13
Figure 1.4: Some extenders used in the Coating Market (courtesy of Imerys Minerals) .....	16
Figure 1.5: Percentages of extenders used in the coating industry in Western Europe ( <i>Adapted from Kline: 2003, Western Europe - All Coatings</i> ) .....	17
Figure 1.6: Current levels of biocide loading in coatings.....	21
Figure 2.1: Drug release from a reservoir device (nanocapsule) .....	27
Figure 2.2: Examples of heavily fouled hulls [48] .....	35
Figure 2.4: Biocides used in this study: OIT in A, and the blend of MIT and CIT, respectively in B and C (with a methyl CH <sub>3</sub> attached to the nitrogen on B and C) .....	38
Figure 2.5: Functional groups present on the surface of porous, amorphous silica [86] .....	40
Figure 2.6: Representation of porous silica, with possible pathway for biocide release .....	40
Figure 2.7: Representation of a Halloysite mineral with pathway of intercalated biocides ....	41
Figure 2.8: Possible pathway for the release of the isothiazoline biocides in the platy minerals, with (A) small and (B) larger particle size.....	41
Figure 3.1: Particle size measurement as used in Malvern instruments [87].....	51
Figure 3.2: Typical particle size distribution curve [88].....	52
Figure 3.3: Biocides used in this study: (OIT), (CIT) and (MIT) respectively in A, B and C (with a methyl CH <sub>3</sub> attached to the nitrogen on B and C) .....	55
Figure 3.4: Thiol degradation of isothiazoline biocides [89].....	58



Figure 3.5: Sites of action of isothiazoline biocides in the Krebs cycle [89] .....	59
Figure 3.8: Schematic of a double beam UV-Vis Spectrometer equipment [91] .....	63
Figure 3.9: CIT/MIT calibration curve obtained from the UV-Vis spectrometer .....	65
Figure 3.10: OIT calibration curve obtained from the UV-Vis spectrometer.....	66
Figure 4.1: Frequency diagram for a broad and narrow particle size distribution [courtesy of Imerys].	71
Figure 4.2: Cumulative (integrated) version of Figure 4.1, showing the % passing (i.e. below) any particular diameter. In this form the “narrow” distribution is called “steep” [courtesy of Imerys].	72
Figure 4.3: The diameter of a circle with the same area as a 2-D projection of a particle may be a useful estimate of its size	73
Figure 4.4: Volume distribution of the platy minerals	75
Figure 4.5: Volume distribution of the non-platy minerals	76
Figure 4.6: Structure of a kaolinite layer [93]	83
Figure 9.7: Proposed intercalation of compounds into a platy clay (done here via an anion exchange [82].	196
Figure 5.1: Schematic of FMC with Polytetrafluoroethylene (PTFE) fluid path [61].....	97
Figure 5.2: Energies of adsorption and desorption of OIT per gram of minerals used in the FMC under flow conditions. ....	99
Figure 5.3: Amount of OIT adsorbed and desorbed per gram of minerals used in the FMC under flow conditions .....	100
Figure 5.4: Calibration curve of OIT biocide of known concentrations obtained from the HPLC .....	105
Figure 5.5: Langmuir system of isotherm classification [96-97].....	108
Figure 5. 6: OIT adsorption of the 4 platy clays used in the experiment: Infilm 939, Suprex, MCBP and NPD.....	110

Figure 5.7: New Zealand halloysite adsorption of OIT .....	111
Figure 5.8: Silica - Carplex CS-5 adsorption of OIT .....	112
Figure 5. 9: CIT/MIT adsorption of the 4 platy clays used in this experiment: Infilm 939, Suprex, MCBP, and NPD 16-A .....	114
Figure 5.10: New Zealand halloysite adsorption of CIT/MIT .....	116
Figure 5.11: Silica - Carplex CS-5 adsorption of CIT/MIT.....	116
Figure 6.1: OIT release profile from adsorbed (◊) and non-adsorbed ( ) OIT to Calcium Silicate T-38.....	129
Figure 6.2: OIT release from adsorbed (◊) and non-adsorbed ( ) OIT to diatomaceous earth celtix.....	130
Figure 6.3: OIT release profile from adsorbed (◊) and non-adsorbed (Δ) OIT to the silica carplex.....	131
Figure 6.4: OIT release profiles from adsorbed (◊) and non-adsorbed (Δ) OIT to the kaolin clay supreme .....	132
Figure 6.5: OIT desorption profiles from paint films with adsorbed (◊) and non-adsorbed OIT (Δ) to montmorillonite clay MCBP .....	133
Figure 7.1: A typical bacteria growth curve. The lag phase can be longer for different organisms [98] .....	144
Figure 7.2: Pseudomonas Aeruginosa growth curve, as observed in laboratory experiments .....	146
Figure 7.3: Cetrimide agar plate showing pseudomonas aeruginosa colony forming units (in green) after 48 hours incubation period .....	147
Figure 7.4: OIT calibration to determine the volume of biocide needed to inhibit or limit the growth of the organism .....	148
Figure 7.5: Pseudomonas colonies formation on paint films containing the kaolin, and subjected to artificial degradation in the QUV over a 1500 hours period .....	149
Figure 7.6: Pseudomonas colonies formation on paint films with silica carplex, subjected to	

artificial degradation in the QUV over a 1500 hours period .....	151
Figure 7.7: Pseudomonas colonies formation on paint films with montmorillonite MCBP, subjected to artificial degradation in the QUV over a 1500 hours period .....	152
Figure 7.8: Percentage of OIT left in the paint films containing kaolin supreme throughout the ageing process .....	155
Figure 7.9: Percentage of OIT left in the paint films containing silica carplex throughout the ageing process .....	156
Figure 7.10: Percentage of OIT left in the paint films containing montmorillonite MCBP throughout the ageing process .....	157
Figure 8.1: Yxy chromaticities in the CIE colour space [99] .....	169
Figure 8.2: L*a*b* colour space [100] .....	170
Figure 8.3: 45 and 20 degrees gloss measurements by the Gardner Gloss meter [101] .....	175
Figure 8.4: A Morest black and white chart .....	176

## LIST OF TABLES

Table 3.1: General characteristics of minerals used in this study .....	45
Table 3.1: Environmental input parameters of isothiazoline biocides and TBT (Source, World Health Organisation, 1990) .....	57
Table 4.1: Size distribution and steepness factors of the minerals used .....	77
Table 4.2: XRF data detailing the percentage of the chemical composition of the nine minerals used .....	81
Table 4.3: XRD data showing percentage of various crystals present in each of the nine minerals used in this study .....	85
Table 4.5: Major differences between a 1:1 and a 2:1 clay .....	93
Table 5.1: Summary of the ratios of heat of sorption (with molar heat of interaction) and amounts of OIT after the FMC run .....	101
Table 5.2: Saturation levels and molecular footprints of the biocides on the minerals biocides used. This saturation level of CIT/MIT on this mineral is listed in Table 5-2, together with the corresponding molecular footprints of the biocide onto the Silica. ....	117
biocides used. This saturation level of CIT/MIT on this mineral is listed in Table 5-2, together with the corresponding molecular footprints of the biocide onto the Silica. ....	118
Table 6.1: Amount of OIT in dried films on Leneta discs .....	127
(MCBP / OIT) still retained more than 40% of its biocide content after seven days. ....	134
(MCBP / OIT) still retained more than 40% of its biocide content after seven days. ....	135
Table 7.1: Composition of powder-OIT preparation for use in the paint film. ....	141
Table 7.2: Number of pseudomonas colony forming units ( $\times 10^5$ ) recorded after paint ageing test in the QUV (at specific times) .....	153
Table 7.3: Percentage of OIT left in the paint films after 1500 hours ageing test .....	158
Table 8.1: Summary of L*A*B*, Gloss and Opacity data of the paint films made .....	177
Table 8.2: Weight loss after 200 scrub cycles .....	180
Table 8.3: Stain resistance of the paints made .....	182
Table 8.4: Viscosity data of the paint (Viscosity readings in Poise) .....	185

Table 8.5: Viscosity measurement data of the paints made, using the Stormer Krebs, the Roto-Thinner and the Sheen and Cone viscometers (Viscosity readings in Poise).....188

## LIST OF TERMS

Å	Angstrom
Al <sub>2</sub> O <sub>3</sub>	Aluminium Oxide
APS	Aminopropyltrimethoxysilane
ATP	Adenosine Triphosphate
B.E.T	Brunauer – Emmett - Teller
BS	British Standard
C.I.E	Commission Internationale d'Eclairage
CaCO <sub>3</sub>	Calcium Carbonate
CaO	Calcium Oxide
CFU	Colony Forming Unit
CH <sub>3</sub>	Methyl
CIT	5-Chloro-2-methyl-4-isothiazolin-3-one
DETA	Diaethylenetriamine
d <sub>F</sub>	Ferret Diameter
ESD	Equivalent Spherical Diameter
EU	European Union
FAD	Flavin Adenine Dinucleotide
Fc	Flow rate
Fe <sub>2</sub> O <sub>3</sub>	Iron Oxide
FMC	Flow Microcalorimetry

GC	Gas Chromatography
GCC	Ground Calcium Carbonate
HPLC	High Performance Liquid Chromatography
ID	Internal diameter
IMO	International Maritime Organisation
K <sub>2</sub> O	Potassium Oxide
Kd	Distribution coefficient
KJ	Kilojoules
Kvolts	Kilovolts
LOI	Loss of Ignition
MCBP	Mineral Colloid BP
MEPC	Maritime Environmental Protection Committee
Mg <sup>2+</sup>	Magnesium
MgO	Magnesium Oxide
MHI	Molar Heat of Interaction
MIC	Minimum Inhibitory Concentration
MIT	2-Methyl-4-isothiazolin-3-one
Mpa	Mega Pascal
Mwt	Molecular Weight
Na <sub>2</sub> O	Sodium Oxide
Na <sub>2</sub> SO <sub>3</sub>	Sodium Sulfite
NAD	Nicotinamide Adenine Dinucleotide
Ne/He	Neon / Helium
NPD	New Product Development
NZH	New Zealand Halloysite
°C	Degree Celcius

OIT	2-Octyl-4-isothiazolin-3-one
PCC	Precipitated Calcium Carbonate
PMGI	Performance Minerals Growth Initiative
P <sub>o</sub>	Initial Light Power
P <sub>s</sub>	Source Light Power
PSD	Particle Size Distribution
PTFE	Polytetrafluoroethylene
Rpm	Revolution per minute
S.A	Surface Area
SEM	Scanning Electron Microscopy
SiO <sub>2</sub>	Silicon Dioxide
SL	Saturation Level (of biocide)
Stddev	Standard Deviation
TBT	Tributyltin
TBT-SPC	Tributyltin Self-Polishing Copolymer
TiO <sub>2</sub>	Titanium Dioxide
Tr	Retention time
UV-Vis	Ultra Violet / Visible
V	Volume
V/V	Volume per Volume
V <sub>r</sub>	Retention volume
W/V	Weight per Volume
Wt%	Weight per cent
XRD	X-ray Diffraction
XRF	X-ray reflectance
ε <sub>λ</sub>	Molar Extension Coefficient

$\theta_i$	Incident Ray
$\theta_r$	Reflected Ray
$\lambda$	Wavelength
$\rho_f$	Density of fluid
$\rho_p$	Density of particle



# **CHAPTER ONE**

## **INTRODUCTION**

## **1.1 Imerys Minerals**

### **1.1.1 History and Development**

Established in 1880, the Imerys group had its origin in mining and metallurgy, with its core business in the extraction and processing of non-ferrous metals. In 1974, under the name of Imetal, the group acquired the French company Huguenot Fenal, hence getting an entry into the clay roof tile market. A year later, the group acquired Copperweld (USA), a company specialising in steel production and metal processing, followed in 1985 by Damrec (France), marking a significant investment in refractories and ceramics. The group's business was then structured around three sectors: Building Materials, Industrial Minerals and Metals Processing.

From 1990 onwards, the Group focused its development on Industrial Minerals and implemented an ambitious acquisitions policy. Imetal established strong positions in white pigments, first in kaolins (Dry Branch Kaolin Company, United States) then in calcium carbonates (Georgia Marble, United States). It then entered the graphite market (Timcal, Switzerland; Stratmin Graphite, Canada). The Group also expanded through acquisitions in refractories (C-E Minerals, United States; Plibrico, Luxembourg), clays (Cératéra, France), ceramic bodies (KPCL, France) and technical ceramics (Refral, France; Lomba and Cedonosa, Spain).

Between 1994 and 1998, Imetal doubled in size, one-third by organic growth and two-thirds by external growth. In 1998, the business was structured around two sectors (Minerals

Processing, Metals Processing) with an operating division-based organisation. The acquisition, in 1999, of English China Clay (ECC), one of the world's foremost specialists in industrial minerals, helped the company to become a global leader in this sector and focussed exclusively on Minerals Processing. Imetal then divested its Metals Processing activity, comprised of the North American companies Copperweld and Copperweld Canada (world leader in bimetallic wires, American leader in specialty tubing), and changed its name to Imerys on September 22, 1999, to reflect that development.

### **1.1.2 Group development from 2000 to 2010**

The Group completed the refocusing process by withdrawing from activities that no longer corresponded to its core business, including dimension stones (Georgia, USA) and trading. The specialty chemicals distribution business (CDM AB, Sweden) was divested in 2004, followed in 2005 by trading in mainly basic refractories (American Minerals, Inc, USA) and roofing products distribution (Larivière, France).

Since 2000, the Group has developed by leveraging its unique know-how. From a varied portfolio of rare resources, Imerys turns industrial minerals into specialties with high added value for its customers. Organised into business groups that correspond to its main markets, the Group is constantly broadening its product range, extending its geographic network into high-growth zones and taking up positions on new markets.

### **1.1.3 Group development by activity**

The **Minerals for Refractories** activity expanded its offering for the refractory and sanitaryware markets and enhanced its global geographic network with the acquisition of

AGS (2006 – France) and Vatutinsky (2007 – Ukraine), both companies specializing in calcined clays. The purchase of a 65% stake in Yilong (Xinjiang) in April 2007 gave Imerys access to an excellent quality andalusite reserve developed to serve the Chinese refractories market.

The **Minerals for Abrasives** activity was created in 2000 with the takeover of the world's leading producer of corundum (fused alumina and bauxite), the Treibacher Schleifmittel group (Austria). A succession of corundum acquisitions were made in the Czech Republic, Germany (2001), Brazil (2002) and China, where a third joint venture was created in 2007 with ZAF, a producer of brown corundum for the Asian abrasives market. In 2007, Imerys added zircon to its portfolio. The Group became the world leader in this mineral - used in the refractories, technical ceramics and automotive sectors - with the successive acquisitions of UCM Group PLC (Great Britain), and Astron China (completed on February 5<sup>th</sup>, 2008). The Minerals for Abrasives division was renamed Fused Minerals.

**Minerals for Filtration** joined the Group in 2005 with the acquisition of the world leader in the sector, World Minerals (United States). This acquisition contributed new minerals (diatomite and perlite), while following a model that is consistent with Imerys' business and skills. Perlite capacities were bolstered in South America in 2007 with the consolidation of Perfiltra (Argentina). With the acquisition in April 2007 of 65% of Xinlong (Xinjiang), China's leading vermiculite producer, Imerys is now the world number two in vermiculite.

New **Minerals for Ceramics** were added to the portfolio, particularly halloysite (New Zealand China Clays, New Zealand - 2000) and fine ceramic clays and feldspar (K-T, United

States and Mexico – 2001; Denain-Anzin Minéraux, Europe - 2005). The Group increased its Asian market presence for applications that mainly serve the sanitaryware industry (MRD-ECC and MRD, Thailand – 2002). In 2007 it developed its reserves of feldspar, an essential component in ceramics manufacturing alongside clays and kaolins, in India (Jumbo Mining), the United States (The Feldspar Corporation) and Turkey.

**Performance Minerals** developed with the extension of calcium carbonate capacities in Central and South America (Quimbarra, chiefly Brazil – 2000), Asia (Honaik, mainly in Malaysia – 2000) and France (AGS-BMP's carbonates activities – 2000). The Group strengthened its positions in Southern Europe (Gran Bianco Carrara, Italy and Blancs Minéraux de Tunisie, Tunisia – 2005) and Turkey (70% stake in Mikro Mineral – 2006).

In **Pigments for Paper**, development focused on ground (GCC) and precipitated (PCC) calcium carbonates, which now account for more than half the Group's sales to the paper industry. Six new production units have been built since 2004, mainly in the Asia-Pacific zone to support the development of local activities, extensive reserves of high quality white marble (GCC) have been acquired in China in recent years. In parallel, an important restructuring plan of its kaolin for paper production announced at mid-2006, enables the Group to have the most competitive platform for both coating and filler kaolins for the paper industry

The Group's **Building Materials** was strengthened in bricks in France with the acquisition of Marcel Rivereau (2004) and, in 2007, a development plan launched in clay bricks to meet high market demand. Clay roof tiles and bricks activities in Spain and Portugal were divested

in 2007.

In **Refractory Solutions**, the acquisition of Lafarge Refractories (2005) made Imerys the European leader in the sector and gave it a foothold in Asia. The merger of this activity with Imerys' existing businesses in the sector (Plibrico) led to the creation of a new entity, Calderys. ACE, the Indian leader in monolithic refractories, joined the Group in 2007, giving it a new dimension in this fast-growing country and consolidating Imerys' world leadership in monolithic refractories. In 2007, Calderys also developed in South Africa with the acquisition of B&B, a refractory product fitter for the local steel industry. Moreover, Imerys has gained leadership in refractory Kiln Furniture in both Asia (Siam Refractory Industry Co, Ltd, Thailand – 2002) and Europe (Burton Apta, Hungary – 2004).

The diversity and geographical scope of Imerys' business have led the company to adopt a decentralised operating management system. Since February 13, 2008, Imerys has reorganised its activities into four business groups.

- Minerals for Ceramics, Refractories, Abrasives and Foundry
- Performance Minerals and Filtration
- Pigments for Paper
- Materials and Monolithics

## 1.2 Company market size

Active in 47 countries with more than 260 locations, Imerys is the world leader in adding value to minerals. It achieved €2.774 billion in annual sales in 2009. The company's global market size is arranged according to the four business groups detailed in the 4 subsections

below (from 1.2.1 to 1.2.4).

### **1.2.1 Minerals for Ceramics, Refractories, Abrasives & Foundry**

This business group has a wide range of extensive, high-quality mineral reserves thanks to its four activities. With expertise in all the techniques needed for transformation, it also offers a diverse range of products that meet the specific requirements of the industries it serves, especially in terms of chemical composition, mechanical properties, thermal and chemical resistance.

Market positions (as of 2010):

- European number 1 in raw materials and ceramic bodies for porcelain
- World number 1 in fused Zirconia
- World number 1 in minerals for refractory applications
- World number 1 in minerals for abrasives
- World number 1 in high performance graphite powders

### **1.2.2 Performance & Filtration Minerals**

The group is made up of the Performance Minerals and Filtration Minerals Group's activities. The Performance Minerals activity provides customers with tailor-made solutions in a highly technical field, based on the processing of kaolins, carbonates, feldspar, mica and ball clays. The development of partnerships with customers is essential within the value-added markets of performance minerals comprising plastics, rubber, coatings, adhesives, caulks and sealants,

health, beauty & nutrition and building & construction materials. The Filtration Minerals activity is the world's leading supplier of diatomite and expanded perlite-based products for filtration. Vermiculite has been complementing the Filtration Minerals portfolio in 2006. The activity has also been strengthened during 2007 with the acquisitions of Perfiltra (perlite) and Xinlong (Vermiculite), both mentioned in section 1.1.3.

Market positions (as of 2010):

- World number 1 in minerals for breathable polymer films
- World number 1 in Mica for engineered plastics and high performance coatings
- World number 1 in perlite-based products for filtration

### **1.2.3 Pigments for Paper**

This comprised the Group's activities in kaolin and calcium carbonates (natural and precipitated) for the paper industry. Its structure is designed to serve the needs of the changing global paper market. Pigments for Paper supply more than 350 paper mills, 26% of which are in North America, 45% in Europe and 29% in the rest of the world, mainly Asia-Pacific, the region driving growth in the paper industry.

Market positions (as of 2010):

- World number 1 in kaolin for paper
- World number 2 in ground calcium carbonate (GCC) for paper
- World number 3 in precipitated calcium carbonate (PCC) for paper



### 1.2.4 Materials & Monolithics

The group gathers the Building Materials and Refractory Solutions Group's activities. It has strong market positions that it continues to develop through substantial capital expenditure and an active innovation policy.

Market positions (as of 2010):

- French number 1 in clay roof tiles, bricks, chimney blocks and natural slates
- World number 1 in alumino-silicate monolithic refractories
- World number 1 in kiln furniture for ceramic applications

Imerys' total sales for the year 2009 were 2.774 billion Euros, with contributions from the four main business groups (this is detailed in Figure 1.1 below).

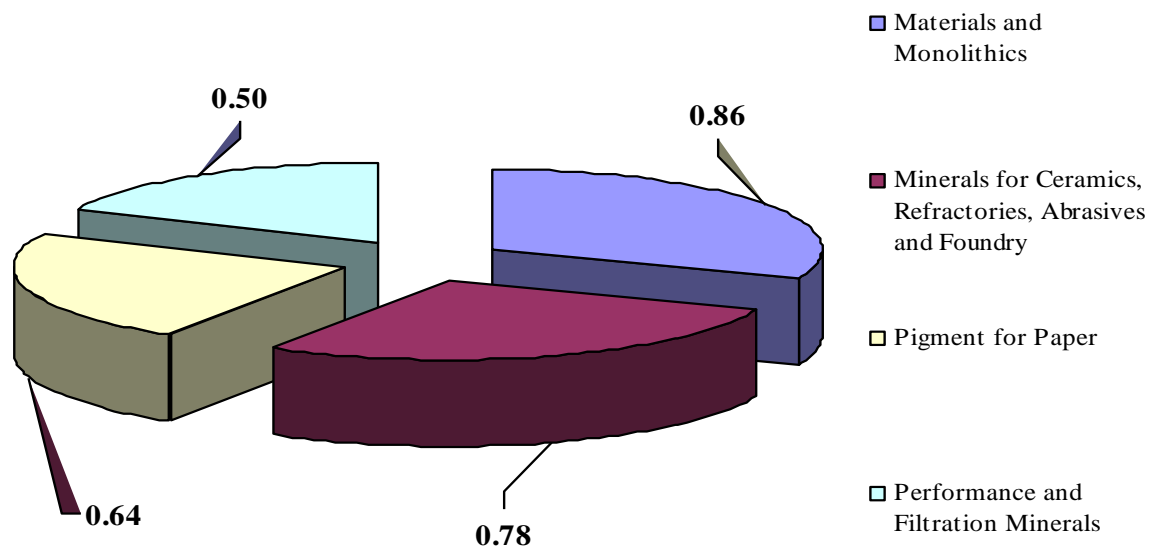


Figure 1.1: 2009 sales by business group (in Billions of Euro)

### **1.3 Overview of clay processing technologies at Imerys**

From Mining to the finished products (according to customer specifications), the company utilises two main processing routes in order to refine its clays: hydrous and calcined process flow. There are many steps involved with each of these processes and they are detailed in Figures 1.2 and 1.3.

### 1.3.1 Steps in hydrous process flow at Sandersville, Georgia, USA

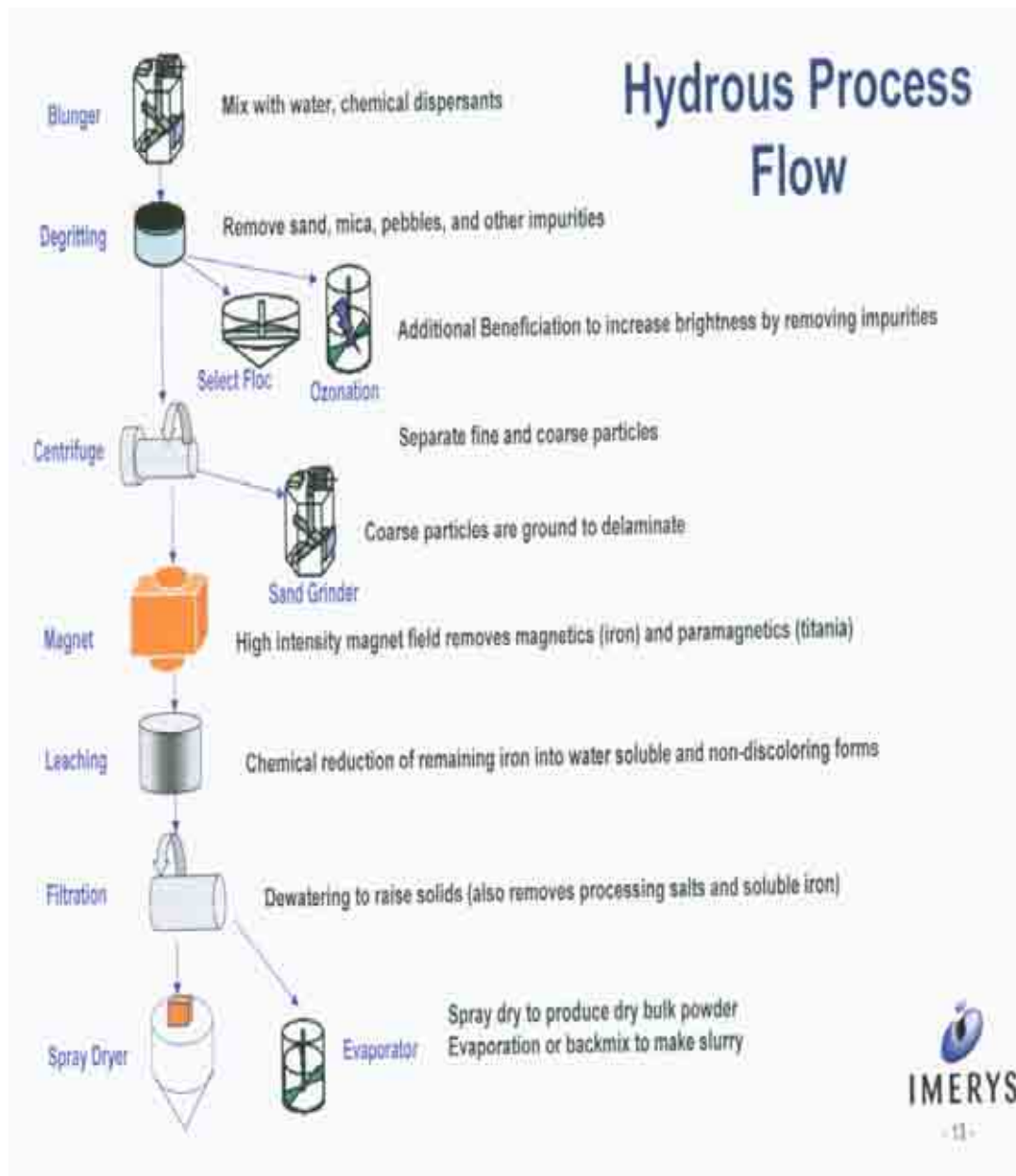


Figure 1.2: Hydrous process flow at Imerys Georgia, USA (courtesy of Imerys Minerals)

In the hydrous process, the clay is first mixed with water and chemical dispersant. This is then followed by the beneficiation process, consisting of:

- The degritting, to remove most impurities from the clay
- The selective flocculation (particles aggregating and settling/flocculating) and ozonisation (water treatment to destroy micro-organisms), to increase the brightness of the clay by further removing more impurities from the mineral
- The centrifugation process, designed to separate the fine particles from the coarse ones (coarse particles are ground in the sand grinder to delaminate them)
- Magnetic separation, which removes magnetic iron and paramagnetic titania from the clay (this will increase the optical property of the final product)
- The leaching process, aimed at chemically reducing the remaining iron into a water soluble and non-discolouring form
- The filtration, which raises the solid level by dewatering the sample, and removing processing salts and water soluble iron
- The spray drying, which produces the dry powder

### 1.3.2 Steps in calcined process flow at Sandersville, Georgia, USA

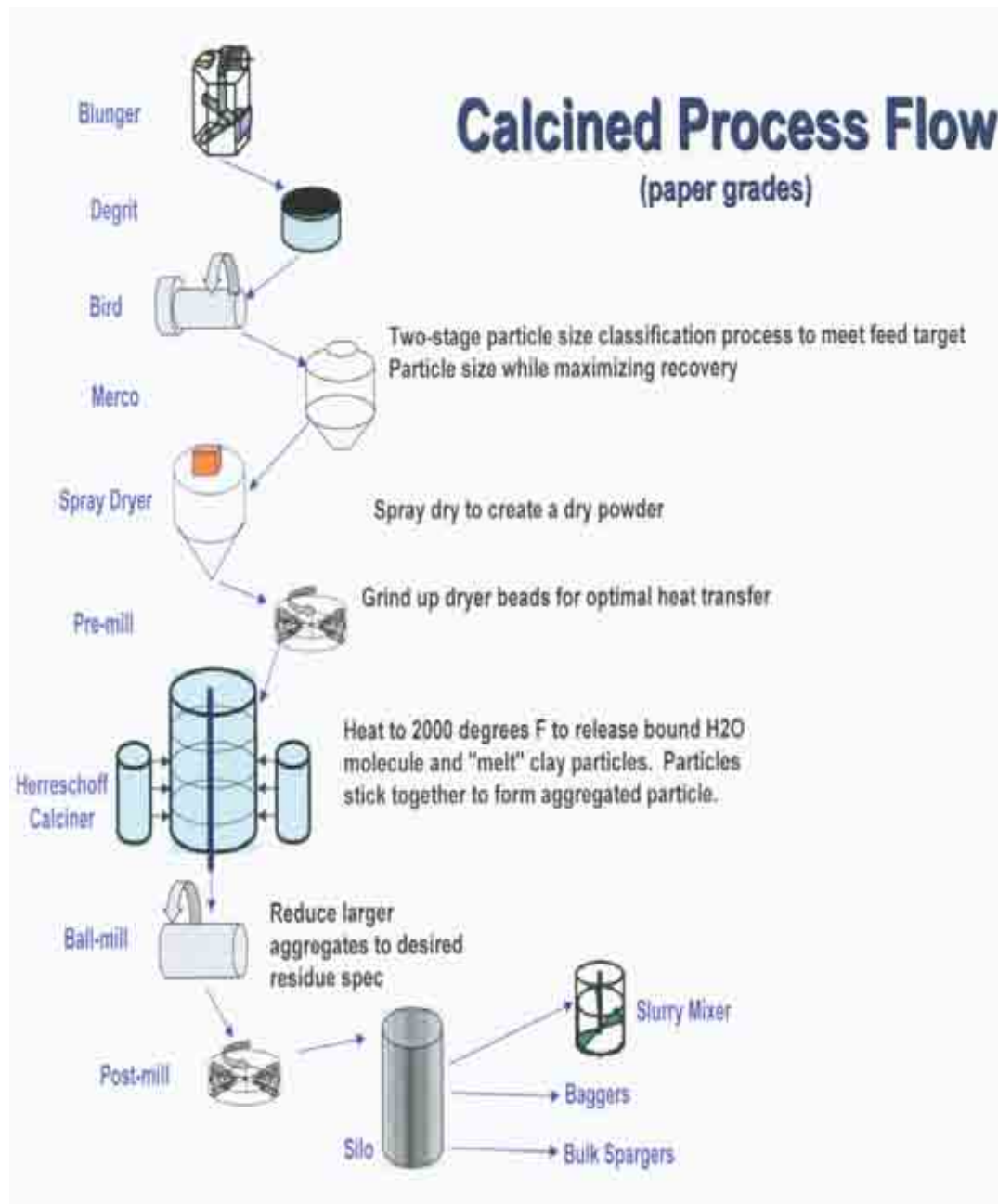


Figure 1.3: Calcined process flow (paper grade) at Imerys Georgia, USA (courtesy of Imerys Minerals)

In the calcined process, the clay is first mixed with water and chemical dispersant. This is

followed by the beneficiation process, consisting of:

- The degrading, to remove most impurities from the clay
- A two-stage centrifugation process, using Bird and Merco industrial centrifuges, to separate the fine particles from the coarse ones
- Spray drying, which produces the dry powder
- Calcination process, where the clay is heated to 1093°C. This process will eliminate all (or most) impurities That remained in the clay and produce large aggregates
- The milling process, where the large aggregates are reduced to smaller desirable size in the ball mill, ready for use

#### **1.4 Overview and objectives of the project**

As stated previously, Imerys possess large reserves of various clays and calcium carbonate. Those minerals, when processed, are mostly used in the paper, paint, plastic and rubber industries as functional fillers and rheology enhancers. The Performance Minerals Growth Initiative (PMGI) group was created in 2003 as part of the Speciality Minerals Division, and symbolised the company's eagerness to develop new products in order to maximise its growth.

This project aims to explore ways by which minerals produced by the company can be used to adsorb and release some biocides in a controlled way in paint films. There are currently high levels of biocide loaded and released from applications such as paints and antimicrobial packaging (see Figure 1.4), and this adds to manufacturing costs, is damaging to non-target organisms in the environment in which these biocides are released. Biocides are also used in

clay slurry tanks by Imerys to control the growth of micro-organisms. It is hoped that the proposed method to control the release of biocides from minerals could help Imerys develop and sell a new generation of minerals suitable for this purpose, and ultimately reduce the amounts of biocide in usage.

Some of the minerals chosen for this work represented a generation of extenders, sold by Imerys, and used in paints. Generally, most extenders will be mineral compounds:

- having a relatively low refractive index (1.4 - 1.7)
- that are insoluble in the paint media

Typical cost of these extenders varies between\_€60 to €800 per tonne (this compared with Titania at €2200 a tonne). A few of those extenders are shown in Figure 1.4.

**Dolomite****Kaolin****GCC****Mica**

Figure 1.4: Some extenders used in the Coating Market (courtesy of Imerys Minerals)

In Western Europe, the estimated total volume of extender used in 2003 was 1.5 million tonnes. This high volume of extender include:

- Kaolin, both hydrous and calcined
- Natural & synthetic barytes
- Other minerals, including mica, diatomite, calcium carbonate and vermiculite.

Figure 1.5 details the percentages of different extenders used in coatings in Western Europe in 2003.



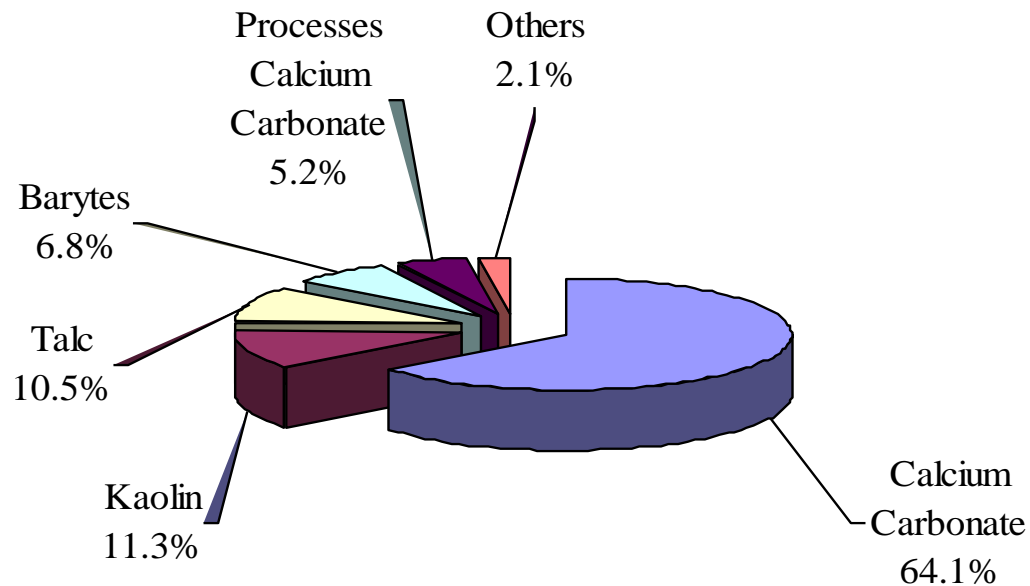


Figure 1.5: Percentages of extenders used in the coating industry in Western Europe (*Adapted from Kline: 2003, Western Europe - All Coatings*)

Imerys Minerals is already present in this market with a large variety of mineral extenders sold to the paint and paper industries. Ground and precipitated calcium carbonates and kaolin account for 80% of the total extenders used in Western Europe, and the company is hoping to develop new products in order to maintain and build their global market position.

Nine minerals were initially chosen for this work, and they were:

- Four Kaolins (Infilm 939, Supreme, Suprex, and NPD-16A). These minerals were chosen because they are relatively inexpensive, produced by Imerys, and generally used in the paper and paint industries as functional fillers

- A montmorillonite (MCBP), used because it is expandable upon hydration, thus opening up the plates and increasing the available surface area for biocide adsorption.
- A halloysite (New Zealand Halloysite). The halloysite was used because of its tubular shape, which has already been tried by Imerys New Zealand in controlled release experiments.[1-2]
- A calcium silicate (T-38) produced and sold by World Minerals, a subsidiary of Imerys Minerals, and used for filtration.
- A diatomaceous earth mineral (Celtix), also produced by World Minerals and used for filtration.
- An amorphous silica (Carplex CS-5) from Degusa, Japan. This mineral was chosen due to its high porosity, and is already used as a chelator agent in breweries, to remove unwanted compounds in beer filtration.

In addition to the industrial functions mentioned, these minerals were selected because of differences in their surface areas, chemical compositions, crystal arrangements, and shapes (described in Table 3-1). It was believed those differences could be exploited for controlled release purposes.

In order to investigate the controlled release potentials of these minerals, it was decided to impregnate them with two biocides of interest, 2-Octyl-4-isothiazolin-3-one (OIT) and the blend of 2-Methyl-4-isothiazolin-3-one (MIT) and 5-Chloro-2-methyl-4-isothiazolin-3-one (CIT), and release the biocide molecules either directly from the minerals, or from paints films, in both static and dynamic environments. The isothiazoline biocides used were chosen because they offer many performance advantages over other biocides. These advantages

include the following:

- They have a broad-spectrum antimicrobial activity and can control the growth of both Gram-negative and Gram-positive bacteria, and fungi (molds and yeasts).
- They are economical. The required dosage concentrations are more cost-effective than other commercial preservatives.
- These biocides are formaldehyde-free, and do not contain or generate formaldehyde (formaldehyde is very toxic when inhaled or present in the food chain, and carcinogenic).
- They offer low use levels (excellent microbe control at low Minimum Inhibitory Concentrations). Typical MIC levels are 6-15 part per million of the combined active components (0.04-0.10% of the product as supplied, volume/volume; see Figure 1.6).
- They have low toxicity, with lower half-lives than other biocides (see Table 3.5).
- Excellent compatibility with common formulation ingredients.
- Excellent stability over a wide pH range (2 to 8.5).
- They are easy to formulate and are supplied as an easy-to-use aqueous solution.
- No side effects: the biocides will not adversely affect a product's physical properties or performance.
- They are environmentally friendly and do not persist in the environment; their breakdown products are essentially benign.

In order to achieve the main aim of the project, the following steps were taken:

- The surface area of each of the nine minerals used was determined by B.E.T.

nitrogen.

- The particle size distribution (PSD) of the minerals was determined using light scattering techniques.
- The minerals used were characterised to determine their chemical compositions using X-ray Fluorescence), crystal structures by X-ray Diffraction, and morphologies by Scanning Electron Microscopy.
- A protocol was developed to adsorb the isothiazoline biocides molecules to the clays (using a bench high shear mill for dry adsorption, and wet adsorption in water, by first making a paste of the minerals).
- The biocide molecules were desorbed in a beaker with water under constant stirring over time, and High Performance Liquid Chromatography (HPLC) was used to measure their concentrations.
- The adsorption and desorption experiments were repeated under flow condition in the Flow Microcalorimeter (FMC), and the various heats produced during the sorption processes were measured to estimate the strengths of the bonds between the biocides and the minerals. This process then gave an indication of the types of adsorption taking place (chemisorption, physisorption), and used to eliminate the less performing minerals.
- The biocide-loaded minerals were added to an external paint formulation. The biocide content of the paint films obtained was first desorbed in water to determine the differences in desorption profiles between the minerals used. Following on this, the paints films were aged over a 1500 hours period, and their potency to destroy *pseudomonas aeruginosa* micro-organisms was investigated throughout that time period.

- Finally, optical, mechanical and rheology properties of the paints were investigated.

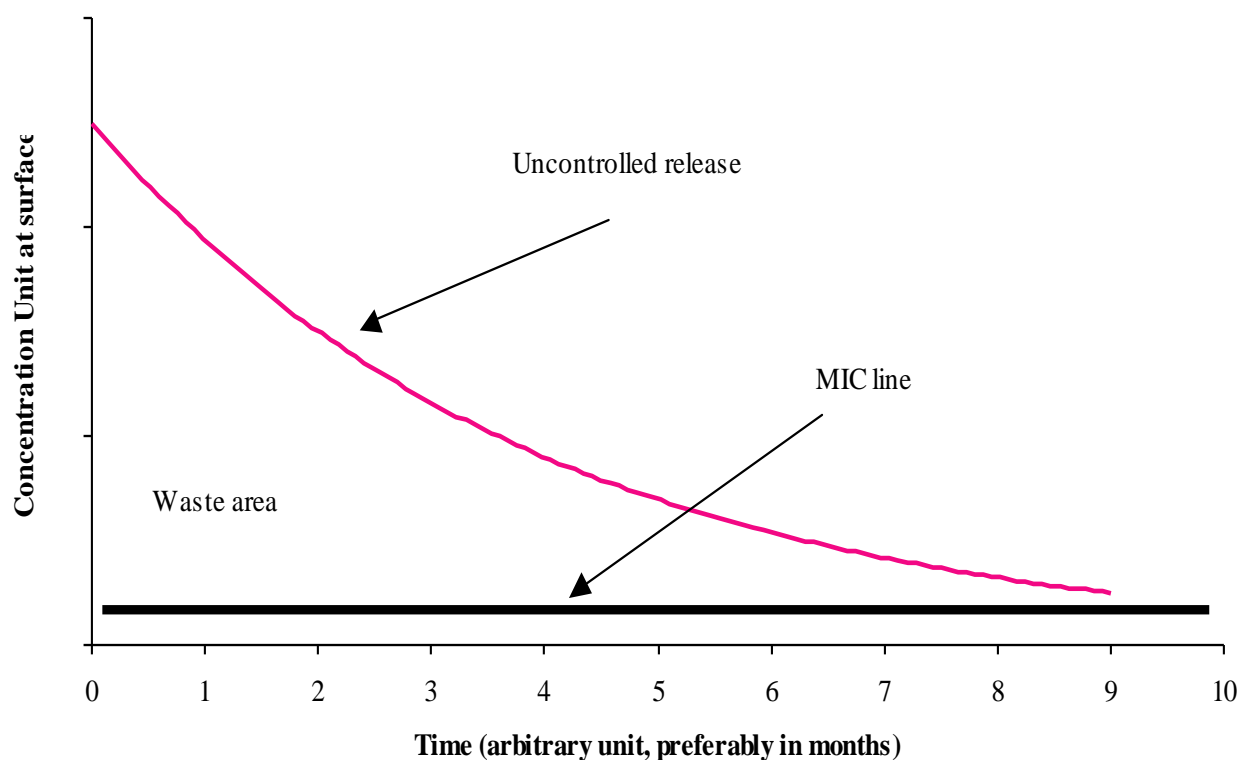


Figure 1.6: Current levels of biocide loading in coatings.

The MIC line (minimum inhibitory concentration, as shown in Figure 1.6), which represents the maximum concentration of biocide required to kill all organisms in a particular system, is a zero order release. The area between the uncontrolled release and MIC lines represents waste and has detrimental environmental and economic effects on the ecosystem and companies respectively.

There are currently several worldwide research groups working on biocide release from paint films, e.g the European Union “Ambio” project [3], and Poseidon in the USA. These research

groups are primarily trying to address issues associated with the toxic nature of the biocides, and the amounts currently being added to the paints, by developing non-biocidal solutions for the problem of marine biofouling. Some of the nine minerals used will be selected for the paint application and the bioassay work if:

- The biocide reasonably strongly adsorbs to the mineral
- The amount of biocide adsorbed is reasonably high
- The biocide desorbs from the mineral over period of time (if it is not permanently attached to the clay)
- The mineral-biocide complex is compatible with the existing paint system (pH and viscosity of the paints of the new formulations must not differ with those of the control)
- The new formulations must be able to kill micro-organisms growing on a paint surface

In the remainder of this thesis, Chapter Two will review the use of controlled release technologies, with specific reference to biocides. Chapter Three outlines the characterisation techniques used for the various materials, with the results of these characterisations detailed in Chapter Four. Chapter Five and Six will respectively outline the adsorption and desorption characteristics of some chosen minerals, while Chapter Seven will discuss the potency of the desorbed OIT biocide in bioassay measurements. In Chapter Eight, the industrial perspective of the project will be discussed, while in Chapter Nine, the various findings of the project will be summarised.

# **CHAPTER TWO**

## **LITERATURE SURVEY**

## 2.1 Introduction

In this chapter, the literature on various aspects of controlled release technologies is reviewed. Particular attention is paid to the various technologies available, the drug (or compound) release mechanisms, the role minerals can and do play, and some of the various biocides found in coatings. Some aspects of controlled release systems in the field of medicine and pharmaceuticals will be explored, as this area has a world-leading advance on any other field, due to the need to minimise or eliminate the side effects of many drugs. Chapter 7 discusses the biocide potency to the organism *pseudomonas aeruginosa* (found on most contaminated surfaces), and it is believed that understanding controlled release mechanisms in the field of modern Medicine could lead the way to creating very good controlled release systems in industries such as paint, agriculture, and food packaging.

### 2.1.1 Overview of controlled release technologies

Controlled release technologies are becoming more and more important, especially in the field of modern medication and pharmaceuticals [4]. Controlled release is the use of formulation components and devices to release a therapeutic at a predictable rate *in vivo* when administered by an injected or non-injected route. An example of controlled release formulation is the transdermal patch containing fentanyl. The rate of drug release from the system is device-led and in theory, the resulting drug plasma levels reach a constant amount per unit time (zero order kinetics).

Another example is the six-month implant of biodegradable microspheres of the peptide,



leuprolide, for treatment of prostate cancer. These formulations avoid the plasma peak and troughs of traditional injections, thus avoiding side effects and making the medicine more effective and acceptable to patients. More recently, controlled release has had to encompass the skills of pharmacology and physiology since the release rates of a drug from a polymer *in vitro* is not the same as what occurs *in vivo*. In addition, researchers in controlled release need to know how drugs cross biological membranes, how they interact with immune cells and how they distribute to different organs. Gene delivery, DNA vaccines, cancer chemotherapy and brain delivery of drugs require drug delivery scientists to get involved in understanding antigen presentation, compartmentalisation within cells, how to target drugs to cancer cells and how to take advantage of receptor-mediated uptake into the brain and other organs. While some of these major medical needs are only beginning to be addressed, there have been significant advances, for example, in conjugating anti-cancer agents to new polymers to give targeted formulations with better pharmacokinetics.

Controlled drug release of drugs in the body at a desired rate has many advantages over conventional forms of dosage and these include the followings [4,5]:

- Minimising deleterious side effects
- Prolonging efficiency time
- Heightening drug bioavailability
- Improving patient compliance
- Protecting sensitive drugs from enzymatic or acidic degradation in the body
- Masking peculiar odours [6]
- Maintaining the patient blood level

One common way of controlling drug delivery is to incorporate the drug into a polymer matrix system [7-10]. The dissolution and diffusion of the drug through the polymer [11, 12], or the swelling and erosion of the matrix [13], are important phenomena in controlling the release characteristics of the formulation. Hydrogel polymers have attracted a great deal of attention over the years because of their valuable applications in controlled and site-specific delivery of drug [14-17], cell encapsulation and tissue engineering [18-20]. Hydrogels have the ability to swell in the presence of water or biological fluids in order to regulate the release of the encapsulated drugs. By controlling the degree of swelling due to crosslinking makes them potential carriers of drugs for controlled release applications [22-24].

### **2.1.2 Overview of drug release mechanisms from polymeric devices**

Drug release from a controlled release system can be achieved by several mechanisms, such as diffusion through a rate-controlling membrane, by osmosis, ion exchange or by degradation of the matrix [25-28]

### **2.1.3 Diffusion controlled release from non-degradable systems**

Diffusion controlled systems can be divided into non-degradable reservoirs and monolithic devices [26, 29]. Reservoir systems provide constant release of a drug over a substantial period. In this system, a core of drug is surrounded by a polymer film that serves as diffusion barrier through which the release of the drug occurs (Figure 2.1). As long as the drug concentration inside the film stays constant, the drug release obeys zero order kinetics.

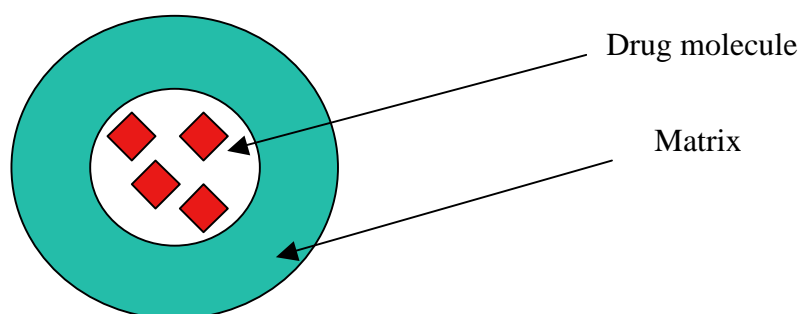


Figure 2.1: Drug release from a reservoir device (nanocapsule)

In monolithic devices of various shapes, the active agent is either dispersed or dissolved in the polymer matrix. In both cases drug diffusion through the polymer matrix is the rate limiting step and the release rates are determined by the choice of the polymer and its consequent effect on the diffusion and partition coefficient of the drug [30].

Mathematical treatment of diffusion depends on whether the drug is dissolved or dispersed in the polymer. In a matrix system, where the drug is dissolved in the polymer matrix, the release follows Fick's law. The following equation describes drug release from a slab-shaped device:

$$\frac{M_t}{M_0} = 4 \left[ \frac{Dt}{\pi h^2} \right]^{1/2} \quad \text{Equation 2.1}$$

where:

$M_t/M_0$  is the fractional released amount of drug ( $\text{mol}/\text{m}^2 \cdot \text{s}$ )

$D$  is the diffusion coefficient of a drug in the matrix ( $\text{m}^2 \text{s}^{-1}$ )

$h$  is the thickness of the slab device (m)

$t$  is time (s).

This equation is valid for the release of the first 60 percent of the drug total (early time approximation). Thereafter the release kinetics follows first order kinetics (late time approximation). The reason for a decrease in the release rate is an increase in the diffusional path length [26, 29, 31]. This problem can be avoided by using special geometry that provides increasing surface areas over time [31].

Higuchi developed an equation for the release of solid drugs dispersed in matrix dosage systems, from which the drug diffuses through non-porous polymer [30]. Drug release is affected, apart from the geometry of the device, also by the concentration of drug. Drug release follows square root of time kinetics until the concentration in the matrix falls below the saturation value ( $C_o > C_s$ ).

$$\frac{dMt}{dt} = \frac{A}{2} \left( \frac{2DC_sC_o}{t} \right)^{1/2} \quad \text{Equation 2.2}$$

In this equation,  $dMt/dt$  is the release rate of drug,  $A$  is the total area of the slab (both sides),  $D$  is the diffusion coefficient of the drug in the matrix,  $C_s$  is the solubility of the drug in a polymeric matrix,  $C_o$  is the total amount of drug (both dissolved and dispersed) in unit volume of the matrix and  $t$  is time (hours). In monolithic systems where excess drug is dispersed, the drug release rate increases with increasing drug concentration. The Higuchi expression is a good predictor of release rates from systems containing 5 to 10 volume per cent of active agent.

At higher drug concentrations, drug particles are in contact with each other and the drug is released by diffusion through the water filled pores [29, 30]. A second form of the Higuchi

equation describes the diffusion of drug from a porous matrix.

$$Q = \left[ \frac{D \varepsilon}{\tau} (2C_o - \varepsilon C_s) C_s t \right]^{1/2} \quad \text{Equation 2.3}$$

In this case the amount of drug released per unit area of the matrix,  $Q$ , depends on the diffusion coefficient of the drug in the matrix ( $D$ ), its solubility in the polymeric matrix ( $C_s$ ), the total amount of the drug (dissolved and dispersed) in unit volume of the matrix ( $C_o$ ), the porosity factor ( $\varepsilon$ ) and the tortuosity factor ( $\tau$ ) of the matrix and time ( $t$ ) [30, 31].

#### 2.1.4 Solvent activation controlled release

In a solvent activation controlled system, the active agent is dissolved or dispersed within a polymeric matrix or is surrounded by a polymer and is generally not able to diffuse through the matrix. Permeation of the moving dissolution medium through the polymer controls the release behaviour of drugs from these systems [30, 32, 33]. Solvent controlled systems can be divided in two types; osmotic and swelling controlled systems. Drug release from the swelling polymer follows Fick's law, when penetration of water into the polymer is rapid as compared to drug diffusion, whereas non-Fickian diffusion is achieved when drug diffusion and the solvent induced relaxations in the polymer are within the same range. When drug diffusion is rapid compared to the constant rate of solvent induced relaxation and swelling in the polymer, zero-order drug release is achieved and drug release is referred to as Case II transport [30]. An osmotic system is constructed by enclosing a drug in a semi-permeable membrane equipped with an orifice. The release rate of drug is governed by the nature of the membrane and the osmotic activity of the drug core. A constant release is maintained as long as the drug core remains saturated [33].

### 2.1.5 Biodegradable systems

The mechanism of biodegradation and drug release from biodegradable controlled release systems can be described in terms of three basic parameters. Firstly, the type of the hydrolytically unstable linkage in the polymer affects the design of the system and next, the position of the labile group in the polymer is important. Secondly the way the biodegradable polymer degrades, either at the surface or uniformly throughout the matrix, affects the device performance substantially. The third significant factor is the device design. The active agent may be covalently attached to the polymer backbone and is released as the bond between drug and polymer cleaves. The active agent may also be dispersed or dissolved into a biodegradable polymer matrix in the same way it is in a monolithic system made from non-biodegradable polymer and the release is controlled by:

- Diffusion
- A combination of diffusion and erosion
- Solely by biodegradation of the matrix [30, 34]

Biodegradable polymers are divided in homogenous (bulk) and heterogeneous (surface eroding) degrading polymers. These mechanisms are the extreme cases and most biodegradable polymer systems constitute a combination of the two types of mechanisms [30, 34]. Degradation is the process of polymer scission by the cleavage of bonds in the polymer backbone. Degradation leads to size reduction of the polymer chains. Erosion is the mass loss of the polymer matrix [34-35].

Homogenous (bulk) degradation appears to be the most common polymer degradation mechanism, where the polymer degrades homogeneously throughout the matrix. The

hydrolysis of bulk degrading polymers usually proceeds by losing molecular weight at first, followed by loss of mass in the second stage when the molecular weight has decreased to 15 000 g/mol or less [36]. The biodegradation rate can be altered by changing the composition (but not the size or the shape) of the polymer [37-38].

Drug release from a matrix undergoing homogenous degradation may be governed by the equations derived from simple diffusion-controlled systems if the drug diffuses rapidly from the device before degradation of the matrix begins. However, bulk degradation causes difficulties in the control of drug release, because the release rate may change as the polymer degrades. As the polymer begins to lose mass, the release rate accelerates because it is determined by a combination of diffusion and simultaneous polymer erosion [39-40]. The bulk degrading polymers most extensively studied are poly(esters), such as copolymers of poly(lactic acid) and poly(glycolic acid).

Surface eroding systems (heterogeneous erosion) lose material from the surface and the erosion rate is dependent on the surface area and the geometry of the device, i.e. the radius to thickness ratio controls the matrix erosion time, rather than the volume of the polymer matrix [36, 41-42]. The molecular weight of the polymer generally does not change significantly as a function of time [30]. Achieving surface erosion, however, requires that the degradation rate of the polymer matrix surface be much faster than the rate of water penetration into the matrix [25].

Zero order drug release is obtained with surface erosion controlled systems such as poly(anhydrides) or poly(orthoesters). The surface eroding system device design is made

easier due to the fact that release rates can be controlled by changes in system thickness and total drug content. In 1976, Hopfenberg and co-workers [43] developed a general mathematical equation for drug release from surface degrading slabs, spheres and infinite cylinders. This model, described in equation 2.4, assumes that the actual erosion process is the rate-limiting step and that the drug release occurs from the primary surface area of the device without seepage from the matrix.

$$\frac{M_t}{M_\infty} = 1 - \left(1 - \frac{k_0 t}{C_0 a}\right)^n \quad \text{Equation 2.4}$$

$M_t/M_\infty$  is the fractional released amount of drug,  $C_0$  is the initial concentration of the drug in the matrix (mole/dm<sup>3</sup>),  $a$  is the initial radius for a sphere or cylinder,  $k_0$  is the zero order rate constant for surface erosion and  $n$  is the shape factor. A shape factor that was defined in the equation by Hopfenberg, has in subsequent studies been applied to other geometrical forms, such as squares and half-spheres [44]. Katzhendler stated that the erosion rates are different in the radial and axial directions [41]. Drug release from a surface-eroding polymer may be controlled solely by erosion of the polymer matrix and the release of drug is constant provided that the surface area of the matrix and the drug concentration remain constant during the drug release period [31]. However, the surface area decreases as the implant is eroded, with a consequent decrease in the release of drug. Consequently, a geometry that does not change its surface area as a function of time is required to attain more uniform and zero order release [26].

True surface erosion where matrix mass loss is equal to the drug release rate is difficult to achieve and often diffusion of the drug molecules may still be rate limiting. For highly water-



soluble drugs especially, the release rate is controlled mainly by diffusion through the matrix, whereas the erosion process controls the release rate of low water-soluble drugs. Thus, the release rate may be a combination of erosion control (zero-order) and diffusion control (square root of time kinetics) [45].

### **2.1.6 Empirical equation for describing drug release**

To simplify the analysis of controlled release data from polymeric devices of varying geometry, an empirical, exponential expression was developed to relate the fractional release of drug to the release time [46-47].

$$\frac{M_t}{M_\infty} = kt^n \quad \text{Equation 2.5}$$

Where  $M_t/M_\infty$  is the fractional solute release,  $t$  is the release time (hours),  $k$  is a constant and  $n$  is the exponent characteristic of the release mechanism [46-47]. This equation applies until 60% of the total amount of drug is released. It predicts that the fractional release of drug is exponentially related to the release time and it adequately describes the release of drug from slabs, spheres, cylinders and discs from both swellable and non-swellable matrices.

## **2.2 Introduction to mechanisms involved in bacterial colonisation (fouling) of surfaces in the paint industry**

Fouling can be defined as the undesirable accumulation of micro-organisms, plants and animals on artificial surfaces immersed in seawater [48] or any other media where the bacterium lives. In the marine environment, all surfaces are affected by the attachment of such fouling organisms. Nevertheless, this attachment process is of vital importance for some

marine life: larvae of invertebrates and spores of algae need to quickly find and bind to a surface in order to complete their life history [49]. Barnacle larvae swim around freely in the water column but in order to complete the transition to adult life, the cyprid larvae (*Balanus Amphitrite*) must attach to a hard surface [49]. Traditionally, the fouling process has been considered to consist of four general stages, [50]:

- Biochemical conditioning: within minutes of its immersion, a clean surface adsorbs dissolved organic molecules such as polysaccharides, proteins and proteoglycans (and possibly inorganic compounds). This adsorption causes the formation of a conditioning film and is essentially governed by physical forces such as Brownian motion, electrostatic interaction and van der Waals forces [51, 52].
- Bacterial colonisation: bacteria and single cell diatoms rapidly settle on this modified surface, again mainly by a physical process [52, 53]. This process takes between 1 to 24 hours
- Unicellular eukaryotic settlement: the transition from a microbial biofilm to a more complex community comprising primary producers, grazers and decomposers (algal spores, marine fungi and protozoa, etc) [48]
- Settlement and growth of larger marine invertebrates together with the growth of macroalgae (seaweeds) [54].

Those phases do not necessary occur sequentially during the fouling process [55] and depend on conditions in the environment such as levels of salinity, temperature and diversity of species. However, adverse effects caused by this biological settlement, in the case of ships, are well known (Figure 2.2). Fouling organisms such as barnacles, mussels and algae are a problem for many boat owners. These organisms attach to the hull, increasing the friction of

the boat in the water. This, in turn, lowers speed, impairs manoeuvrability and ultimately increases fuel consumption [56]. It is estimated that fuel consumption increases 6% for every 100  $\mu\text{m}$  increase in the average hull roughness caused by fouling organisms [57-60]. This microbial spoilage costs around 25 billion Euros (£18 bn) annually to the European Union [61]. In order to prevent the attachment of fouling organisms, paints containing bioactive molecules (biocides) are used to protect pleasure, commercial and military boats.



Figure 2.2: Examples of heavily fouled hulls [48]

### 2.3 Biocides in the coating industry

Mariners from ancient times were aware of the problems resulting from fouling organisms. The ancient Phoenicians and Carthaginians were said to have used pitch and possibly copper sheathing on their ship's bottoms, while wax, tar and asphaltum were used by other ancient cultures [62, 63]. The Greeks and Romans both used lead sheathing, which the Romans secured by copper nails. Copper has been in general use by the British Navy since 1780 [18].

From these early beginnings, antifouling paints incorporating copper salts developed. Copper binds to sulphur containing cell constituents, leading to a variety of responses associated with heavy metal toxicity [49]. The introduction of iron ships in 18<sup>th</sup> century lead to the withdrawal of copper sheathing in antifouling coatings [64].

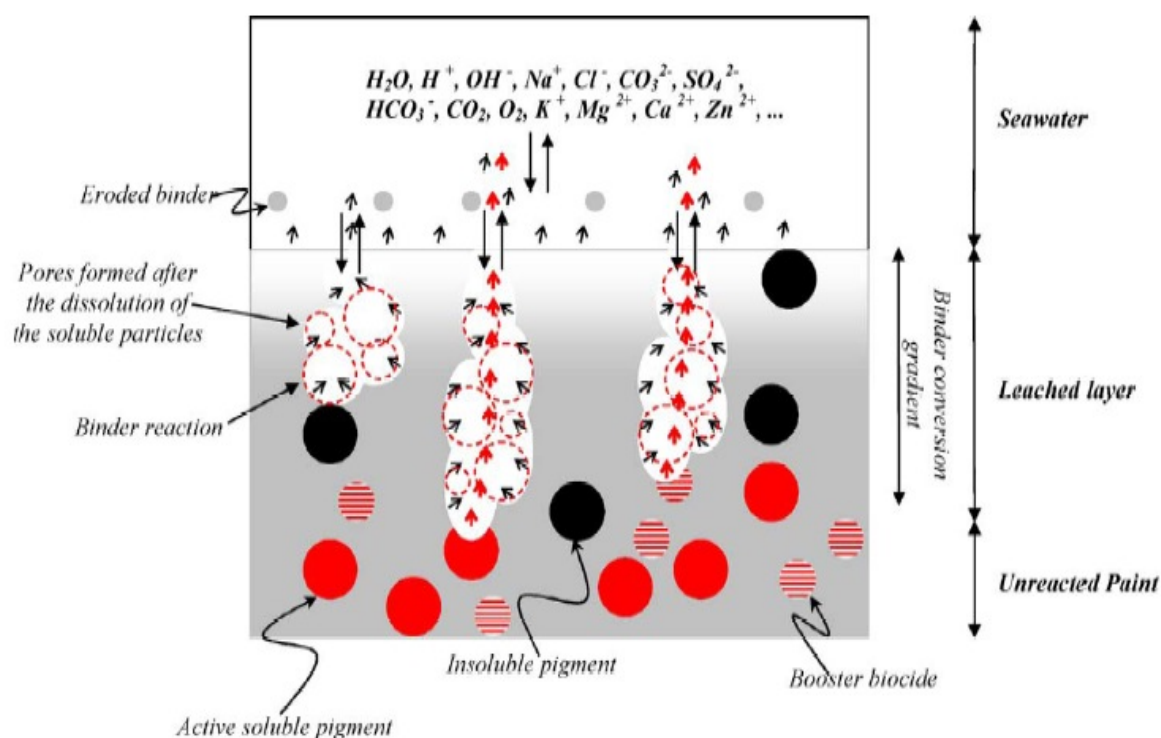


Figure 2.3: Schematic illustration of the behaviour of a biocide-based antifouling system exposed to seawater [48]

In the 1800s, a variety of paints were developed based on the idea of dispersing a toxicant in a polymeric vehicle. Copper oxide, arsenic, and mercury oxide were popular antifoulants. Solvents included turpentine oil, naphtha, and benzene. Linseed oil, shellac varnish, tar, and various kinds of resin were used as binders [62, 63]. But it was not until the mid 1950s that Van de Kerk and co-workers reported on the possibilities of the broad-spectrum high-toxicity Tributyltin (TBT) in antifoulant coatings [65]. By the early 1960s, the excellent antifoulant

properties of TBT were discovered and commercialised. A wide range of other compounds is used as biocides in antifouling coatings today, including cuprous oxide, Irganol 1051, diuron, SeaNine 211 and Dichlofluanid. The release of these biocides from the paints is markedly affected by seawater conditions such as temperature and salinity [66].

Throughout the history of navigation, Tributyltin self-polishing copolymer paints (TBT-SPC) have been the most successful in combating biofouling on ships. Around 70% of the world fleet use these paints [67, 68], and this has led to important economic benefits [69, 70]. TBT saves the US Navy an estimated \$US 150 million annually [71]. Nevertheless, biocides are essentially toxic to the environment and affect non-target organisms [56]. Studies have shown that Irganol and Diuron persist in the environment [72, 73]. These 2 compounds, together with TBT and copper, have had damaging effects on the reproduction and growth of various marine life forms [74, 75] and can pass through the food chain. These studies have led the Marine Environmental Protection Committee (MEPC) of the IMO (International Maritime Organisation) to recommend a global ban on the use of TBT and the withdrawal of other toxic compounds for use in marine coatings [76].

A new generation of generic substances, based on the isothiazolinone structure, are being developed and introduced by paint manufacturers. These biocides are said to be electrophilically active and readily react with their surrounding environment, thus facilitating their catabolism [77]. Two of those isothiazoline biocides were used in this study, and they were: 2-Octyl-4-isothiazolin-3-one (OIT), and the blend of 2-Methyl-4-isothiazolin-3-one (MIT) and 5-Chloro-2-Methyl-4-isothiazolin-3-one (CIT), referred to as CIT/MIT (see Figure 2.4).

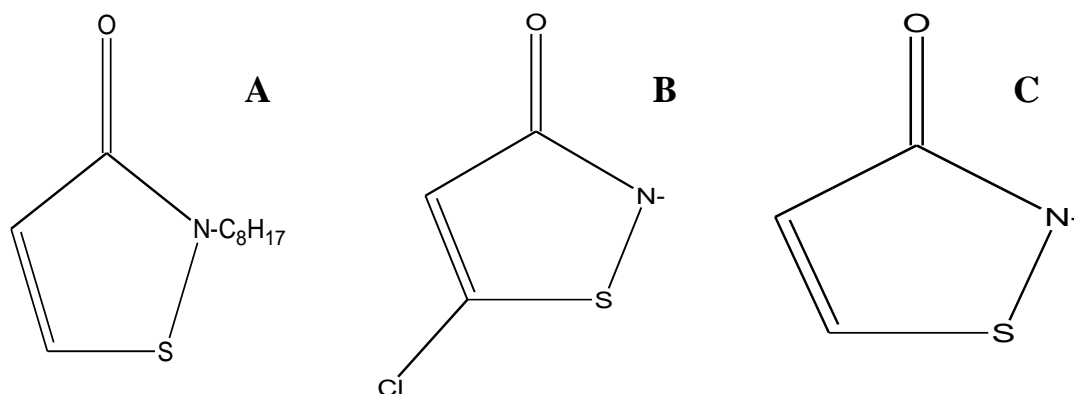


Figure 2.4: Biocides used in this study: OIT in A, and the blend of MIT and CIT, respectively in B and C (with a methyl CH<sub>3</sub> attached to the nitrogen on B and C)

## 2.4 Roles of Minerals

The impregnation of powders by active compounds (often using spray drying or fluidised bed agglomeration) has also become a very attractive process in the past few years. It has been shown to be appropriate for food ingredients as well as for chemicals, drugs and cosmetics [78]. It is important, using this technique, to build a barrier between the components in the particle and the environment for protection against oxygen, light, and water. The efficiency of protection and controlled release depends on the composition and structure of the wall and operating conditions (temperature, humidity, pH and pressure) during the production of the particle [78].

## 2.5 Biocides and minerals in antifouling coatings

Minerals could be used to carry biocides in order to limit the bioavailability of these

compounds in seawater and shield them from the ill effects of environmental exposure. Montmorillonite has been used to carry the herbicides Hexazinone [79] and Sulfentrazone [80] for slow release in soil. Clay-liposomes have also been used to carry herbicides and reduce their leakage in groundwater [81]. Hydrotalcite-like anionic clays have been intercalated with anti-inflammatory agents for controlled-release formulations [82]. The isothiazolinone-based biocides mentioned above have been encapsulated within a protective framework (silica and zeolites used as carriers), and their release has been controlled by way of varying the pore size of these carriers [79]. The silica carrier has many functional groups involved in the interaction with the biocide. Broadly speaking silica is considered to be a polymer of silicic acid consisting of inter-linked  $\text{SiO}_4$  tetrahedra. This construction terminates by the formation of siloxane bridges ( $\text{Si-O-Si}$ ) or silanol groups ( $\text{SiOH}$ , in Figure 2.5). The surface chemistry of silica is dominated by the nature, distribution and accessibility of these structures [83–85]. Siloxane sites may also be differentiated as:  $(\text{-SiO-})_2$ ,  $(\text{-SiO-})_3$ ,  $(\text{-SiO-})_5$ , or  $(\text{-SiO-})_6$  rings. Silanol sites may be distinguished as: isolated (single or free) silanols; vicinal (or bridged) silanols, which are characterised by their ability to hydrogen bond; and geminal silanols, which consist of two hydroxyls attached to the same silicon atom and as such are too close to mutually hydrogen bond. These functional groups are believed to be involved in the interaction between the mineral and the biocide.

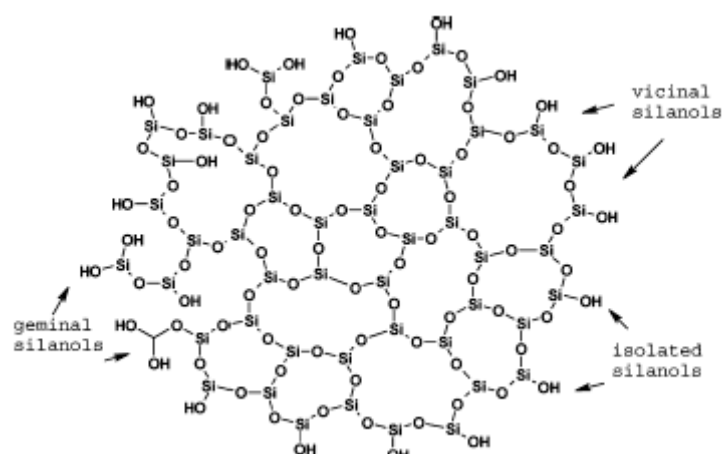


Figure 2.5: Functional groups present on the surface of porous, amorphous silica [86]

The highly porous silica can be “filled” with the biocides in its core, with the release being controlled by the pore size of the mineral (see Figure 2.6). This technique can work with both the amorphous and the irregular shape silica.

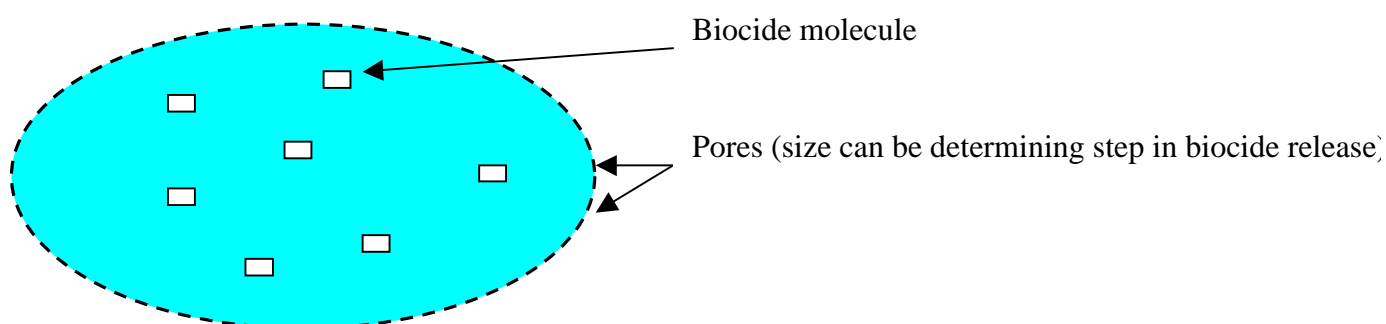


Figure 2.6: Representation of porous silica, with possible pathway for biocide release

Rod-shape minerals such as halloysite are normally hollow cylinders containing air <sup>[78]</sup>. This air can be removed under vacuum, and replaced with the biocide for slow release, with the length of the cylinder slowing down this release (see figure 2.7).



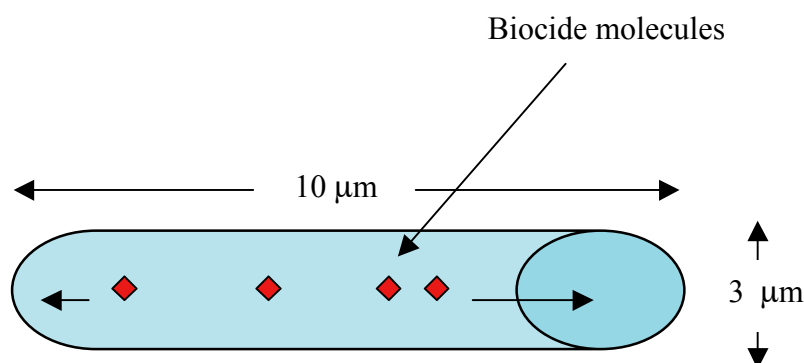


Figure 2.7: Representation of a Halloysite mineral with pathway of intercalated biocides

The biocide can equally be inserted within the plates of platy clays such as Kaolin and Montmorillonite (see figure 2.7). The tortuosity of the space between the plates could slow down the release of the encapsulated biocides.



Figure 2.8: Possible pathway for the release of the isothiazoline biocides in the platy minerals, with (A) small and (B) larger particle size

Despite these advances in research on coatings, there is an ongoing trend to find the next generation of biocide-free coatings (both antifoulant and other domestic coatings). The US paint giant Poseidon is currently developing compounds such as Frescalin and Menthridan (mostly from seaweeds) that employ a repellent, rather a toxic mechanism, in their

antifouling coatings (these substances are believed to interact with calcium channels on the organism's cilia to prevent its attachment). These compounds are still at the early stage of development and more time is needed to assess their effectiveness.

In Chapter 3, the methods of characterisation of the minerals used in this project are presented, together with the biocides selected (and the reasons for the choice of these biocides). The advantages (and some of the disadvantages) of these methods are also discussed.

The scientific literature reviewed suggested there was little work done in the area of controlled release of drugs or other compounds using minerals as carriers, especially platy clays with low surface area (ranging from 10 to 40 m<sup>2</sup>g<sup>-1</sup>). Controlled drug delivery using minerals could, however, have advantages in many fields if a reliable release system is found, and these could include:

- No rejection by the body of the mineral carrier used, as no antibody will be made against it.
- Drugs “sequestered” within a mineral framework can still be protected from enzymatic or acidic degradation in the body (depending on the shape of the mineral used).
- In a paint, the mineral will act both as a rheology enhancer and a carrier of the compound of interest.
- The compounds of interest can be released at a desired rate, thus reducing wastage linked to environmental pollution and increased costs to manufacturer.

# **CHAPTER THREE**

## **MATERIAL CHARACTERISATION**

### **3.1 Introduction**

Nine different minerals and two isothiazoline biocides were used in this study. These materials were characterised by a variety of techniques. The surface areas of the minerals were measured by the B.E.T. nitrogen method; the crystallography, chemical composition and morphology of the same mineral powders were obtained by XRD, XRF and SEM methods respectively. The minerals' particle size analysis was obtained using Light Scattering. The adsorption of the isothiazoline biocides onto the minerals was studied by measuring the adsorption isotherms using High Performance Liquid Chromatography (and sometimes by UV-Vis), while Flow Microcalorimetry was used to determine the strength of adsorption of the biocide on the surfaces of the mineral powders.

### **3.2 Minerals used and characterisation methods**

The minerals used in this study are shown in Table 3-1.

Table 3.1: General characteristics of minerals used in this study

Trade name	Mineral	General composition	Surface area m <sup>2</sup> /g	Shape
Infilm 939	Kaolin	Al <sub>2</sub> O <sub>3</sub> . 2SiO <sub>2</sub> . 2H <sub>2</sub> O <sup>(*)</sup>	22	Platy
Supreme	Kaolin	Al <sub>2</sub> O <sub>3</sub> . 2SiO <sub>2</sub> . 2H <sub>2</sub> O	17	Platy
NPD 16A	Kaolin	Al <sub>2</sub> O <sub>3</sub> . 2SiO <sub>2</sub> . 2H <sub>2</sub> O	23	Platy
Suprex	Kaolin	Al <sub>2</sub> O <sub>3</sub> . 2SiO <sub>2</sub> . 2H <sub>2</sub> O	25	Platy
MCBP	Montmorillonite	Na <sub>0.2</sub> Ca <sub>0.1</sub> Al <sub>2</sub> Si <sub>4</sub> O <sub>10</sub> (OH) <sub>2</sub> (H <sub>2</sub> O) <sub>10</sub>	39 <sup>(**)</sup> & 800 <sup>(***)</sup>	Platy
T-38	Calcium Silicate	Ca <sub>2</sub> SiO <sub>4</sub>	122	Irregular
Celtix	Diatomaceous Earth	SiO <sub>2</sub> (mostly)	24	Irregular
Carplex CS-5	Amorphous Silica	SiO <sub>2</sub>	150	Amorphous
NZ Halloysite	Halloysite	Si <sub>2</sub> Al <sub>2</sub> O <sub>5</sub> (OH) <sub>4</sub> .2H <sub>2</sub> O	50	Tubular

<sup>(\*)</sup>: General formula of Kaolin, with its principal component, Kaolinite, having the formula Al<sub>2</sub>Si<sub>2</sub>O<sub>5</sub>(OH)<sub>4</sub>

<sup>(\*\*)</sup> and <sup>(\*\*\*)</sup>: surface area of Montmorillonite as a dry and wet powder respectively.

The first four platy clays in Table 3.1 (with the exception of infilm 939, which was obtained from Imerys Georgia, USA) were produced and processed by Imerys in Cornwall, England, and are regularly used in the paper and paint industries as rheology modifiers. T-38 (calcium silicate) and Celtix (diatomaceous earth) were obtained from World Minerals, a subsidiary of Imerys, based in California, USA. The halloysite was received from Imerys New Zealand. Carplex CS-5 is produced by Degussa, Japan. MCBP (montmorillonite) was obtained from Southern Clay Products in the USA. These minerals were selected because of differences in their surface areas, chemical compositions and shapes, as described in Table 3-1. In addition

to those differences, their industrial functions also made them candidates of interest in this study:

- Carplex is sold by Degussa primarily as a chelator agent in breweries, to remove unwanted compounds in beer filtration.
- Celtix and T-38 are both sold by World Minerals and are used in filtration.
- New Zealand halloysite is said to have controlled release characteristics because of its tubular shape [1,2].
- Suprex was processed without the use of a chemical dispersant.

### **3.2.1 Crystallography analysis by XRD method**

At Imerys, the XRD equipment used was a Philips PW1710, and is generally used in conjunction with XRF. It is a powerful non-destructive technique for characterizing crystalline materials and provides a mineralogical breakdown of substances such as mica, feldspar and kaolinite. Samples are analyzed as powders with grains in random orientations and the technique can provide information on structures, phases, crystal orientations and other structural parameters such as average grain size, crystallinity, strain and crystal defects. XRD peaks are produced by constructive interference of monochromatic beam scattered from each set of lattice planes at specific angles. The peak intensities are determined by the atomic decoration within the lattice planes. Consequently, a X-ray diffraction pattern is the fingerprint of the periodic atomic arrangements in a given material. An on-line search of a standard database for X-ray powder diffraction pattern enables quick phase identification for a large variety of crystalline samples. Advantages associated with X-ray diffraction include:

- Very quick identification of materials
- Minimum or no sample preparation
- Large library of crystalline structures
- Computer-aided material identification
- Technique is completely non-destructive and analysis performed at ambient conditions

The limitations associated with XRD include the difficulty to characterise a sample if more than one phase is present, and difficulty in orientation if no crystals are present.

### **3.2.2 Chemical composition analysis by X-ray fluorescence method**

XRF is one of the most widely used instrumental methods at Imerys for the determination of the chemical composition of various minerals, and is based on fluorescence effect (XRF equipment used at Imerys is the Panalytical Magix Pro). Samples to be analysed are compressed powder pellets or fused glass discs and exposed to x-ray radiation (generally between 10 and 100 kVolts), leading to the ionisation of their component atoms. The ionisation consists of the ejection of one or more electrons from the atom and occurs if the atom is exposed to radiation with energy greater than its ionisation potential. This ionisation creates “vacancies” or “holes” in the inner electron shells of the sample atoms and renders the electronic structure of the atom unstable. These vacancies are filled with electrons from higher energy levels. The de-excitation processes that follows (with atoms returning to the ground state) lead to the emission of X-rays, which are characteristic for the emitting element. Using this technique, one can determine the atomic composition of a given sample. The term fluorescence is applied to phenomena in which the absorption of higher-energy

radiation results in the re-emission of lower-energy radiation. Advantages associated with XRF include:

- XRF is ideal for the measurement of most elements (major and minor), and is thus a preferred technique for whole rock characterisation.
- The fusion technique minimises particle size effects that could otherwise cause problems with the measurement process.
- Numerous trace elements can also be determined from the same fused disc, e.g. Y, Nb, Zr. The discs themselves can be stored indefinitely.

XRF nevertheless present some limitations, including:

- Fluorescent X-rays can be easily absorbed by the sample itself (self-absorption). It is therefore important that the sample matrix matches as closely as possible to that of the calibration standards. If this is not possible, then empirical correction factors must be applied.
- Lighter elements are not easily determined by XRF as they have inherently less sensitivity. The lower energy XRF emission from these elements means that they have less penetrating power and hence less sensitivity.
- Sample fusion enhances the XRF measurement technique by minimising particle size effects but, sometimes, refractory minerals dissolve slowly and do not give satisfactory fusion.

### **3.2.3 Powders' morphology detection by Scanning Electron Microscopy (SEM)**

Electron Microscopes were developed due to the limitations of Light Microscopes, which are



limited by the physics of light to 500x or 1000x magnification and a resolution of 0.2 micrometers. They function exactly as their optical counterparts except that they use a focused beam of electrons instead of light to create an image of the specimen and gain information as to its structure and composition. The SEM equipment used at Imerys is the Jeol 6700F Field Emission Scanning Electron Microscope. The basic steps involved in all electron microscopes are:

- A stream of electrons is formed by the electron source and accelerated toward the specimen using a positive electrical potential
- This stream is then confined and focused, using metal apertures and magnetic lenses, into a narrow, focused, monochromatic beam.
- This beam is focused onto the sample using a magnetic lens
- Interactions occur inside the irradiated sample, affecting the electron beam

These interactions and effects are detected and transformed into an image.

An electron microscope can help the user determine the following information:

- Topography - The surface features of an object or "how it looks", its texture; direct relation between these features and materials properties (hardness, reflectivity...etc.)
- Morphology - The shape and size of the particles making up the object; direct relation between these structures and materials properties (ductility, strength, reactivity...etc.)

Electron microscopes are nevertheless expensive to buy and maintain. They are dynamic rather than static in their operation: requiring extremely stable high voltage supplies, extremely stable currents to each electromagnetic coil/lens, continuously-pumped high/ultra-

high vacuum systems and a cooling water supply circulation through the lenses and pumps. Sample preparation time is also a lengthy process and there is a possibility of sample damage during the preparation. Samples also need to be viewed in vacuum to avoid scattering electrons by air molecules. The main advantage of SEM over light microscopy is the increased depth of field. Small object and particles that would normally escape the field of view of light microscope can be imaged on the SEM.

### **3.2.4 Particle size analysis by Light Scattering (using the Malvern Mastersizer)**

Extenders (like clay minerals) are manufactured in a wide range of finenesses and are used in the paint industry to fulfill specific requirements in very different coating systems. To cover the requirements of paint manufacturers, many different qualities are manufactured in order to accommodate some or all of the most important properties of coatings listed below:

- Rheology
- Opacity
- Suspension properties
- Packing density
- Storage stability
- Hold out / Leveling
- Density
- Sanding properties
- Gloss
- Wet scrub resistance
- Surface smoothness
- Corrosion resistance
- Brightness
- Exterior durability

The paint chemist can influence these properties by correctly selecting extenders with the appropriate granulometry. The granulometry or particle size distribution of an extender is

characterised in general by the particle size distribution curve illustrated in Figure 3.2. Using the Malvern Mastersizer ATM13 at Imerys, one can determine the weight mean particle size of various minerals in solution. This instrument uses the principles of Mie scattering with a low powered Ne/He laser. The suspension (containing the particles) is illuminated using a parallel beam of light (see Figure 3.1). The scattered light is collected and focused onto a detector at the focal point of the lens. The distribution of scattered light can then be converted, mathematically, into a particle volume distribution. <sup>[21, 35]</sup>

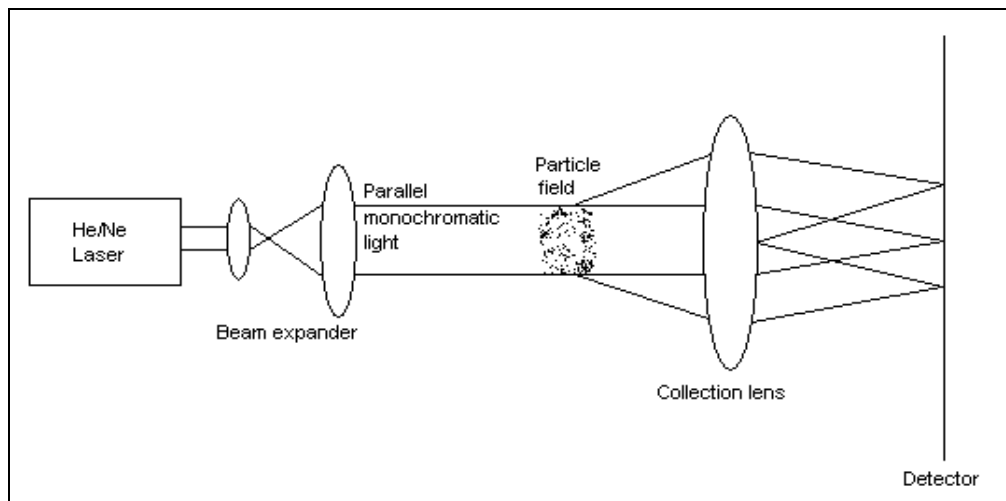


Figure 3.1: Particle size measurement as used in Malvern instruments [87]

The particle diameters are calculated from the measured volume of the particle, found by assuming a spherical shape. This is disadvantageous with kaolin, as particles are usually flat platelets and so the size recorded for a particle is dependent on the angle at which the beam of light hits each particle [87].

The most important points are: The “Top Cut” ( $d_{98}$ ) which gives the diameter of extender

particle so that at least 98 % of the particles by weight are finer i.e. in principle the coarsest particle present. The “Mean Particle Size” ( $d_{50}$ ) representing the size of particle so that 50 % of the particles by weight are coarser or finer (see Figure 3.2).

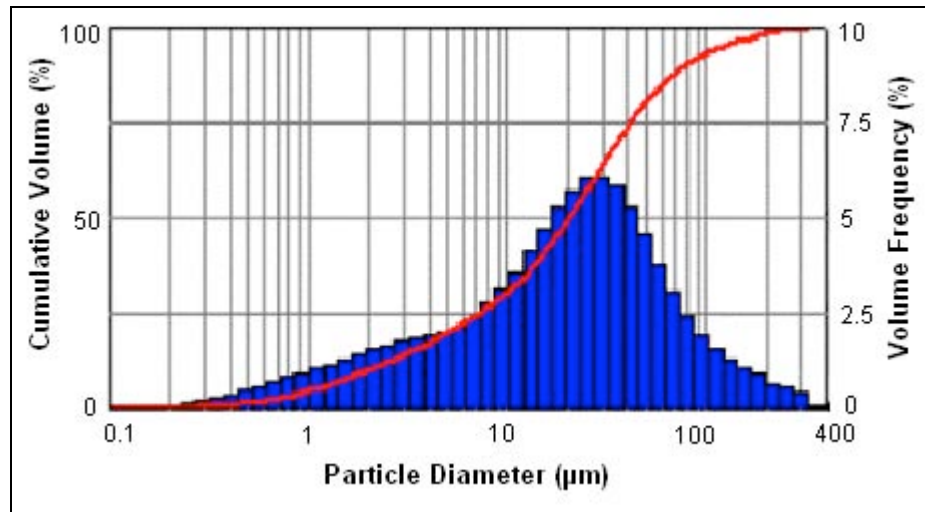


Figure 3.2: Typical particle size distribution curve [88]

The scattered light technique provides a fast response time, which is advantageous in many situations. Problems are encountered with kaolin suspensions at high solid volume fractions. These fractions are so opaque they must be diluted in order to allow the scattered light to pass through them. Studies have shown that a minimum of 5 to 10% of the laser light needs to pass through the sample in order to obtain reliable results.

### 3.2.5 Surface area measurement by B.E.T. (Brunauer Emmett and Teller)

Gas adsorption is the most widely used and accurate technique for total surface area measurements. Gas molecules of known sizes are condensed onto the unknown sample surface. By completely covering the surface and opening the pores of each particle with a

condensed gas the surface area analyser can characterise the surface, including irregularities and pore interiors down to an atomic level. Nitrogen is often the gas used as its molecular size is well established, it is inert and is available in high purity at a reasonable cost. The “outgassed” sample under high vacuum in its sample tube is immersed in a coolant bath of liquid nitrogen at  $-195^{\circ}\text{C}$ . At this stage the sample is ready to attract gas molecules onto it when they are admitted to the sample tube.

At Imerys, the specific surface area of powders is measured using the Tristar equipment manufactured by Micrometrics, Georgia, USA. This area is determined using measurements made at three partial pressures. Nitrogen is used as the adsorbate in conjunction with helium as the carrier. All samples are out-gassed at  $180^{\circ}\text{C}$  before testing. The specific surface area is determined by measuring the quantity of nitrogen gas that is adsorbed as a monomolecular layer on the test sample. The adsorption is carried out at temperatures close to the boiling point of the adsorbate. This is achieved by immersing the test sample in a Dewar flask containing liquid nitrogen. Under these specific conditions the area covered by a molecule of gas is accurately known. Thus, the area of the test material may be determined by measuring the number of molecules adsorbed. A sensitive pressure transducer measures the change in pressure occurring in the sample chamber and thereby quantifies the volume adsorbed. At Imerys, samples to be analysed are prepared by the Analytical department as follow:

- If the sample is a powder, between 5 and 10 g are transferred to the oven and dried.
- If the sample is a slurry, ensure that it is thoroughly mixed either by stirring it with the bench stirrer, mixing it on the rotating rollers or by shaking its container vigorously.

- If the sample is a deflocculated slurry, pour sufficient to give about 10 g dry weight equivalent into a small dish and place it in the oven.
- If the sample is a flocculated slurry, filter sufficient to give between 5 g and 10 g dry weight equivalent through a fine hardened filter paper. (At this stage sample weight is not critical). Place the cake in the oven and dry it.

After this drying period, the sample is remove from the oven and dispersed adequately by crushing it with a pestle and mortar. 1.5 g of this test material is then weighed and placed into the sample tube, which is in turn placed into the heating element of the Tristar (set at 180°C). Nitrogen and hellium cylinders are then turned on at pressure of approximatly 1 bar. At the end of this heating period, the sample tube and its content are transferred to the “cool” zone of the FlowPrep equipment to allow the tube to cool to a touch. After this cooling period, the filler is gently placed into the sample tube, ensuring that the Dewar flask if filled with liquid nitrogen. The flask is then placed on the intrument’s platform, and measuremnet can start. At the end of the measurement, the specific surface area is expressed as m<sup>2</sup>/g and shown on the printout of the computer attached to the equipment. The test is ISO9001 compliant, and its precision is  $\pm 3$  % of the value of the test material.

### 3.3 Biocide selection and measurement

The biocides used in this study were obtained from Clariant, UK, and were: 2-octyl-4-isothiazolin-3-one (OIT) and the blend of 5-chloro-2-methyl-4-isothiazolin-3-one, and 2-methyl-4-isothiazolin-3-one (CIT/MIT). The blend of CIT/MIT was in a ratio of 3 to 1 by volume. These biocides represent a new generation of generic substances based on the isothiazoline chemistry, and are being developed and introduced by major paint manufacturers. They are being used in paints to replace the more traditional biocides such as silver, mercury, tributyltin (TBT), irganol, diuron and copper, which have had damaging effects on the environment and on the reproduction and growth of various marine life forms.

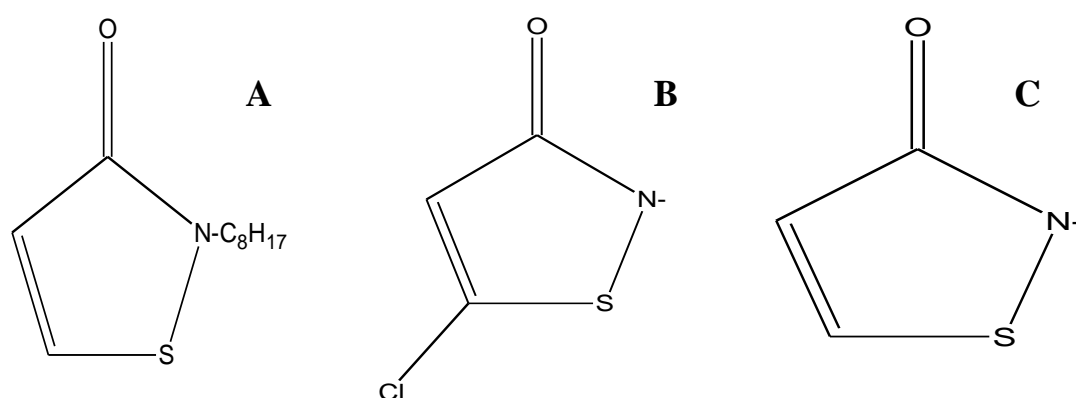


Figure 3.3: Biocides used in this study: (OIT), (CIT) and (MIT) respectively in A, B and C (with a methyl CH<sub>3</sub> attached to the nitrogen on B and C)

#### 3.3.1 Biocide selection

The isothiazoline biocides used were chosen because they offer many performance advantages over other biocides. These advantages include the following:

- They have a broad-spectrum antimicrobial activity and can control the growth of Gram-negative and Gram-positive bacteria, and fungi (molds and yeasts).
- They are economical. The required concentrations generally are more cost-effective than other commercial preservatives.
- They are formaldehyde-free, and do not contain or generate formaldehyde (formaldehyde is very toxic when inhaled or present in the food chain, and carcinogenic).
- They offer low use levels (excellent microbe control at low concentrations). Typical use levels are 6-15 part per million of the combined active components (0.04-0.10% of the product as supplied, volume/volume).
- They have low toxicity as their half-lives are lower than other biocides (see Table 3.1).
- Excellent compatibility with common formulation ingredients.
- Excellent stability over a wide pH range (2 to 8.5).
- They are easy to formulate and are supplied as an easy-to-use aqueous solution.
- No side effects: the biocides will not adversely affect a product's physical properties or performance.
- They are environmentally friendly and do not persist in the environment; their breakdown products are essentially benign.



Table 3.1: Environmental input parameters of isothiazoline biocides and TBT (Source, World Health Organisation, 1990)

Parameters	Isothiazolines	Tributyltin (TBT)
Half life (sea water)	1 day	9 days
Half life (sediment)	0.04 day	162 days
Bio-concentration factor (*)	14	10,000
Adsorption coefficient (**)	1666	8,000

(\*): Concentration of a chemical in a tissue per concentration in water; accumulation of pollutants through chemical partitioning from aqueous phase to organic phase

(\*\*): Mass of adsorbed substance per unit mass of adsorbent / concentration of substance in solution

### 3.3.2 Degradation of isothiazolines

Isothiazoline biocides are electrophilically active and readily react with their surrounding environment to facilitate their degradation. The isothiazolone molecule interacts with thiol groups in enzyme proteins (co-enzymes or redox cofactors, see Figure 3.4) in the cell, prohibiting the normal interaction of the enzyme (by inhibition of the active site of the enzymes). These enzymes are important in the biochemical cycles through which the cell obtains its energy. Therefore the cell slows and eventually dies (see Figure 3.4). The by-products of their degradation consist mainly of urea and carbonic acid, which are harmless to the environment.

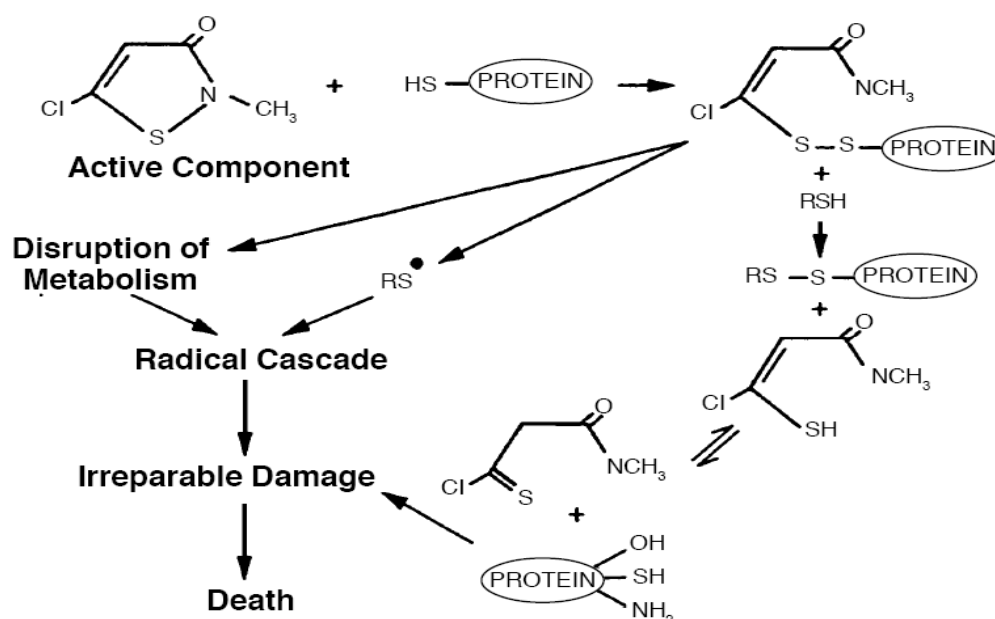


Figure 3.4: Thiol degradation of isothiazoline biocides [89].

The biocides can also interact with primary amines in redox cofactors (see Figure 3.5) Nicotinamide Adenine Dinucleotide (NAD) and Flavin Adenine Dinucleotide (FAD). These redox cofactors normally remove  $H^+$  ions from the Krebs cycle for ATP production (Adenosine Triphosphate, the energy of the cell). In pure aqueous solutions the isothiazoline ring opening is initiated by simple hydrolytic cleavage of the S-N bond, which is the reaction occurring in the presence of strong nucleophiles such as primary and secondary amines and particularly thiol derivatives.

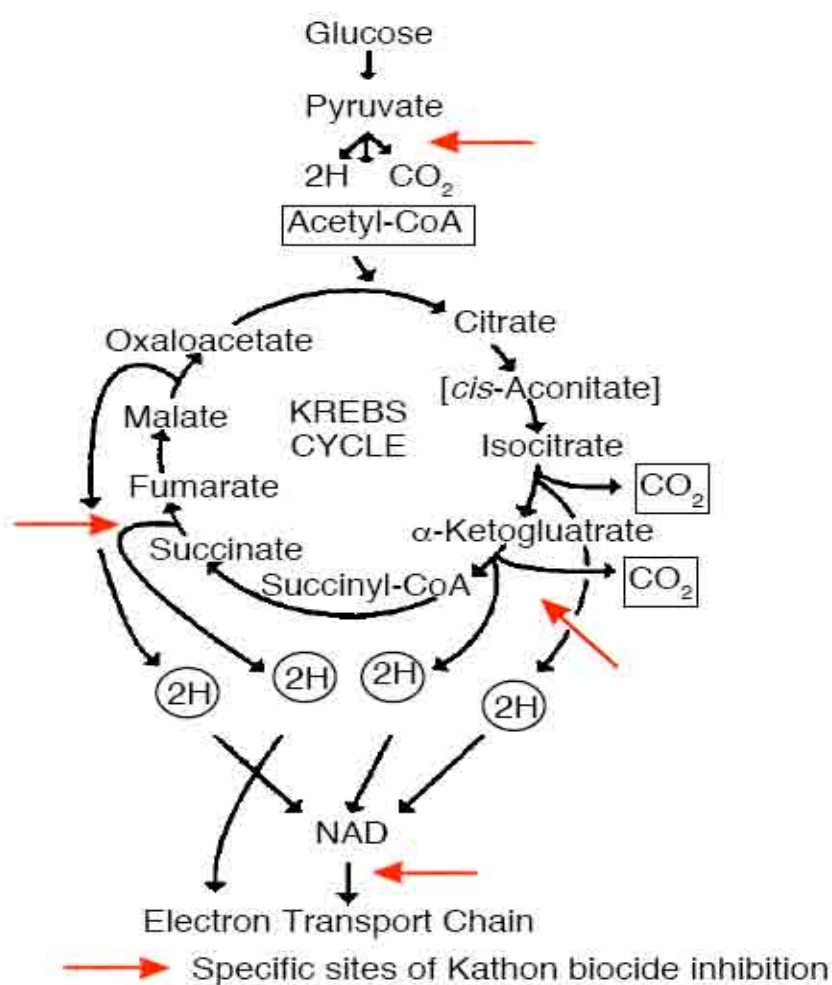


Figure 3.5: Sites of action of isothiazoline biocides in the Krebs cycle [89]

### 3.3.3 Concentration measurement by HPLC

High performance liquid chromatography (HPLC) is a form of column chromatography commonly used in biochemistry and analytical chemistry research laboratories. It is often referred to as high-pressure liquid chromatography and is used to separate components of a mixture by using a variety of chemical interactions between the substance being analyzed (analyte) and the chromatography column.

### 3.3.3.1 Principles of HPLC system

The basis of all forms of chromatography is the partition or distribution coefficient ( $K_d$ ), which is the way in which a compound distributes itself between two immiscible phases. For two immiscible phases A and B, the value of  $K_d$  is a constant at a given temperature and is given by the expression:

$$\frac{\text{Concentration in phase A}}{\text{Concentration in phase B}} = K_d \quad \text{Equation 3.1}$$

All chromatographic systems consist of:

- A stationary phase, which may be a solid, gel, liquid or a solid/liquid mixture that is immobilised
- A mobile phase, which may be liquid or gaseous and which flows over or through the stationary phase

In isocratic HPLC (one solvent system), the analyte is forced through a column of the stationary phase by pumping a liquid (mobile phase) at high pressure through the column. The analyte is introduced in a small volume to the stream of mobile phase (between 10 and 30  $\mu\text{l}$ ), and is retarded by specific chemical or physical interactions with the stationary phase as it traverses the length of the column. The amount of retardation depends on the nature of the analyte, stationary phase and mobile phase composition. The time at which a specific analyte elutes (comes out of the end of the column) is called the retention time ( $t_R$ , in min) and is considered a unique identifying characteristic of a given analyte. The retention volume ( $V_R$ , in ml) is the volume of mobile phase required to elute the analyte. These 2 parameters

are related by the flow rate,  $F_C$  (ml/min), of the mobile phase through the column:

$$V_R = t_R F_C \quad \text{Equation 3.2}$$

The use of pressure increases the linear velocity giving the components less time to diffuse within the column, leading to improved resolution in the resulting chromatogram. Common solvents used include any miscible combinations of water or various organic liquids (most commons are methanol and acetonitrile). Water may contain buffers or salts to assist in the separation of the analyte components, or compounds such as trifluoroacetic acid, which acts as an ion-pairing agent. In this study, the HPLC was used to quantify the biocide molecules in solutions after the adsorption/desorption processes (Chapters 5, 6 and 7).

### 3.3.4 Concentration measurement by UV-Vis

Ultraviolet (UV) and Visible (VIS) light can cause electronic transitions. When a molecule absorbs UV-VIS radiation, the absorbed energy excites an electron into an empty, higher energy orbital. The absorbance of energy can be plotted against the wavelength to yield a UV-VIS spectrum. Ultraviolet radiation has wavelengths in the range of 200-400 nm. Visible light has wavelengths in the range of 400-800 nm. Any species with an extended system of alternating double and single bonds will absorb UV light, and anything with colour absorbs visible light, making UV-VIS spectroscopy applicable to a wide range of samples.

UV-Vis spectroscopy has many uses including detection of eluting components in high performance liquid chromatography (HPLC), determination of the oxidation state of a metal centre of a cofactor (such as haeme in haemoglobin), or determination of the maximum

absorbance of a compound prior to a photochemical reaction. Most organic compounds that absorb UV-VIS radiation contain conjugated pi-bonds. Both the shape of the peak(s) and the wavelength of maximum absorbance can give information about the structure of the compound.

In analytical applications it is advantageous to measure the concentration of an analyte independent of the effects of reflection, solvent absorption, or other interference [Ref]. The Beer-Lambert law (also called the Beer-Lambert-Bouguer law) describes the linear relationship between absorbance and concentration of an absorber of electromagnetic radiation. The general Beer-Lambert law is usually written as:

$$A = \varepsilon_{\lambda} c l$$

**Equation 3.3**

where  $A$  is the absorbance,  $\varepsilon_{\lambda}$  is the molar extinction coefficient for the absorber at wavelength  $\lambda$  (in nm),  $c$  is the concentration of the absorbing solution in  $\text{mol.dm}^{-3}$ , and  $l$  is the path length through the solution (or thickness, in cm). Experimental measurements are usually made in terms of transmittance ( $T$ ), which is defined as:

$$T = \frac{P}{P_0}$$

**Equation 3.4**

where  $P$  is the power of light after it passes through the sample and  $P_0$  is the initial light power. A 100% value for  $T$  represents a totally transparent substance, with no radiation being absorbed, whereas a zero value for  $T$  represents a totally opaque substance, or complete absorption. The relation between  $A$  and  $T$  is:

$$A = -\log(T) = -\log\left(\frac{P}{P_0}\right) \quad \text{Equation 3.5}$$

### 3.3.4.1 UV-VIS at Imerys

The UV-Vis spectrometer at Imerys is a double beam equipment capable of identifying the two transmittance measurements that are necessary to determine the concentration of an analyte in solution, and is shown schematically in Figure 3.8.

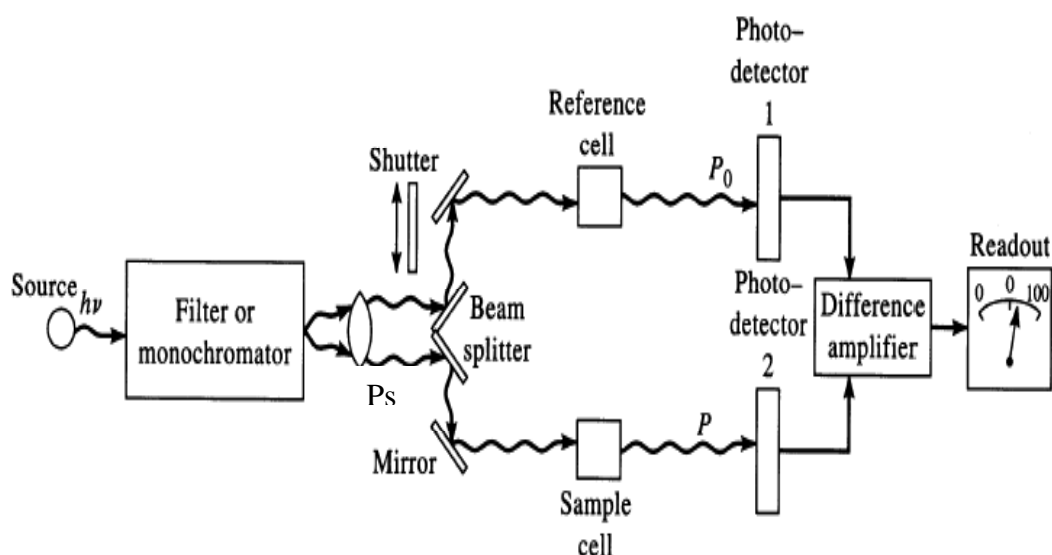


Figure 3.6: Schematic of a double beam UV-Vis Spectrometer equipment [91]

The top branch of Figure 3.8 (to the reference cell) is for solvent only and the bottom branch is for an absorbing sample in the same solvent. In this example,  $P_s$  is the source light power that is incident on a sample,  $P$  is the measured light power after passing through the analyte, solvent, and sample holder, and  $P_0$  is the measured light power after passing through only the

solvent and sample holder. The measured transmittance in this case is attributed to the analyte only. The reference measurement is made simultaneously with the sample measurement. These two values are then loaded onto the computer to generate the full spectrum (reference value is subtracted from the reference value). Modern absorption instruments can usually display the data as transmittance, percentage-transmittance, or absorbance. An unknown concentration of an analyte can be determined by measuring the amount of light that a sample absorbs and applying Beer's law. If the absorptivity coefficient is not known, the unknown concentration can be determined using a working curve of absorbance versus concentration derived from standards. In this case, one sample of OIT and one of CIT/MIT were separately measured on the UV-VIS at wavelengths between 190 and 700 nm to determine the wavelengths at which optimum absorbances were obtained (280 nm for OIT and 277 nm for CIT/MIT). Samples of the biocides of known concentrations were made and measured at these wavelengths in order to obtain a working calibration curve for the remainder of the samples (see Figures 3.9 and 3.10).



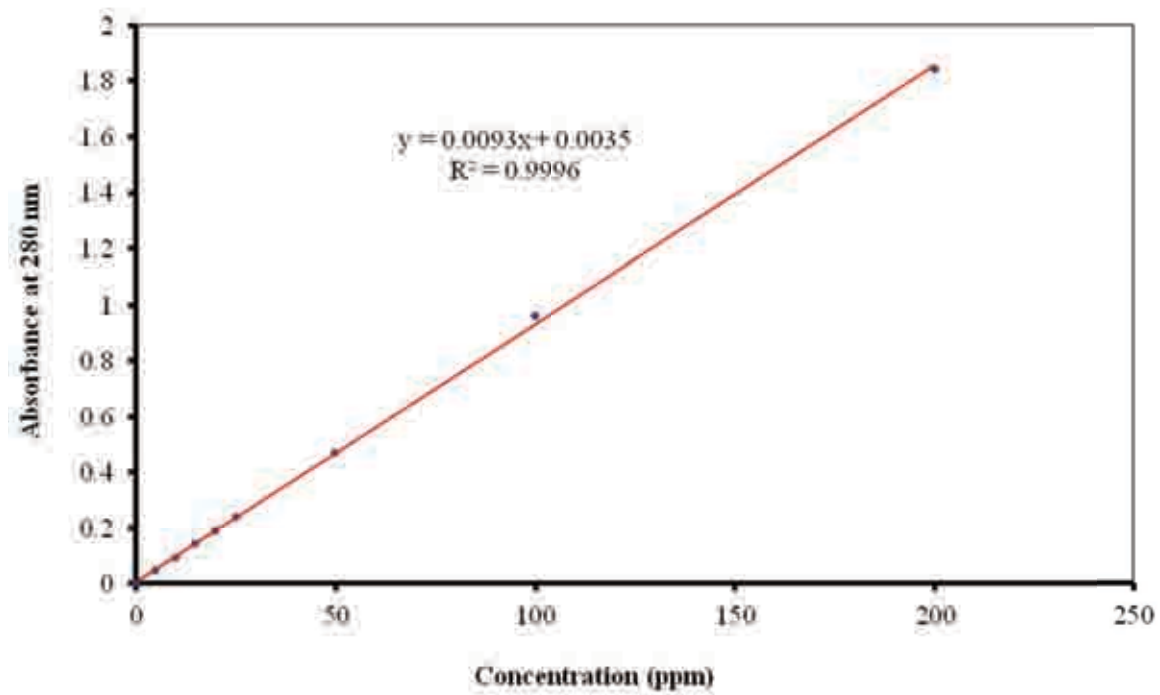


Figure 3.7: CIT/MIT calibration curve obtained from the UV-Vis spectrometer

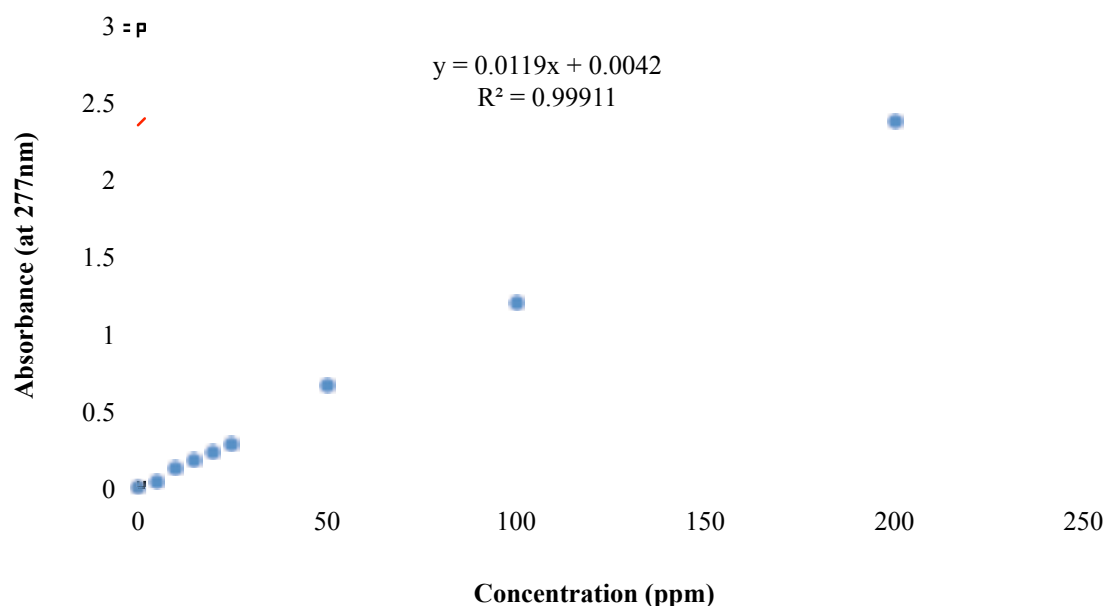


Figure 3.8: OIT calibration curve obtained from the UV-Vis spectrometer

#### 3.3.4.2 Advantages and limitations of the UV-VIS in relation to Beer-Lambert law

The UV-VIS spectrometer offers the advantage of being a very rapid method of determining the concentration of various compounds in samples. The technique is also simple to use and not labour intensive. Samples can be measured over a very wide range of wavelengths in order to determine the maximum absorbance of the particle(s) being analysed.

The linearity of the Beer-Lambert law can be limited by chemical and instrumental factors.

The causes of nonlinearity include [90]:

- deviations in absorptivity coefficients at high concentrations (above 0.01 Molar) due to electrostatic interactions between molecules in close proximity

- scattering of light due to particulates in the sample
- fluorescence or phosphorescence of the sample
- changes in refractive index at high analyte concentration
- shifts in chemical equilibrium as a function of concentration
- non-monochromatic radiation, deviations can be minimized by using a relatively flat part of the absorption spectrum such as the maximum of an absorption band
- stray light

### **3.4 Strength of biocide adsorption onto minerals**

The ability of organic as well as inorganic materials to participate in adsorption, adhesion and catalysis is facilitated by their surface geometry and bulk porosity. The method of Flow Microcalorimetry (FMC) has been used to study the association of these particulates with probes having known acid-base characteristics.

#### **3.4.1 General principles of Flow Microcalorimetry (FMC)**

To assist in the selection of appropriate carriers (see Table 3-1), Flow Microcalorimetry was used to better understand the nature of the interactions between the biocide and active sites on those carriers. The Flow Microcalorimeter (FMC) is able to measure heat exchanged as a result of adsorption/desorption occurring under flow conditions [86]. A differential Refractometer, downstream to the calorimeter, allows quantification of an adsorbate (the biocide, in this case). The amount of solute adsorbed on the solid is calculated from the comparison of parallel experiments conducted with the solid and a non-adsorbing probe. The difference between the refractometer signals of the two experiments permits the calculation of the amount of adsorption. In aqueous solutions, heat flux into or out of the sample almost

always happens on reaction. These reactions may involve a wide variety of situations, e.g., the interaction of two molecules (such as an isothiazoline biocide and its guest), changes in the conformation of complex macromolecules (such as proteins or DNA), or even in the structure of very complex multimolecular colloidal drug delivery systems (such as liposomes). Microcalorimetry uses a suite of techniques and appropriate calibrations to directly measure enthalpies associated with adsorption and desorption, and heat capacity changes that arise when chemical reactions occur.

### **3.4.2 Possible FMC results**

Calorimetric and concentration measurements obtained from the FMC can uncover the nature of interactions between the substrates (carriers) and the biocide (either it is a physisorption or a chemisorption effect). These interactions can take the following forms:

- Total adsorption – no desorption
- Total adsorption – partial desorption
- Total adsorption – total desorption
- Partial adsorption – no desorption
- Partial adsorption – partial desorption
- Partial adsorption – total desorption
- No adsorption

The ideal solution would be for the minerals used to adsorb a fairly large amount of the biocide, and release it over a long period of time (Total adsorption and total desorption over time, preferably months, or even years). In Chapter 4, the results of the minerals characterisation are presented and discussed.

# **CHAPTER FOUR**

## **RESULTS OF MINERAL CHARACTERISATION**

#### 4.1 Mineral characterisation studies

In this chapter, the results of the characterisation of the nine minerals in Table 3-1 (crystallography, crystal structure, particle size and morphology) are presented. An attempt is made to relate these structural factors to the potential for controlled release of the isothiazoline biocides (OIT and CIT/MIT). It is expected that in order to be a suitable substrate for sorption and bioassay studies, a mineral must:

- Have almost little or no structural water in its core (as the amount of water affects the purity of the mineral and can inhibit the adsorption of the biocides)
- Have a high degree of purity (in this case, the FeO content of the mineral must be minimal, as it affects the optical property of the paint formulations containing the mineral)
- Have small particle size following the milling process, as this will increase the available surface area of the mineral per gram, potentially leading to larger amounts of biocide being adsorbed

#### 4.2 Mineral size distribution analysis by the Mastersizer

Industrial minerals are often sold in the form of aggregates, powders or slurries. The form is often dictated by the eventual application: dry or damp aggregates for concrete, powders as additives to plastics, while water based paint and paper coatings may require well dispersed suspensions.

The size of the particles in each system is influential in the behaviour of the final material;

the smoothness (gloss) of a paint film, the strength of a ceramic article, the appearance of concrete. For this reason the industry has evolved standard measures of the particle size distribution.

The term distribution is important because the particles are rarely all the same size; instead they are many sizes and the statistical term “distribution” is used to describe the range of particle sizes present. A powder with both very small and very large particles is said to have a wide distribution, whereas a powder in which all the particles have similar sizes is called a narrow (or steep) distribution. These terms are born from the graphical representations used to describe distributions, which are called frequency diagrams or histograms. This type of graph shows the fraction (most often mass, but sometimes volume or number) of particles in each size range, as in Figure 4.1.

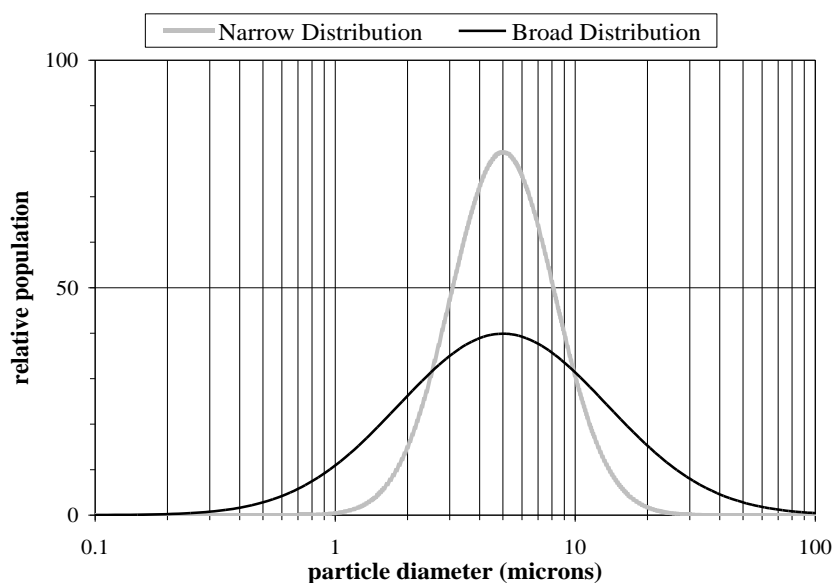


Figure 4.1: Frequency diagram for a broad and narrow particle size distribution [courtesy of Imerys].

Note that a logarithmic scale is often used, as particle size distributions often have a lognormal character

Distributions are however often shown in their integrated (cumulative) form as in Figure 4.2. The cumulative form allows direct reading of the “% passing”, “i.e. smaller than a specified size” (see Figure 4.1). This is widely considered a more intuitive way to describe a size distribution. It also has the key advantage that several distributions may be plotted on the same graph allowing easy comparison.

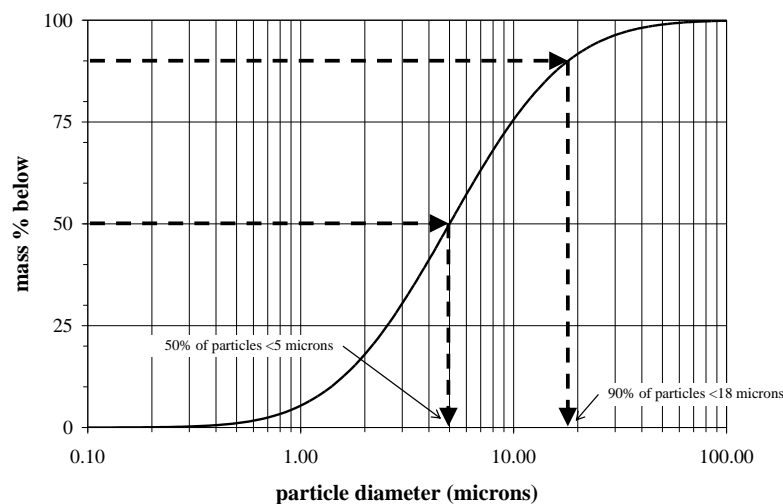


Figure 4.2: Cumulative (integrated) version of Figure 4.1, showing the % passing (i.e. below) any particular diameter. In this form the “narrow” distribution is called “steep” [courtesy of Imerys].

The  $d_{50}$  and  $d_{90}$  refers to 50% and 90% respectively of particles present below a particular diameter (can be read off the X-axis). As opposed to a population of particles that are all the same size (monodisperse), most powders have particles that are of several sizes



(polydisperse), forming a distribution. Most modern systems can calculate the distribution with no *a priori* assumptions, meaning that irregular distributions, such as those with two peaks (bimodal) or more, can be measured.

The particle's diameter (the hydrodynamic diameter) is calculated from the measured volume of the particle, found by assuming a spherical shape. This can be disadvantageous with the minerals used, as the particles are often non spherical (e.g. Kaolin) and so the sizes recorded were dependent on the angle at which light hits each particle [61].

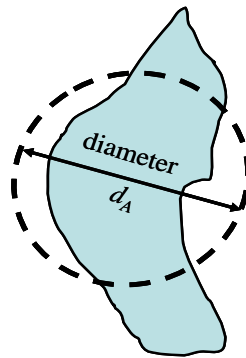


Figure 4.3: The diameter of a circle with the same area as a 2-D projection of a particle may be a useful estimate of its size

The equivalent sphere diameters can be obtained in several ways:

- Diameter of the sphere with the equal volume  $d_v$ . This can be calculated from the volume using:

$$d_v = \left( \frac{6V}{\pi} \right)^{1/3} \quad \text{Equation 4.1}$$

where  $V$  is the volume of the particle. The volume may be measured, for example, with 3-D imaging systems.

- Diameter of the sphere with equal surface area  $d_s$ .

$$d_s = \left( \frac{A}{4\pi} \right)^{1/2} \quad \text{Equation 4.2}$$

where  $A$  is the surface area of the particle (in  $\text{m}^2/\text{g}$ ). The surface area may be measured with techniques such as Nitrogen BET.

#### 4.2.1 Materials and Methods

A 5 g sample of mineral powder was mixed in a beaker with 5 ml of deionised water (a dispersant solution containing 1% w/v sodium carbonate and 0.5% w/v sodium hexametaphosphate may be added for a better dispersion). Droplets of this suspension were then transferred to the Mastersizer's own water tank for analysis (particles were illuminated using a parallel beam of light, usually from a low-power He/Ne laser). Laser diffraction particle size analysis is based on the scientific phenomenon that particles in a laser beam scatter laser light at angles that are inversely proportional to the size of the particles. Large particles scatter at small forward angles while small particles scatter light at wider angles. By the use of Fourier and Reverse Fourier optics, this scattering is imaged to an array of detectors at the focal plane of the optics. There is a direct relationship between the distribution of the scattered light energy on these detectors and the particle size distribution which gives rise to it. The Mastersizer software uses Mie theory to obtain an optimal analysis of this light energy distribution to arrive at the size distribution of the particles.

Data obtained were logged into an Excel spreadsheet to plot a cumulative "mass percent finer

than” distribution, both as a curve and table. More comprehensive results, including a particle number distribution, can also be obtained.

#### 4.2.2 Results

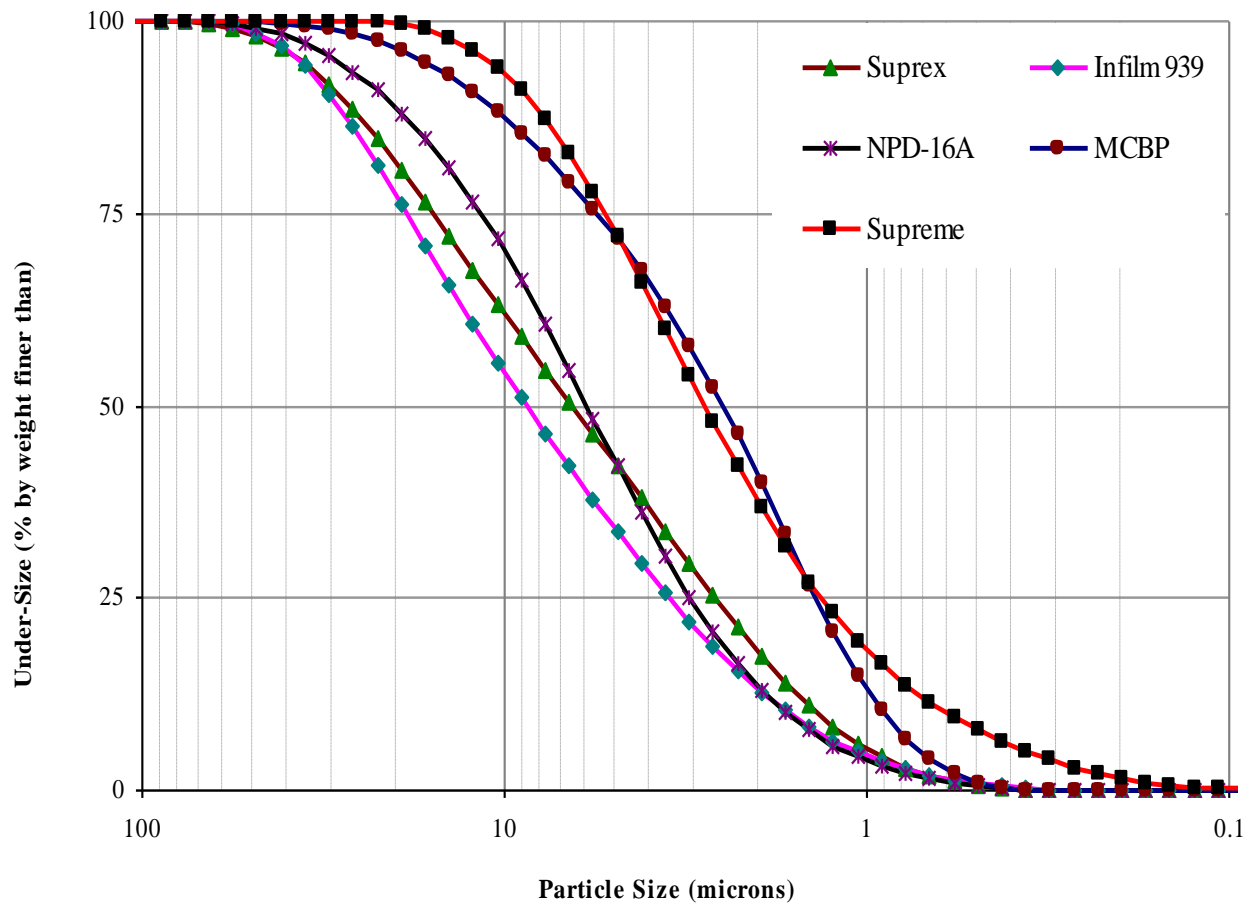


Figure 4.4: Volume distribution of the platy minerals

The volume distributions shown on Figure 4.4 indicated that the particle sizes for all the platy minerals used ranged from 0.1 to around 98 microns. The shapes of the curves were flatter rather than steeper for all the six minerals. These observations confirmed that the particles were polydispersed, with a broad distribution range. It appeared from the distribution range

that there were more particles below 10  $\mu\text{m}$  size than above for all the minerals.

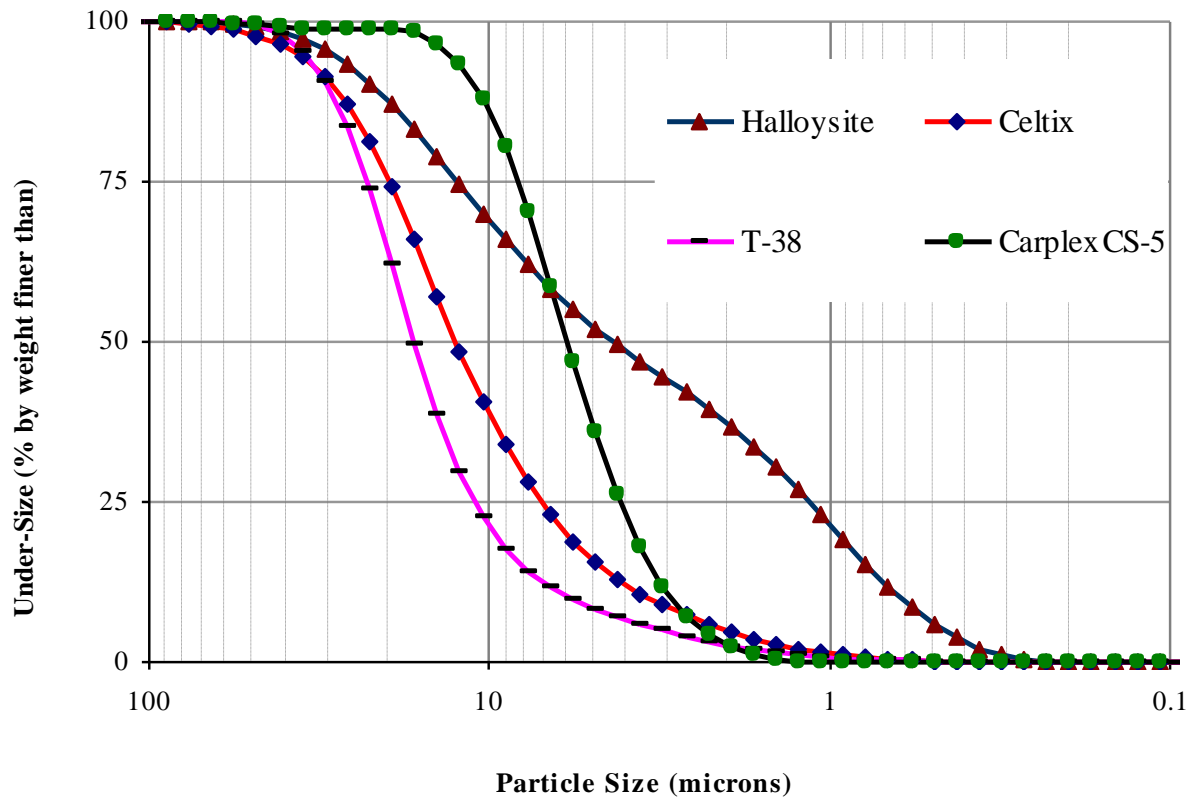


Figure 4.5: Volume distribution of the non-platy minerals

The volume distributions shown on Figure 4.5 indicated that the particle sizes for all the irregular and rod-shaped minerals used ranged from 0.1 to around 98 microns. The shapes of the curves were flat for the New Zealand halloysite, and steep for the amorphous silica-based minerals (calcium silicate T-38, diatomaceous earth Celtix and silica Carplex CS-5). These observations confirmed that all the particles were polydispersed, with both a broad and narrow distribution range for halloysite and the amorphous minerals respectively. It appeared from the distribution range that there were more particles below 10 microns size than above for all the minerals (except for T-38 and Celtix).

The steepness,  $d_{30}$ ,  $d_{50}$ ,  $d_{70}$  and  $d_{98}$  values of the minerals are presented in Table 4.1

Table 4.1: Size distribution and steepness factors of the minerals used.

Minerals	$d_{30}$	$d_{50}$	$d_{70}$	$d_{98}$ (top cut)	Steepness ( $d_{70} / d_{30}$ )
Kaolin-Infilm 939	4.3	8.7	16.2	46.1	3.8
Kaolin-Suprex	3.1	6.5	13.3	47.5	4.3
New Zealand Halloysite	1.4	4.3	10.5	39.1	7.4
Kaolin-Supreme	1.6	3.1	5	18.3	3.1
Kaolin-NPD-16A	3.6	6	10	40.1	2.8
Silica-Carplex	4.5	6	7.7	16.2	1.7
Calcium silicate-T-38	12.3	16.7	21.5	41.1	1.7
Diatomaceous Earth-Celtix	8.2	12.6	18	49.8	2.2
Montmorillonite-MCBP	1.56	2.5	4.6	25.1	2.9

(All values, except the steepness ratios, are in  $\mu\text{m}$ )

As previously stated, if a  $d_{50}$  value of a particular mineral is X, this meant that 50 per cent by weight of the particles present is below X (and 50% above it). Within the mineral processing industries, this value is considered important in evaluating the particle size of various minerals. The  $d_{50}$  values in Table 4-1 indicated that montmorillonite MCBP was the finest mineral, closely followed by kaolin supreme, New Zealand halloysite, carplex, NPD-16A, kaolins suprex and infilm 939, diatomaceous earth celtix and calcium silicate T-38

respectively.

The “Top Cut”  $d_{98}$  values showed that the silica (Carplex), the kaolinite (supreme) and the montmorillonite (MCBP) were the finest three clays of the group of minerals studied. The kaolin Supreme is an Imerys mineral, readily available, with a relatively small surface area ( $17 \text{ m}^2\text{g}^{-1}$ ), but the best  $d_{98}$ , and the second best  $d_{50}$  and  $d_{70}$  of all the minerals in Table 4-1. Those attributes have made this mineral an ideal candidate for use in the remainder of all experiments carried out in this project.

The terms  $d_{50}$  and  $d_{98}$  are of particular importance when considering fine particles. An additional property is the steepness of the particle size distribution curve (see Table 4.1). Various definitions are used in the mineral processing industry to describe this property. Imerys prefers to use the term “steepness factor”. This steepness factor is the quotient of the  $d_{70}$  and the  $d_{30}$  values. A curve with the steepness factor  $\geq 2$  is described as “flat” and those with the factor of  $< 2$  as “steep”. In other words, a fine extender (mineral used in the paint and/or paper industries) with a flat particle distribution curve contains a wide range of different size particles e.g. from under  $0.1 \mu\text{m}$  to  $3 \mu\text{m}$ . An extender with a steep particle size distribution curve contains particles within a narrow size range. Ideally such an extender would be isodiametric (all particles would be of the same size). Particle size is very important in the paper and coating industries. In the coating industry, an extender with a high isodiametric particle content offers the following advantages:

- Increased opacity in heavily filled interior emulsion paints
- Easy dispersion in oil-based, synthetic binders

- Excellent gloss and the best gloss retention in very glossy systems
- Shortening of the drying time of water-reducible coatings through the capillary effect
- Spacing extender with optimal particle size distribution for the partial replacement of titanium dioxide (very expensive)

The silica Carplex and the calcium silicate T-38 were the only two minerals with steep distribution curves, having a steepness factor of 1.7. The various percentage values still showed Carplex was finer (smaller particle sizes) than T-38 (large particles size with narrow distribution). Diatomaceous Earth Celtix, the kaolins NPD 16A, Supreme, Infilm 939, Suprex, the Montmorillonite MCBP, and New Zealand Halloysite all had very flat distribution curves, with the Halloysite's curve being the broadest (see Figure 4.5), possibly due to its tubular shape.

### **4.3 Mineral characterisation by X-ray Fluorescence (XRF)**

The chemical composition of all the minerals used in this study, arising from their general composition detailed in Table 3.1 of Chapter 3, was determined by XRF. This technique was ideal for the measurement of most elements (major and minor), and was thus a preferred technique for whole rock characterisation.

#### **4.3.1 Materials and Method**

The minerals (10 g of material is generally used) were prepared as compressed powder pellets or fused glass disc and excited with x-ray radiation, normally generated by an x-ray tube operating at a potential of 32 kVolts. The tests were performed at high temperature (1000°C) in order to eliminate any volatile compounds such as structural “combined water” trapped

within the samples (hydrates or hydroxy-compounds). The elimination of this trapped water lead to the structure of the minerals alone to be characterised. The amount of water present was determined from a Loss On Ignition (LOI) test, where samples were ignited in a suitable container (platinum, unglazed porcelain or vitreous silica) at 1000°C for about 1 hour, and the weight loss determined. This method may also be used to determine the levels of carbon dioxide present in carbonate based minerals. The level of purity of two minerals of similar structures can be determined by this method (the amount of impurity liberated).

#### **4.3.2 Results**

Results obtained from the XRF analysis of the minerals are in table 4.2, with major and minor trace elements recorded.



Table 4.2: XRF data detailing the percentage of the chemical composition of the nine minerals used

Table 4.2: XRF data detailing the percentage of the chemical composition of the nine minerals used

	Al <sub>2</sub> O <sub>3</sub>	SiO <sub>2</sub>	K <sub>2</sub> O	Fe <sub>2</sub> O <sub>3</sub>	TiO <sub>2</sub>	CaO	MgO	Na <sub>2</sub> O	LOI	Total
Kaolin - Infilm 939	39.1	45.1	mtd *	0.61	1.05	0.05	mtd	0.13	13.87	99.91
Montmorillonite - MCBP	18.1	65	mtd	3.73	0.11	0.81	2.8	3.39	6.02	99.96
Silica - Carplex CS-5	mtd	99.88	mtd	0.11	mtd	mtd	mtd	mtd	mtd	99.99
NZ Halloysite	38.7	45.8	mtd	0.48	0.11	mtd	mtd	mtd	14.91	99.89
Kaolin - Supreme	37.7	47.7	0.9	0.68	0.02	mtd	0.19	0	12.79	99.98
Calcium Silicate T-38	1.18	46.29	0.25	0.84	0.09	30.86	0.3	0.43	19.15	99.39
Diatomaceous Earth - Celtix	1.7	91.7	mtd	0.76	0.1	0.54	0.52	0.4	4.28	100
Kaolin - NPD-16A	35.5	48.1	1.78	0.55	0.03	mtd	0.09	0.47	13.48	100
Kaolin - Suprex	37.7	45.5	mtd	1.38	1.46	mtd	0	mtd	13.96	100

(\*): Minor trace detected (less than 0.01 %)

Table 4-2 shows the various chemical components of the minerals used in this study. The Loss On Ignition (LOI) values showed that, with the exception of the silica, all the minerals had some structural water trapped within them. The percentages of water liberated from infilm 939, supreme, suprex and NPD-16A were very similar, as these minerals had the same kaolinite structure and almost the same processing route. Suprex, with a LOI of 19.96%, had the most structural water in its core. This indicated that, of all the minerals tested, it was the least pure mineral before this initial test. The test also indicated that the silica obtained from Degussa was very pure, with almost no LOI value. This is due to its chemical structure,  $\text{SiO}_2$ , with no bound water.

Kaolinite (the main constituent of most clays) has the formula  $\text{Al}_2\text{Si}_2\text{O}_5(\text{OH})_4$ . Its structure arises from the combination of silica ( $\text{SiO}_2$ ) and aluminium oxide ( $\text{Al}_2\text{O}_3$ ) layers into a hexagonal sheet (see Figure 4.6). Hydrogen bonding between the alternating oxygen and hydroxyl surfaces causes these platelets to stack together, sometimes resulting in stacks up to 100  $\mu\text{m}$  in length which consist of hundreds of thousands of layers [92]. The presence of this structure in all the minerals used (with the exception of silica-Carplex, calcium silicate T-38, and diatomaceous earth-Celtix) was shown using this XRF. It was hoped the hydrogen bonds between the oxygen and hydroxyl surface could be broken, upon hydration of the minerals, to allow the biocide to be intercalated.

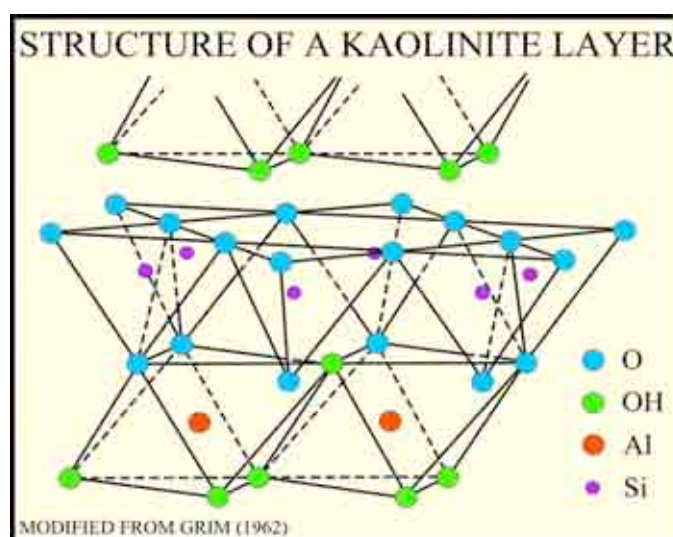


Figure 4.6: Structure of a kaolinite layer [93]

Table 4-2 also showed that the silica Carplex CS-5 was the highest grade of the three  $\text{SiO}_2$  based minerals used, with the silicon dioxide comprising 99.88% of the minerals. The diatomaceous earth Celtix had 91.7% of  $\text{SiO}_2$ , with minor traces of  $\text{Al}_2\text{O}_3$ ,  $\text{Fe}_2\text{O}_3$ ,  $\text{CaO}$ ,  $\text{MgO}$  and  $\text{Na}_2\text{O}$  also detected. The calcium silicate T-38 (formed by the reaction of calcium oxide and silica) contained 46.29% of  $\text{SiO}_2$  and 30.86% of  $\text{CaO}$ . Nevertheless, minor traces of  $\text{Al}_2\text{O}_3$ ,  $\text{Fe}_2\text{O}_3$ ,  $\text{MgO}$  and  $\text{Na}_2\text{O}$ ,  $\text{K}_2\text{O}$  and  $\text{CaCO}_3$  were also detected in this analysis.

The presence of iron oxide ( $\text{Fe}_2\text{O}_3$ ), also known as hematite, could affect the optical property (whiteness and yellowness) of these minerals in industrial paint applications. Great care is generally taken during the beneficiation process (explained in Chapter 1) of these minerals to remove this element by means of magnetic separation and/or bleaching. The montmorillonite MCBP seemed to have the highest percentage of  $\text{Fe}_2\text{O}_3$ , at 3.73%. The effect of these ions on the paint's mechanical and optical properties is fully discussed in Chapter 8.

#### **4.4 Material characterisation by X-ray Diffraction (XRD)**

In this study, the XRD method was used to obtain information on the nature of the crystals present in the minerals used.

##### **4.4.1 Material and method**

Samples were analysed as powders (10 g) with grains in random orientations. The samples were placed in an intense beam of X-rays of a single wavelength (monochromatic X-rays), producing the regular pattern of reflections. As the crystal was gradually rotated, previous reflections disappeared and new ones appeared; the intensity of every spot was recorded at every orientation of the crystal. Multiple data sets were collected, with each set covering slightly more than half a full rotation of the crystal and typically containing tens of thousands of reflection intensities. Data collected were combined computationally with complementary chemical information to produce and refine a model of the arrangement of atoms within the crystal. The final, refined model of the atomic arrangement (crystal structure) can then be stored in a computer database. Consequently, X-ray diffraction pattern is the fingerprint of the periodic atomic arrangements in a given material.

##### **4.4.2 Results**

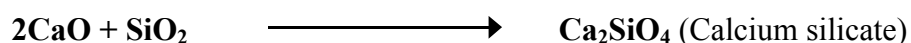
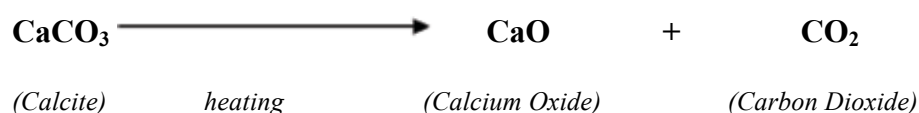
XRD data for the minerals used are summarised in Table 4.3.

Table 4.3: XRD data showing percentage of various crystals present in each of the nine minerals used in this study

	Kaolinite	Mica	Quartz	Feldspar	Calcite	Amorphous Silica	Anatase	Halloysite/Kaolin	Montmorillonite
Kaolin - Infilin 939	98						2		
Montmorillonite - MCBP	None detected		10		2				88
Silica - Carplex						99.9			
New Zealand - Halloysite			1					99	
Kaolin - Supreme	94	4	1	1					
Calcium Silicate - T-38			8.5		13	79.5			
Diatomaceous Earth - Celtix			1.5		1	97.5			
Kaolin - NPD-16A	89	6	1	4					
Kaolin - Suprex	97		1				2		

The XRD data in Table 4-3 confirmed the presence of kaolinite as the major constituent of all the following minerals: infilm 939, supreme, suprex and NPD-16A. A trace of anatase (a form of  $\text{TiO}_2$ ) was also found in infilm 939 and suprex, two almost identical minerals, with the same processing route and origin, but only differing by the absence of dispersant in the latter.

Carplex, celtix and T-38 were the only minerals that almost entirely consist of amorphous silica (99.9%, 97.5% and 79.5% respectively). Traces of crystalline silica (quartz), and calcite (most stable polymorph of  $\text{CaCO}_3$ ) were also detected in MCBP, supreme, suprex, T-38 and celtix. The presence of calcite in T-38 (calcium silicate) was not unusual, as Calcite will form Calcium Oxide ( $\text{CaO}$ ) upon heating.  $\text{CaO}$  can, in turn, reacts with  $\text{SiO}_2$  (in various ratios) to make Calcium Silicate. The two reactions are as follows:



The presence of halloysite and montmorillonite was also confirmed in the respective minerals.

#### 4.5 Morphology assessment by Scanning Electron Microscopy (SEM)

The SEM was used to assess the shapes of the minerals in Table 4:3 in order to determine

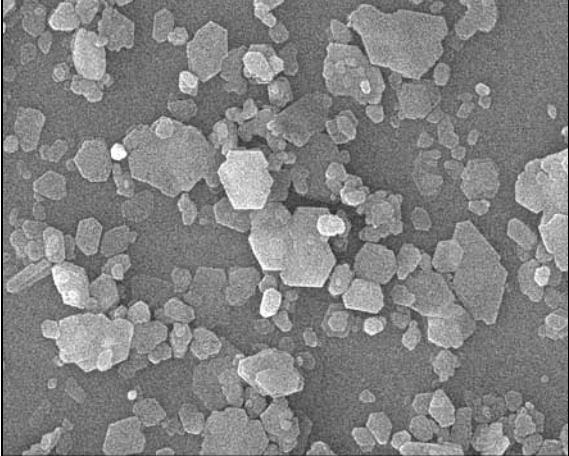
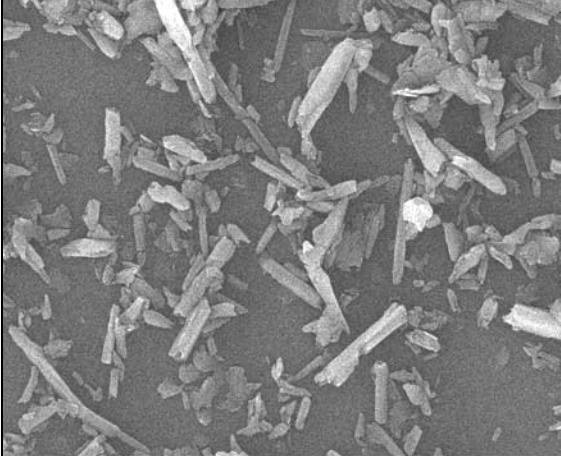
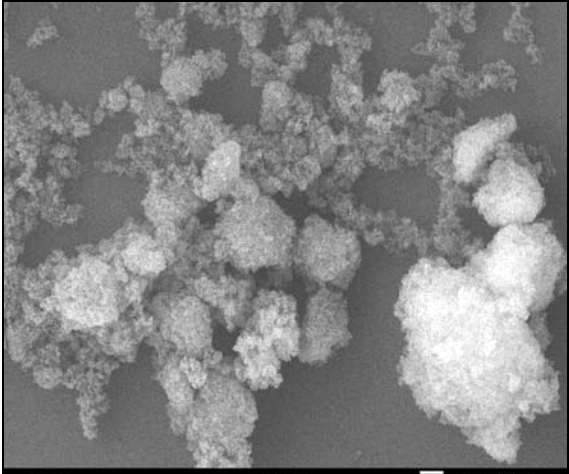
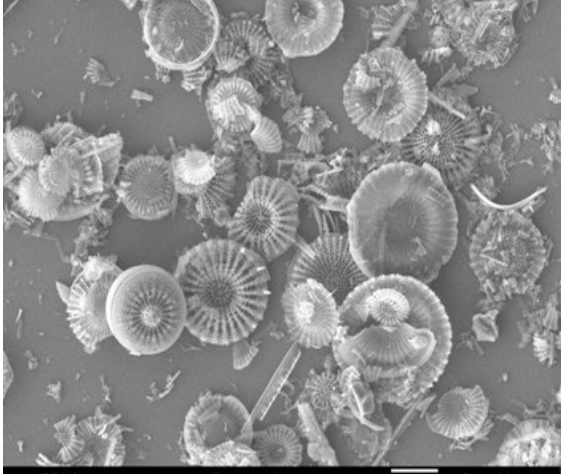
how these minerals could perform as controlled release media. The principles underpinning this technique were explained in section 3.1.3 of Chapter 3.

#### **4.5.1 Material and method**

Samples of dried powder (5 g) were coated in a thin film of gold to prevent charge build-up in the microscope and erosion, which could lead to image distortion. Coating was performed in a sputter coater. The sample was placed on conductive carbon film on an earthed SEM stub in an inert argon atmosphere. A cathode ray tube was then used to coat the sample. The cathode is made of gold, and as a very high voltage was applied to the tube, the argon in the sputter coater ionised. Bombardment of the gold in the cathode by ionised argon atoms sputtered off gold atoms from the cathode onto the earthed sample, effectively scanning its surface.

### 4.5.2 Results

Table 4.4: Electron micrographs of different minerals

<p><b>Platy mineral - Kaolin (Infilm 939)</b></p>	<p><b>Rod-shaped mineral - New Zealand Halloysite</b></p>
	
<p><b>Amorphous mineral – Silica (Carplex CS-5)</b></p>	<p><b>Irregular-shaped mineral diatomaceous Earth (Celtix)</b></p>
	



The SEM revealed four different shapes materials, and it was hoped each of these could be exploited for controlled release purposes. The platy minerals (the Kaolins Infilm 939, Supreme, Suprex, NPD-16A and Montmorillonite MCBP) showed a more hexagonal shape under the microscope, due to the presence of kaolinite detected by XRD. Several of these hexagonal layers stack together to give the platy character of these clays, and it was hoped to use the interlayer spaces as media to carry the biocide.

The halloysite was shown to have a tubular shape under the microscope. Halloysite is an aluminosilicate clay mined from natural deposits in countries such as America, Brazil, China, France, Japan, South Korea and Turkey. It is chemically similar to kaolin, but differs in having a hollow microtubular rather than a stacked plate-like structure [94]. Halloysite typically is formed by hydrothermal alteration of aluminosilicate minerals. A mismatch in the two-layered alignment of the tetrahedral sheet of silica bonded to the octahedral or gibbsite sheet of alumina causes the wall to curve into the cylindrical shape [95]. The mineral can also occur intermixed with Dickite, Kaolin, Montmorillonite and other clay minerals. It was hoped to utilize the hollow tube to store the biocide and provide a slow release mechanism of the correct quantity.

The amorphous silica and the irregular “mushroom-like shape” calcium silicate T-38 and diatomaceous earth Celtix minerals were also shown under the SEM. Although T-38 and Celtix were shown to have a large amount of amorphous material, they also contained some quartz and calcium carbonate (calcite), possibly conferring them the irregular shape observed (see Table 4-3 for crystal composition). These minerals are normally used on the market for filtration purpose because of their porous structure and ability to carry considerable amount of material in their core. It was hoped, in this project, to use these sponge-like minerals for

controlled release of the OIT biocide.

#### **4.6 Discussion**

It was necessary to characterise the minerals used in this study in order to understand how best they could be used for the controlled release of the biocides OIT and CIT/MIT. The characteristics of importance were the chemical compositions, crystal structures, morphologies and particle size distributions.

In order to determine the particle size distributions of the nine minerals used, it was preferable to measure them whilst they are in a wet dispersion. The use of dry measurement techniques could have lead to inaccurate results due to the agglomerates in the particles. These minerals are most often used as a suspension in water during the manufacturing processes, and so a particle size measurement in this state was thought more useful, allowing the behaviour of the clay in suspension to be determined and characterised. However, Mie theory holds good for all particulate materials in all transparent media – liquids or gases or even transparent solids and thus a new Mastersizer equipment is able to measure suspensions, emulsions, spray droplets, smokes, vapours or even dry powders, giving the user unparalleled versatility of measurement capability. The Mastersizer Side-angle and backscatter detectors allow the extension of the dynamic range with no sacrifice in resolution.

The particle size calculations using the Malvern Mastersizer required that the particles were well dispersed and disaggregated, and were sufficiently diluted in the fluid so that adjacent particles did not interfere with one another. This does not work particularly well for particles below 100 nm due to the effects of Brownian motion. The method was also somewhat

dependent on consistent particle density, as denser particles will settle faster. The hydrodynamic ESD is an important measure and is extensively used in the mineral processing industries, and is particularly useful because the Stokes settling principle is widely used to dewater or classify particles into different size fractions. For regularly shaped particles, such as spheres or cubes, the correlations work reasonably well and have been developed and refined over many years. The models still work reasonably well for slightly irregular particles; this accounts for perhaps the majority of particles, but care needs to be taken for some particular circumstances. Hollow or porous particles, acicular or filamentary particles, lamellar or platy particles can all give misleading output from the light-scattering models, and the results therefore need to be treated with caution. The “Top Cut”  $d_{98}$  values showed that the silica (Carplex), the kaolinite (Supreme) and the montmorillonite (MCBP) were the finest three clays of the group of minerals studied. Most of Imerys’ minerals are used in the paper and coating industries, and it was necessary to determine how fine each of the nine minerals was. This property was important as a fine mineral can influence the rheology, density, scrub and corrosion resistance, and packing density of the paint formulation in which it is (even if a mineral was found to be a very good controlled release medium, it may still have to be reasonably fine for use in paints or paper). Carplex (the silica), MCBP (the montmorillonite) and supreme (the kaolin) were selected for the paint and bioassay work described in see Chapter 7 for this reason.

The XRD experiments described the crystal nature of the nine minerals used. The presence of kaolinite, halloysite and montmorillonite in the phyllosilicate minerals (halloysite, suprex, supreme, MCBP, NPD-16A and infilm 939) was confirmed, with infilm 939 appearing to be the “purest” of all the kaolinite at 98%. The technique was also able to show the amorphous

nature of the three silicate minerals (carplex, T-38 and celtix). Quartz was also present in many other minerals. Oxygen is the most abundant element in the earth's crust, and Silicon is the second most abundant. Due to such abundance, the formation of silica ( $\text{SiO}_2$ ) in nature is very common. This explained why traces of silica were found in all but two of the minerals examined. The chemical compositions of these crystals were analysed by the XRF.

Using the XRF technique, it was possible to eliminate the structural “combined water” trapped within the samples by Loss On Ignition (LOI) test. LOI values showed that, with the exception of the silica, all other minerals had trapped water within their cores. Major elements found included silicon dioxide (in all minerals), aluminium oxide (in all but the amorphous silica), and calcium oxide (only found in the calcium silicate T-38). The presence of oxygen and silicon in all the minerals was expected. The presence of aluminium oxide ( $\text{Al}_2\text{O}_3$ ), an amphoteric oxide of aluminium produced by the Bayer process from bauxite, can confer an abrasive nature to the minerals in which it is a constituent, due to its hardness.

The kaolinite-based minerals used in this study (supreme, suprex, MCBP, infilm 939, NPD-16A, New Zealand halloysite) are part of the phyllosilicates (from the Greek *phyllon*, leaf), or sheet silicates. They form parallel sheets of silicates tetrahedral with  $\text{Si}_2\text{O}_5$ , and are sometimes referred to as 1:1 or 2:1 clay. A 2:1 clay consists of an octahedral sheet sandwiched between two tetrahedral sheets (montmorillonite), whereas a 1:1 clay would consist of one tetrahedral sheet and one octahedral sheet (suprex, supreme, infilm 939, NPD-16A and New Zealand halloysite). These sheets are linked through oxygen atoms <sup>[72]</sup>, and it was hoped to intercalate them with the biocides in these controlled release experiments. The main differences between these two clays are summarised in Table 4.5.

Table 4.5: Major differences between a 1:1 and a 2:1 clay

Characteristic	Kaolinite	Montmorillonite
Layer type	1:1	2:1
Typical chemical formula	$[\text{Si}_4] \text{Al}_4\text{O}_{10}(\text{OH})_8$	$\text{M}_x[\text{Si}_8]\text{Al}_{3.2}\text{Fe}_{0.2}\text{Mg}_{0.6}\text{O}_{20}(\text{OH})$
Particle size ( $\mu\text{m}$ )	0.5 – 5.0	0.01 – 1.0
Specific Surface area ( $\text{m}^2/\text{g}$ )	7 – 30	600 - 800
Shrink/swell potential	Non-expansive	Highly expansive
Interlayer space	None (very small)	Very large
Cation Exchange Capacity ( $\text{cmol}_c/\text{kg soil}$ )	2 - 15	80 - 150

The three silica-based minerals used (carplex CS-5, T-38 and celtix) are thought to interact with the isothiazoline biocides in a different way (see section 2.6 of Chapter 2).

Scanning Electron Microscopy (SEM) was used to examine the shapes of the minerals used because it was more useful for looking at morphological changes than other types of microscopy methods. Using this technique, four different shape minerals were revealed:

- Platy for the four kaolins and the montmorillonite (suprex, supreme, NPD-16A, infilm 939 and MCBP)
- Rod-shape for the New Zealand halloysite
- Amorphous for the silica (Carplex CS-5)
- Irregular for the diatomaceous earth and calcium silicate (celtix and T-38)

It was hoped that the morphologies described above could help entrap and slowly release the isothiazoline biocides.

The characterisation experiments uncovered the shapes, chemical compositions, crystal structures, and particle size distributions of the nine minerals used. In the next Chapter, an attempt will be made to discover how these characteristics of the minerals could be used to adsorb the isothiazoline biocides in both static and dynamic environments. Flow Microcalorimetry will be used to estimate the sorption energies (and amounts of biocide), and HPLC will measure the concentration of biocide in solution after the adsorption in the high shear mill.

# **CHAPTER FIVE**

## **ADSORPTION ISOTHERM STUDIES**

In this chapter, data from the Flow Microcalorimeter (FMC) and adsorption isotherms of the isothiazoline biocides (OIT and CIT/MIT) onto the minerals are presented and discussed. The molecular footprints of the biocides on selected mineral surfaces were also determined. These measurements were made in order to assess the suitability of the minerals for controlled release of biocides in paint films (described in chapter 7).

## **5.1 Flow Microcalorimetry (FMC)**

The biocide used in this experiment was OIT. It was the only one of the two isothiazolines that could be obtained in its pure form (100%). Running the pure biocide on the FMC was necessary to assess the true amount of the adsorbent on the minerals' surface and the energies gained or liberated as a result of the interaction processes.

### **5.1.1 Materials and Methods**

The FMC used was a Microscal 3V upgraded to an all-PTFE fluid path (see Figure 5.1). The instrument was linked to a Microscal thermistor bridge control unit that was connected to one channel of a Perkin–Elmer 970 series data station. The FMC cell outlet was connected to a Waters 410 differential refractometer; the electrical output of the latter was connected to the second channel of the 970 series data station. Energy calibration of the FMC was achieved via passage of  $3 \times 10^{-4}$  W electric power for 300 seconds through a filament integrated into the cell outlet connector. Calibration of the differential refractometer was achieved using a 20  $\mu$ l loop, i.e. a 20  $\mu$ l OIT solution of known concentration. The 970 series interfaces were linked to a PC for data manipulation using Perkin–Elmer Total Chrom version 6.3.1 software. The FMC studies were conducted using a cell temperature of 27 °C ( $\pm 1$  °C) and a probe



concentration of 0.3% w/v. The solvent flow rate was  $4 \text{ ml h}^{-1}$ . The mineral powders were weighed into a graduated tube such that the tapped volume of the sample was  $0.15 \text{ cm}^3$ .

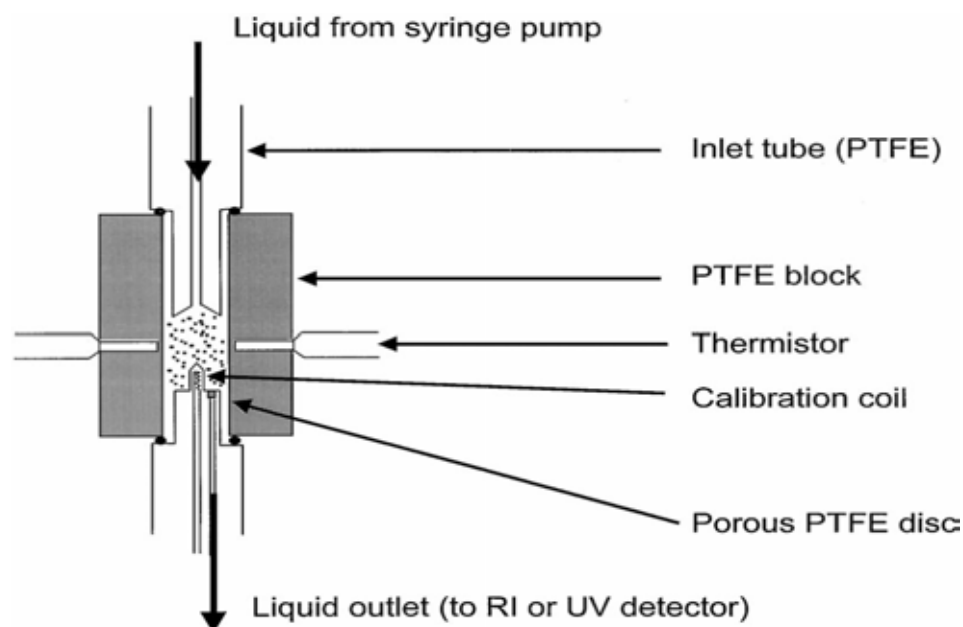


Figure 5.1: Schematic of FMC with Polytetrafluoroethylene (PTFE) fluid path [61]

The experimental error of the FMC measurements was in the order of  $\pm 2.5\%$ , obtained by averaging over multiple replicates. Decahydronaphthalene was used as the non-adsorbing probe, and cyclohexane (HPLC grade dried over  $4\text{\AA}$  molecular sieve) as the solvent for the isothiazolinone. The probe and the solvent were both obtained from Sigma-Aldrich. OIT (100% pure) was obtained from Thor Chemicals in Germany. All nine minerals detailed in Table 4-1 were used. The amount of probe adsorbed was determined by subtraction of the non-adsorbing probe trace from the adsorbing probe trace, once limiting deflection had been obtained. The area of the resulting peak is proportional to the amount adsorbed or desorbed. The thermal and differential refractometer responses were calibrated using 2 and 7 calibration peaks, respectively.

Within the FMC cell the adsorbent (volume  $0.15\text{ cm}^3$ ; 350–800 mg) was equilibrated, with cyclohexane, for 18 h before measurements commenced. This conditioning period was necessary to remove the vast majority of loosely bound surface water from the substrates. Initially the adsorbate in cyclohexane was passed through the cell containing the adsorbents (each in turn), and after adsorption had taken place cyclohexane was passed through the cell to facilitate desorption. For both adsorption and desorption measurements, the data reported are that for the average result between two runs.

The ratio of the adsorption energy (per unit area or unit mass of the substrate) to the desorption energy can be considered to be a measure of how strongly the probe was retained on the surface of the clays. A zero desorption energy means that the probe was irreversibly (very strongly) adsorbed under the conditions used. If the adsorption energy is equal to the desorption energy, adsorption of the probe is completely reversible and the biocide can be considered weakly adsorbed.

### 5.1.2 Results

The results of the FMC work are presented in Figures 5.2 (heat), 5.3 (amount), and summarised in Table 5.1

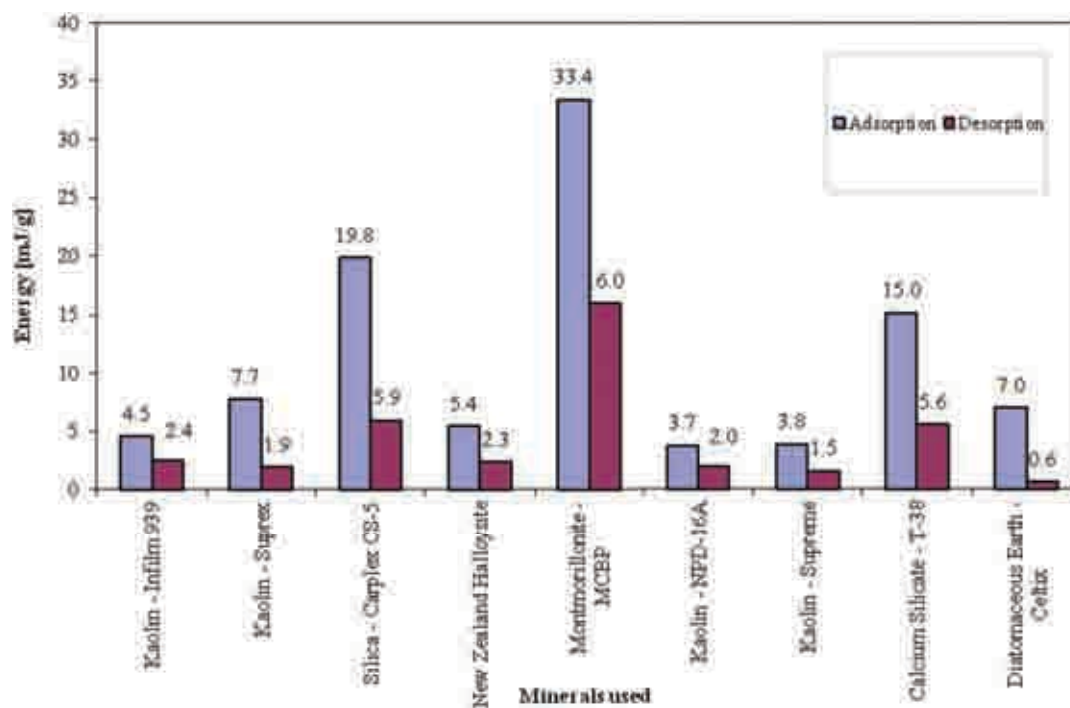


Figure 5.2: Energies of adsorption and desorption of OIT per gram of minerals used in the FMC under flow conditions.

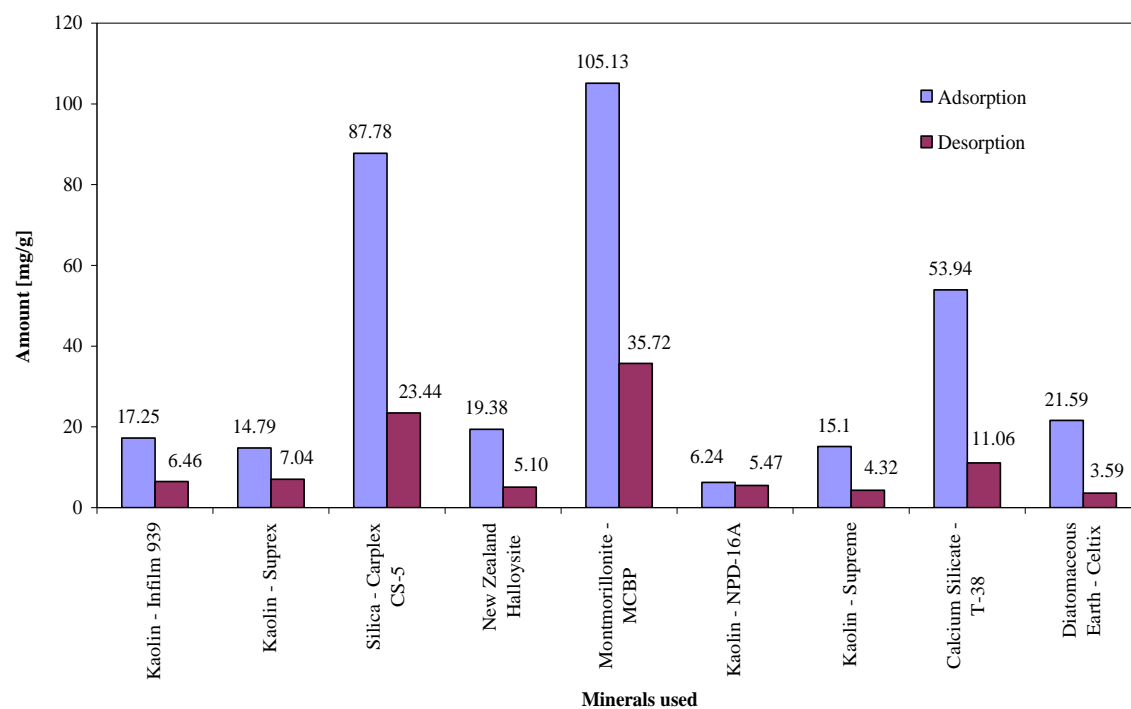


Figure 5.3: Amount of OIT adsorbed and desorbed per gram of minerals used in the FMC under flow conditions

Table 5.1: Summary of the ratios of heat of sorption (with molar heat of interaction) and amounts of OIT after the FMC run

	Surface area (m <sup>2</sup> /g)	Energy ratios (Adsorption/ Desorption)	Amount ratios (Adsorption/ Desorption)	Molar Heat of Interaction (kJ/mole OIT) (M.h.i <sup>*</sup> )
Kaolin (Infilm 939)	22	1.87	2.67	0.06
Kaolin (Suprex)	25	4.05	2.1	0.05
Silica (Carplex CS-5)	150	3.35	3.74	0.05
NZ Halloysite	50	2.34	3.8	0.06
Montmorillonite (MCBP)	39 or 800 <sup>(**)</sup>	2.08	2.94	0.07
Kaolin (NPD 16-A)	23	1.85	1.14	0.12
Kaolin (Supreme)	17	2.53	3.49	0.05
Calcium Silicate (T-38)	122	2.67	4.88	0.06
Diatomaceous Earth (Celtix)	24	11.66	6.01	0.07

The molar heat of interaction was calculated using equations 5.1 and 5.2

$$\text{OIT adsorbed (mole)} = \text{amount adsorbed (g)} / 213 \text{ (1 mole OIT)} \quad \text{Equation 5.1}$$

$$\text{M.h.i} = \text{Heat of adsorption (kJ)} / \text{OIT adsorbed (mole)} \quad \text{Equation 5.2}$$

<sup>(\*\*)</sup> When MCBP is dry or wet, respectively

Figure 5.2 showed that the heat of adsorption energies were greater than the desorption energies for all the minerals used. Energy ratio values in Table 5-1 were all over 1, indicating that some (or most) of the OIT molecules remained on the minerals' surface after desorption had taken place. However, differences in the values of adsorption energies could be due to variations in accessible surface areas of the minerals (and the strength of the biocide's bond onto the surfaces). Figures 5.2 and 5.3 show that the highest surface area minerals, the montmorillonite MCBP, the silica carplex CS-5 and the calcium silicate T-38 strongly adsorbed the OIT molecule, possibly due to their high surface area and level of porosity respectively. The sorption energies and the amounts of OIT on all the kaolins and halloysite minerals were very low, possibly reflecting their lower surface areas. Porous and irregular shaped minerals (carplex, celtix and T-38) showed the highest sorption ratios of OIT (amount), contrary to the tubular New Zealand halloysite. This indicated that porous minerals carried more biocide molecules. The heat of desorption for all the probes indicated significant irreversible adsorption. The diatomaceous earth celtix and the kaolin suprex, with ratios of 11.6 and 4.05 respectively, appeared to almost irreversibly holding on to OIT, indicating that they would be poor controlled release substrates within the timeframe of the experiment. On the contrary, the attachment of OIT to the kaolin NPD-16A could be said to be totally reversible (amount ratio of 1.14), perhaps also indicating that this mineral could not be used in controlled release experiments, as the biocides would be released too quickly. The molar heat of interaction was similar for all the minerals, with the exception of NPD-16A (0.13 kJ/mole OIT). These primary adsorption results indicated that the New Zealand halloysite, the diatomaceous earth celtix and the kaolin suprex could be ruled out as good candidates for controlled release purposes.

## 5.2 Adsorption Isotherms

The isotherm experimental protocol used in this study was taken from an Ineos Silica patent (US patent number 6905698) and modified before used (minerals used and amounts were different from those in the patent, together with the way the biocide was inserted into the Halloysite tubes). In the adsorption experiments, it was assumed that the amount of biocide not present in water had adsorbed to the surface of the carriers. The adsorption capacity of six of the minerals in Table 5-1 (the kaolins infilm 939, suprex, NPD-16A, the New Zealand halloysite, the silica carplex and the montmorillonite MCBP) was determined experimentally by measuring the adsorption equilibrium isotherms (static environment). In order to achieve this, High Performance Liquid Chromatography (HPLC) was used to measure the concentration of the desorbed biocide molecules in solution. The adsorption isotherms of celtix, supreme and T-38 were not determined as these minerals were unavailable at the time and only the FMC measurements previously described were used to determine their suitability for controlled release.

### 5.2.1 Material and Method

The isothiazoline biocides used in this study (OIT and CIT/MIT) were obtained from Clariant UK. The CIT/MIT in solution had a concentration of 1.59 wt %, and in a ratio of 3:1 with a molecular weight of 137.5 Dalton. OIT was also supplied as a solution with a concentration of 45.7 wt %, and a molecular weight of 213 Dalton. Six carriers (Infilm 939, Suprex, New Zealand halloysite, and NPD-16A, carplex CS-5 and mineral colloid BP) were selected for use in this study. Due to the lack of a controlled-release mineral on the market, the silica carplex CS-5 was used as a control. This mineral:

- Possesses a high degree of porosity, which is useful in sorption isotherm studies
- Has the ability (and is currently used in industry) to carry unwanted compounds present in beer production
- Has a high surface area

### 5.2.2 HPLC settings

The HPLC used was an isocratic system from Hitachi. It is composed of a pump, a UV detector, a column oven, an autosampler, an organiser for eluents and washing solutions, and a computer with appropriate software (EZCHROM elite) for data analysis. The mobile phases (eluents) used for analysing the two biocides in this study were composed of:

- For CIT/MIT: 12% acetonitrile, 1% glacial acetic acid and 87% deionised water
- For OIT: 25% deionised water and 75% acetonitrile.

These solvents were degassed prior to use (by stirring gently until all air bubbles have disappeared. A second degassing also takes place in the HPLC, before the eluent flows through the column). The HPLC works as follows:

- The solvent was delivered by the pump (via its own degasser)
- The sample was then injected by the autosampler
- The injected sample was separated in the column, whose temperature was kept constant at 30°C by the column oven
- The separated sample was thereafter detected in the form of a signal by the detector and peaks were observed on a graph at the time the separated sample exit the column.



The flow rate of the mobile phase was 1 ml/min and the autosampler was programmed to inject 30  $\mu$ l per sample in the column. Running time for each sample was 9 and 20 minutes for OIT and CIT/MIT respectively.

Samples of known concentration of biocides were prepared in order to obtain calibration curves used to determine the concentration of biocide in the aliquots (see Figure 5.4).

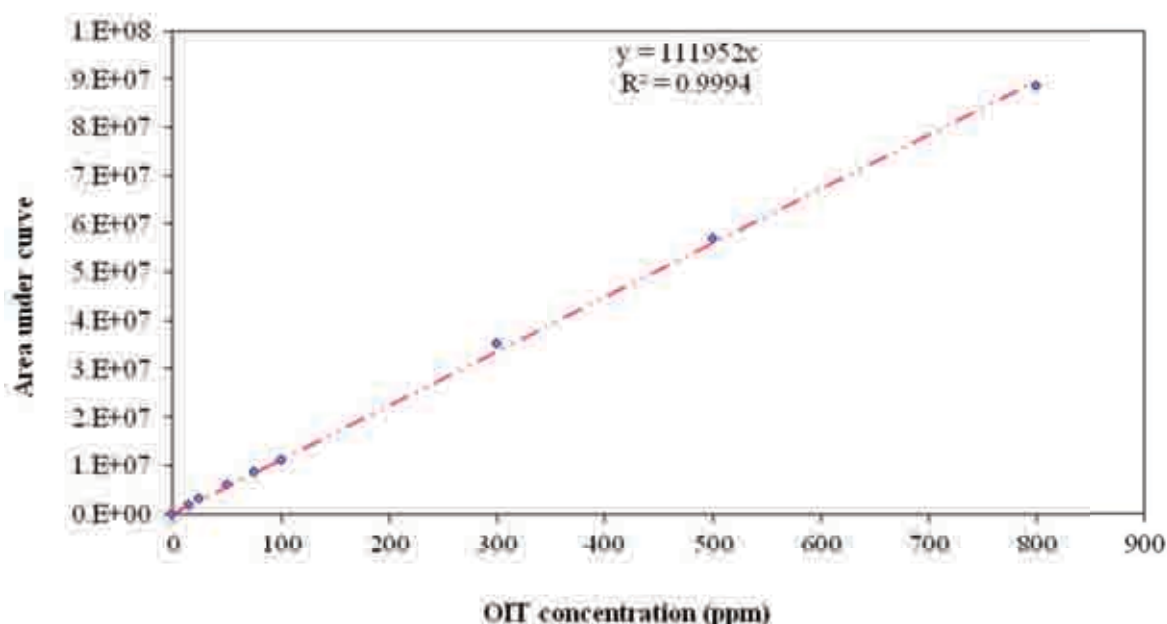


Figure 5.4: Calibration curve of OIT biocide of known concentrations obtained from the HPLC

### 5.2.3 Methods of adsorption

With the exception of New Zealand halloysite, the carriers (minerals) were impregnated with the biocides using a high shear mill (mixing the biocide and carrier for 1 minute). Varying volumes of biocides were used in the adsorption process (25, 50, 75, 100, 200, 300, 500, and

800  $\mu$ l). Due to density differences between the powders, varying amounts of mineral were used (in the mill) in this process and they were:

- 10 g for each of the two kaolins Infilm 939 and suprex, and also of the montmorillonite MCBP
- 5 g for the kaolin NPD-16A
- 2.5 g for the silica carplex CS-5

The impregnation of the halloysite tubes was achieved by mixing, in a beaker, 5 g of the mineral in solution of biocide prepared using the biocide volumes stated above. The biocide-Halloysite solutions were then placed in a vacuum oven (under vacuum) for two hours in order to:

- Displace air trapped within the Halloysite tubes
- Allow the biocides to penetrate the tubes

#### **5.2.4 Adsorption isotherm studies**

After the adsorption process, the impregnated carriers were then charged to deionised water (making a total volume of 1 litre) and allowed to equilibrate under constant stirring, for 180 minutes (using a magnetic stirrer). This process was performed separately for each of the carriers, with the exception of New Zealand halloysite. Aliquots of the suspension were taken at time interval, between 1 minute and 3 hours, and filtered using 0.4 $\mu$ m Millipore filters. Aliquots were also taken after encapsulating the biocides in the Halloysite tubes under vacuum in order to estimate the amount of the molecules that remains in solutions.

In order to assess the amount of the biocide that had eluted into solution and produce an adsorption isotherm for each of the minerals and biocides used, samples of known biocide concentrations were made and calibration graphs were produced (see Figure 5.4). All samples and aliquots were run on the HPLC. The shapes of the isotherms obtained were analysed according to Langmuir's classification of isotherms. Langmuir developed a theoretical basis for the classification of adsorption isotherms for solutes in dilute solution, which relates their characteristic shapes to parameters of the solvent and any second solute. This approach was based on four main assumptions:

- Maximum monolayer coverage ( $\theta$ )
- No interaction between adsorbate atoms / molecules
- Coverage is independent of binding energy
- There is a thermodynamic equilibrium of adsorption ( $k_a$ ) and desorption ( $k_d$ ) rate, ( $d\theta / dt$ ) being equal

Three of the four main classes (S, L, H) developed by Langmuir (see Figure 5.5) are accounted for by differences in relative magnitude of the activation energies of desorption of solutes and solvent. The S-shaped isotherm is also accounted for by an additional concentration-dependence of this parameter, implying cooperative adsorption. The linear (C) class is explained by penetration of the substrate's micropores by the solute, with or without the solvent, whereby new adsorption sites are opened up; the theory predicts the experimentally found sharp inflection to a plateau in the C-curves. Curves of the other classes can also in some cases show a linear branch above the turning point, representing conditions like those for C-curves.

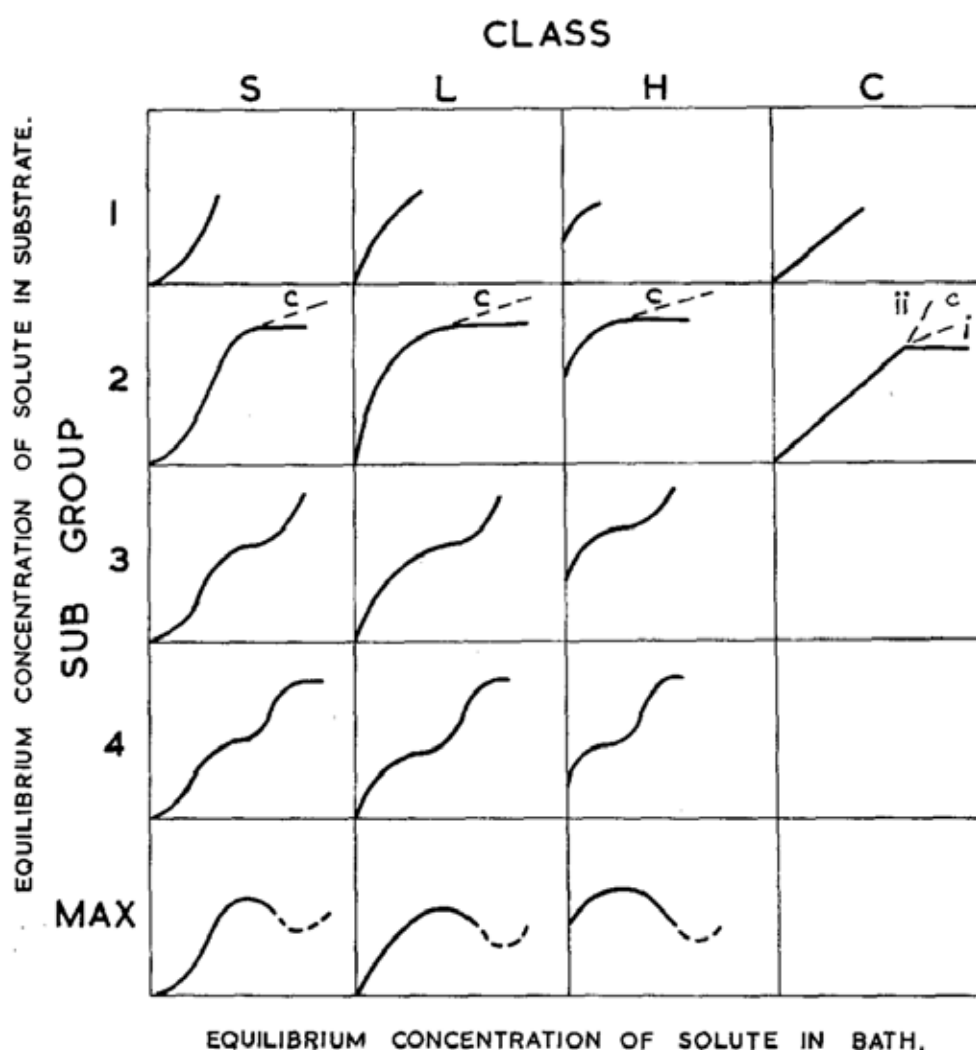


Figure 5.5: Langmuir system of isotherm classification [96-97].

The 2c subgroup indicates microporosity in the substrate, and in the C-class, the second branch of the curve in the subgroup 2 may be horizontal, or have a less steep ( $C_i$ ) or a steeper ( $C_{ii}$ ) slope than the main portion, according to the nature of the system. Though only subgroups progressing from I through 4 are shown these obviously can be extended to 5 or beyond if further rises and steps occur [96-97].

### 5.2.5 Results for OIT Adsorption on the selected minerals

Adsorption isotherms of OIT were carried out to determine the biocide loading capacities of the minerals. The molecular footprints of the biocide on the minerals (the area each molecule occupies on the surface) were calculated using this set of equations:

$$SL_1 \text{ (mmol m}^{-2}\text{)} = SL_0 \text{ (mg m}^{-2}\text{)} / \text{Mwt} \quad \text{Equation 5.3}$$

$$SL_2 \text{ (molecule m}^{-2}\text{)} = SL_1 \times 0.001 \times AV \quad \text{Equation 5.4}$$

$$\text{Molecular footprint (}\text{\AA}^2\text{ / molecule)} = 10^{20} / SL_2 \quad \text{Equation 5.5}$$

where SL is the biocide saturation level, Mwt its molecular weight, and AV the Avogadro number ( $6.02 \times 10^{23}$ ). The areas occupied by the biocide molecule on the surface of the minerals could also be obtained by calculating the bond lengths within the OIT molecule (both vertically and horizontally). This could give an indication of the geometrical position of the molecule on the surfaces of the minerals.

F  
N

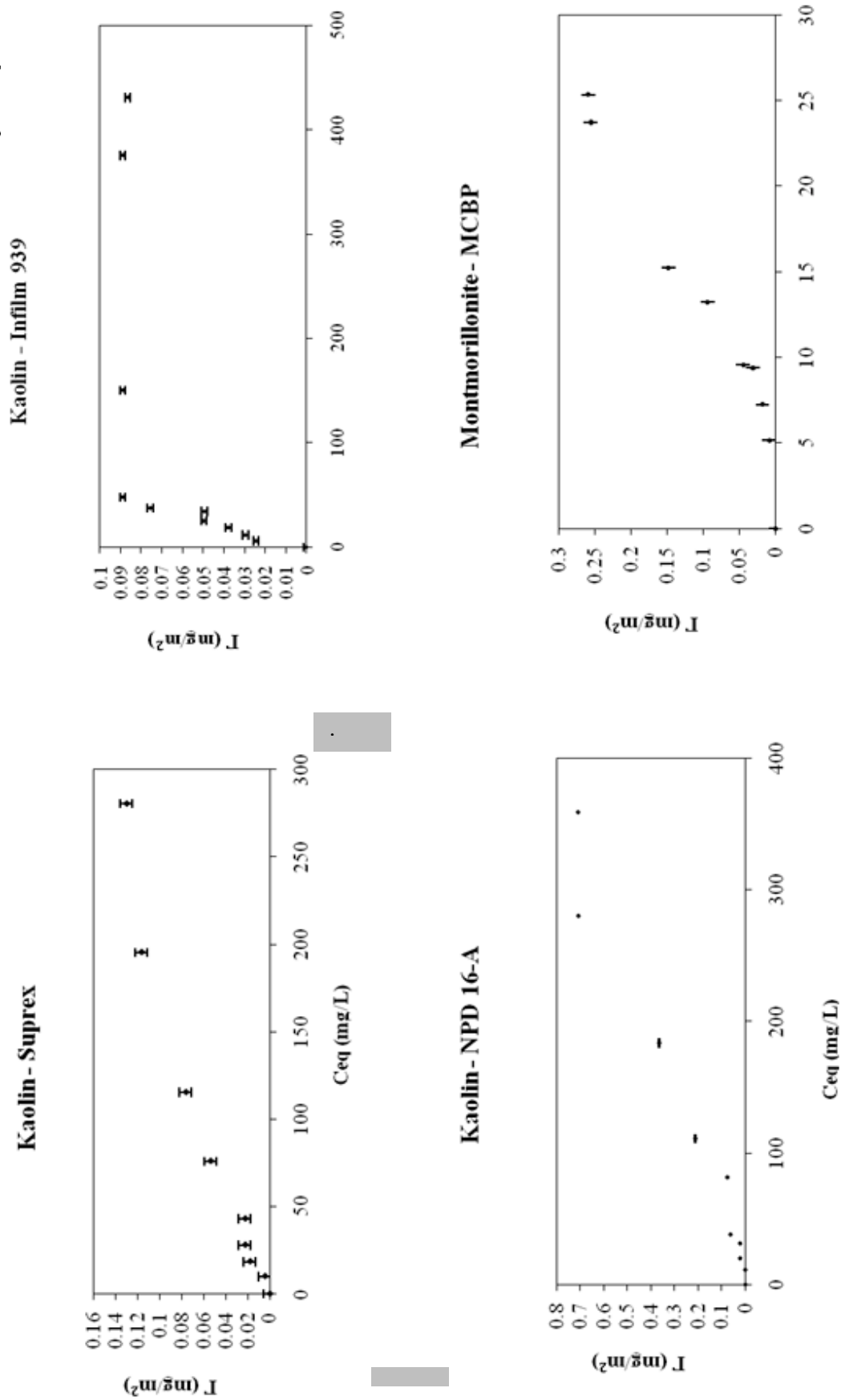


Figure 5. 6: OIT adsorption of the 4 platy clays used in the experiment: Infilm 939, Suprex, MCBP, and NPD 16-A

Figure 5.5 shows the adsorption of OIT on the four platy clays used. The maximum amounts adsorbed (saturation levels) are listed in Table 5-2, together with the corresponding areas the biocide occupies on the various minerals. For each of the points on the 4 curves, 8 measurements were made, and the means were taken to determine the concentration of the biocide in water. NPD-16A appears to have the highest OIT saturation level, followed by MCBP. The shape of the isotherms suggested that they were of the S and L classes Langmuir isotherms [96-97] . Suprex, infilm 939, and NPD-16A have an L-2 type Langmuir isotherm (isotherms with a convex shape and with a plateau). L-type isotherms are normally constant as the concentration approaches zero. The high surface area montmorillonite has an S-2 type Langmuir isotherm (isotherms with a concave shape at lower concentrations, also with a plateau).

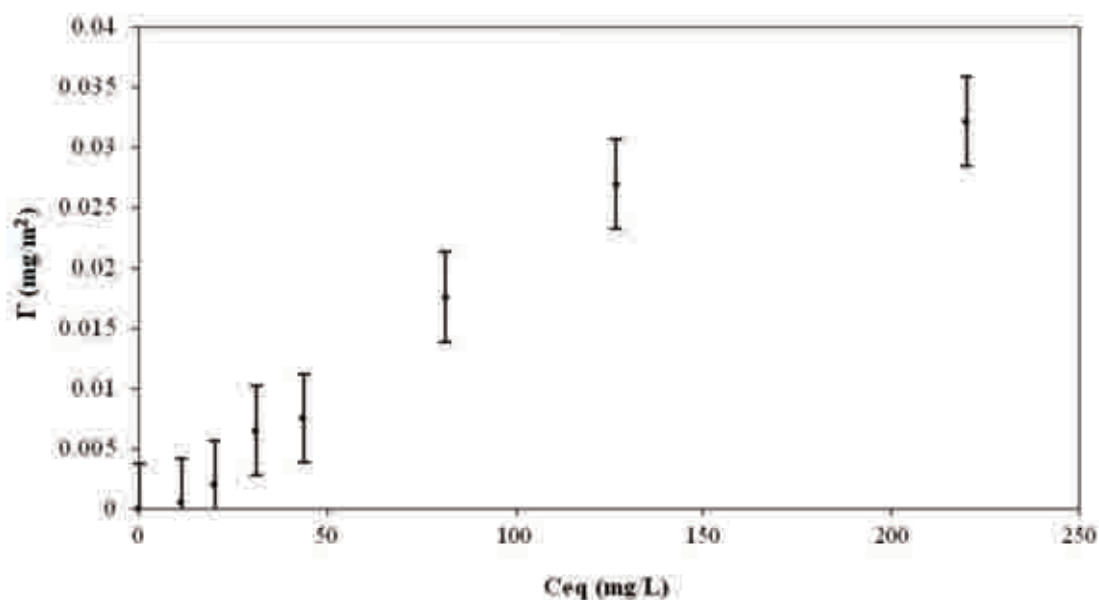


Figure 5.7: New Zealand halloysite adsorption of OIT

Figure 5.7 shows the isotherm for this tubular mineral was also of the L-2 type (Langmuir), with a convex shape and a plateau indicating the saturation level of the biocide. The biocide saturation level for this mineral is smaller than those of the platy minerals. This was in line with the findings of the isotherm study on the FMC. The saturation level and its corresponding footprint are listed in Table 5-2

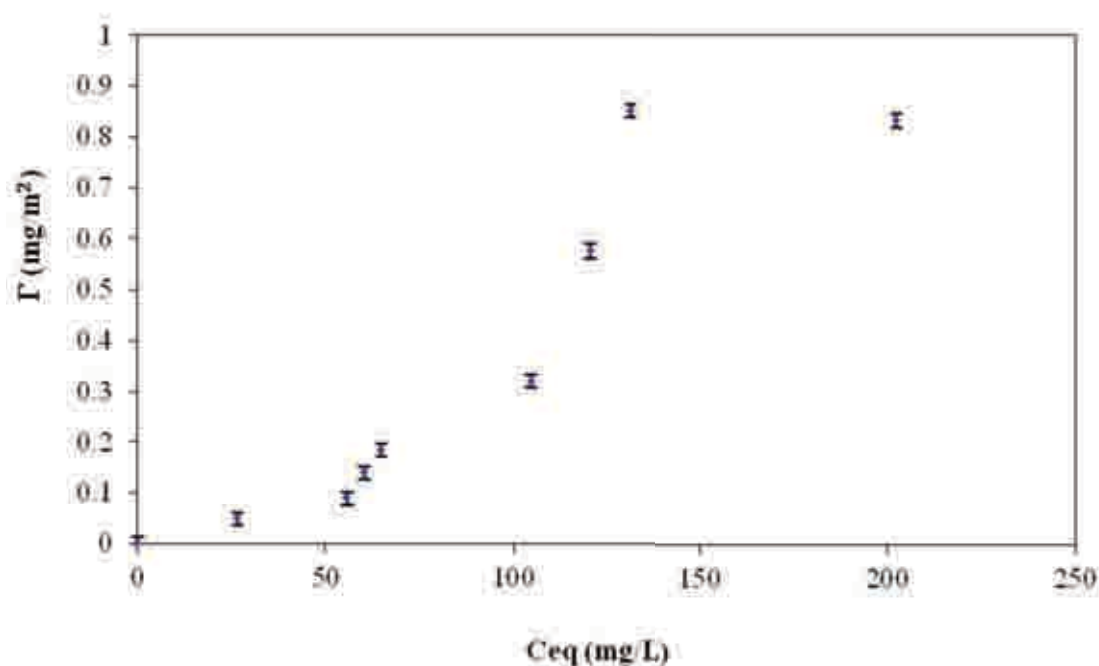


Figure 5.8: Silica - Carplex CS-5 adsorption of OIT

The isotherm for the carplex mineral is shown in Figure 5.8, and of the S-2 type (Langmuir), with a concave shape and a plateau. The saturation level appears to be the highest of all the minerals tested (almost 0.9 mg/m<sup>2</sup>), and is listed in Table 5-2, together with the corresponding molecular footprint of the biocide onto the Silica.



**5.2.6 Adsorption of CIT/MIT on carriers**

Adsorption isotherms of CIT/MIT were also carried out on the same six minerals mentioned in section 5.2.1 in order to estimate their loading capacities.

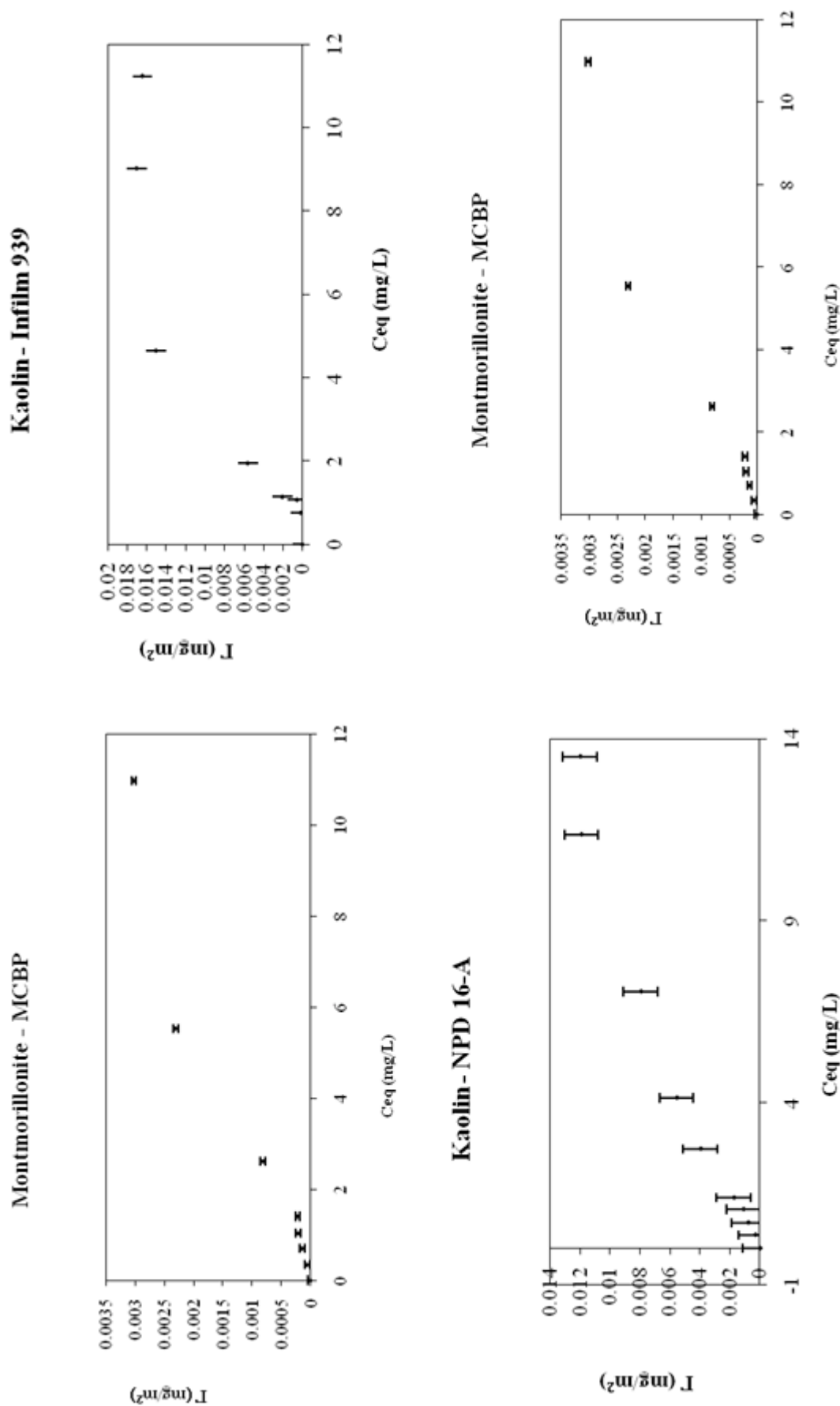
Fi  
Su

Figure 5.9 shows the adsorption of CIT/MIT on the same four platy clays as in Figure 5.8. The biocide's saturation levels are listed in Table 5-2, together with the corresponding areas it occupies on the various minerals. For each of the points on the 4 curves, 8 measurements were made, and the means were taken to determine the concentration of the biocide in water. Infil 939 appears to have the highest saturation level for CIT/MIT, followed by NPD-16A, with MCBP having the lowest level of adsorbed biocide. This was almost the reverse of the previous experiment where Infil had the lowest level for OIT, and could be due in part to the different functional groups of the two biocides ( $C_8H_{17}$  on OIT and  $CH_3$  on CIT/MIT) adsorbing differently to the surface of the minerals. The shapes of the isotherms were very similar to those of CIT/MIT. Suprex, infilm 939, and NPD-16A have an L-2 type Langmuir isotherm (isotherms with a convex shape and with a plateau, constant as concentration approaches zero). The high surface area Montmorillonite has an S-2 type Langmuir isotherm (isotherms with a concave shape at lower concentrations, also with a plateau).

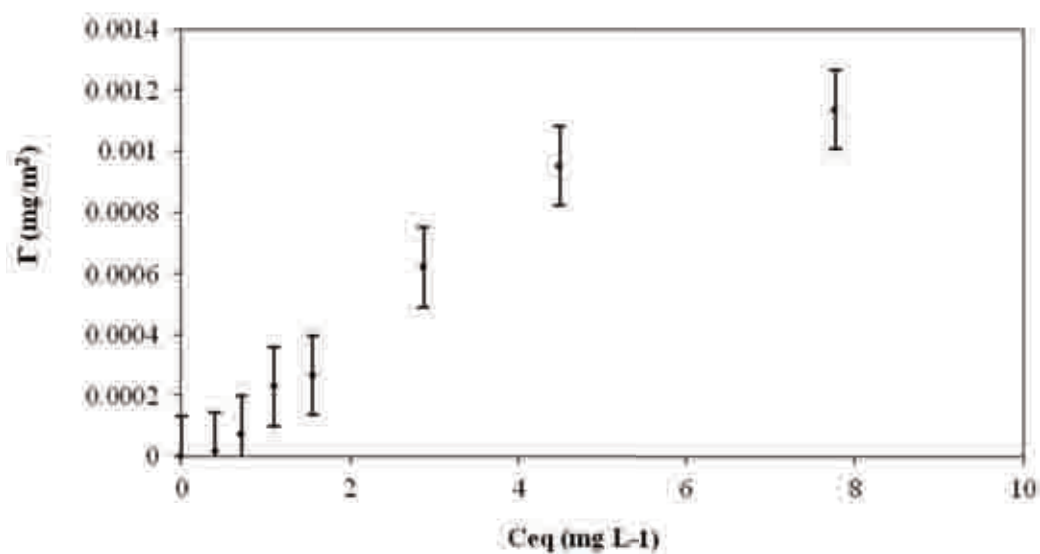


Figure 5.10: New Zealand halloysite adsorption of CIT/MIT

The isotherm for the tubular halloysite shown in Figure 5.10 was also of the L-2 type (Langmuir), with a convex shape and a plateau indicating the saturation level of the biocide. The biocide saturation level for this mineral was smaller than those of the platy minerals, possibly due to its shape and very small pore diameter. The saturation level and its corresponding footprint are listed in Table 5-2

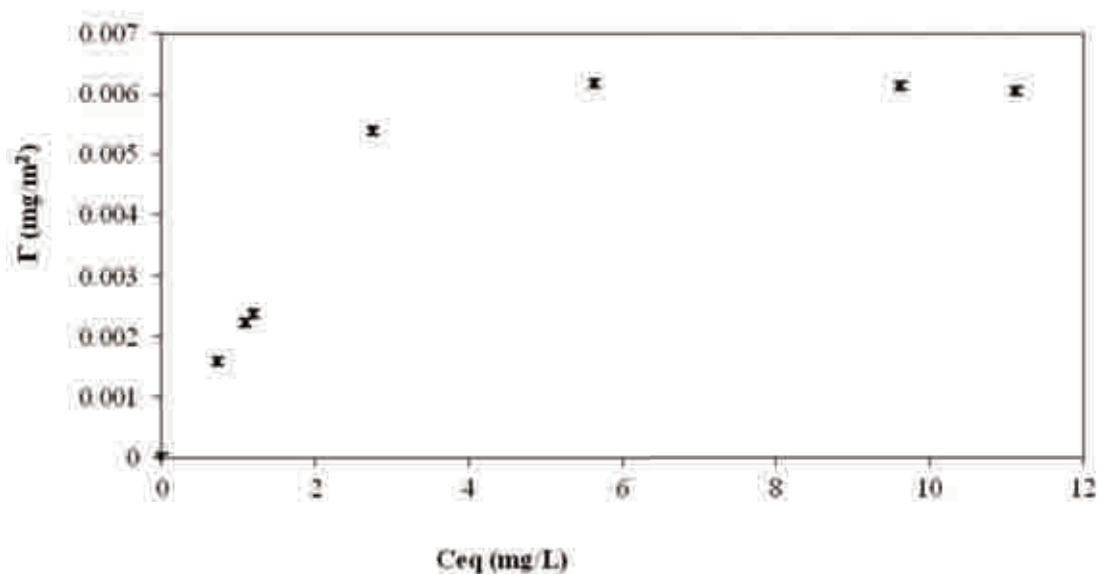


Figure 5.11: Silica - Carplex CS-5 adsorption of CIT/MIT

Figure 5.11 shows the adsorption isotherm for carplex mineral. The isotherm for this amorphous and highly porous mineral was of the L-2 type (Langmuir), with a convex shape and a plateau indicating the saturation level of the biocide. This isotherm was of the S type when OIT was adsorbed to the mineral, but changed to the L type when CIT/MIT was adsorbed, and may be due to the difference in the chemistry of the functional groups of the

Table 5.2: Saturation levels and molecular footprints of the biocides on the minerals

	S.A. (m <sup>2</sup> /g)	OIT			CMTT			Ratio CMTT/MTT to OIT [3]
		Saturation level (mg/m <sup>2</sup> )	Footprint (Å <sup>2</sup> /molecule) [1]	Isotherm shape	Saturation level (mg/m <sup>2</sup> )	Footprint (Å <sup>2</sup> /molecule)	Isotherm shape	
Kaolin Suprex	25	0.13	272	L-2	0.005	7100	L-2	26.1
Kaolin Infilm 939	22	0.08	410	L-2	0.016	2218	L-2	5.4
Kaolin NPD- 16A	22.8	0.7	50	L-2	0.01	3550	L-2	71
New Zealand Halloysite	50	0.03	1104	L-2	0.001	35500	L-2	32.1
Silica Carplex	150	0.83	43	S-2	0.006	5916	L-2	138.8
Montmorillonite MCEP	39 & 800 [3]	0.26	136	S-2	0.003	11833	S-2	87

[1] Area occupied by the biocide molecule on the surface of the minerals

[2] Ratios in table indicate those of footprint data between CMTT/MTT and OIT

[3] Surface area when MCEP is dry and wet respectively

biocides used. This saturation level of CIT/MIT on this mineral is listed in Table 5-2, together with the corresponding molecular footprints of the biocide onto the Silica.

The areas occupied by OIT on the minerals were calculated from the corresponding saturation level values of the biocide on the isotherm curves (see Table 5:2). These areas indicated that:

- The area occupied by one molecule of OIT adsorbing on Carplex CS-5 was  $43 \text{ \AA}^2$ , with the biocide's footprint on this mineral being 2, 3.2, 6.4, 9.6 and 26 times lower than those of NPD-16A, MCBP, suprex, infilm 939 and New Zealand halloysite respectively. This silica was the best performing mineral in term of space occupied by the OIT molecules.
- Of the three kaolins used, NPD-16A can carry 5.4 times more OIT than suprex and 8.2 more than infilm 939, although these minerals have similar surface areas (22.8, 25 and  $22 \text{ m}^2/\text{g}$  respectively). This is probably due to differences in their surface chemistries and crystal arrangement, effects of chemical and/or mechanical surface treatment.
- OIT occupies 3.2 times more space on MCBP than on carplex CS-5 (surface areas are  $800$  and  $150 \text{ m}^2/\text{g}$  respectively). This is primarily due to differences in the basic structures of the minerals, with MCBP being a platy 3 layer 2:1 clay, and carplex an amorphous silica, and also to the ways these minerals adsorb the biocide (see Figure 5.6 and 5.8 for MCBP and carplex adsorption respectively).
- There was no surface area effect as thought prior to the experiments (where the highest surface area minerals will adsorb more biocides molecules than the lower

surface area kaolin), as NPD-16A ( $20.8 \text{ m}^2\text{g}^{-1}$ ) outperformed MCBP ( $800 \text{ m}^2\text{g}^{-1}$ ).

- The standard deviations for the points on all the isotherms were very low, varying between  $0.001$  and  $0.108 \text{ mg/m}^2$ , suggesting the data points were closely clustered around the mean values.

For CIT/MIT biocide, the molecular footprints indicated that:

- The mineral that adsorbs the most biocide was Infilin 939. The footprint of the biocide on this mineral was 1.6, 2.6, 3.2, 5.3 and 16 times lower than those of NPD-16A, carplex CS-5, suprex, MCBP, and New Zealand halloysite respectively.
- The dispersant-free kaolin (suprex) seemed less favourable to the biocide absorption and could adsorb 3.2 times less CIT/MIT than Infilin 939, although both minerals possess similar surface areas. This was probably due to the lack of chemical surface treatment of suprex causing most of the clay's layers to stick together, and consequently reducing the available surface area for biocide adsorption
- Kaolin NPD-16A can carry 10 times more CIT/MIT than the halloysite despite the latter having more than twice the surface area of the former. This is probably due to the morphologies of the clays, with the platy kaolin NPD 16A more likely to expose the areas between its plates to the biocide than the tubular halloysite (which required air trapped in the tubes to be pumped out under vacuum, and replaced by the biocide)
- Of the three kaolins examined, NPD-16A can also carry twice as much biocide than suprex, but 1.6 times less than infilm 939. This is probably due to the effects of different chemical and/or mechanical surface treatments of the minerals
- The silica carplex CS-5 could carry twice as much CIT/MIT than the

montmorillonite MCBP, although the surface area of the montmorillonite is 5.3 times higher (in the wet form) than that of the silica. However, it was found that the lower surface area kaolin NPD-16A ( $22.8 \text{ m}^2/\text{g}$ ) performed much better than both silica and MCBP. This is an indication that, like with the OIT molecules, there was no surface area effect

### 5.3 Discussion

Carplex CS-5, a silica from Degussa, Japan, was used in this study as a control because it showed, in previous studies, the potential to absorb more biocides than silica of higher surface areas tested.

The biocide adsorption process showed that low surface area minerals were able to carry the isothiazoline biocides, contrary to previous studies stating otherwise [86]. The ratios in Table 5:2 were those of the footprint data between the two biocide molecules. They indicated that all the minerals used in the adsorption process favour OIT (with OIT occupying less space on the minerals). This could be due to the orientation of the biocide molecules as they adsorb onto the minerals, with the more hydrophobic octyl side chain on OIT away from the minerals' surfaces, whereas the hydrophilic Methyl on CIT/MIT was participating in the adsorption process. From the footprint ratio values, infilm 939 seemed to be more efficient at carrying the two biocides, albeit in small quantities. It appeared that with an appropriate surface treatment (use of an appropriate surfactant with a strong affinity to the biocide, or milling the clay in order to increase the surface area available for the biocide), this mineral could be efficient at carrying greater quantities of both OIT and CIT/MIT. The silica's high ratio value suggested that the mineral's structure favoured the OIT molecule.



The shape of the isotherms gave an indication of the way the biocide molecules covered the surface of the carriers. Langmuir isotherms implied that:

- There was a co-operative adsorption between the absorbates (biocides) and the substrates (minerals)
- There was monolayer coverage of the minerals' surfaces by the biocide molecules.

The HPLC used was very sensitive and accurate (as described in section 3.2.3.3), detecting biocide concentrations between 1 and 2000 parts per million. Most of the data obtained were repeated, using a UV-Vis spectrophotometer, albeit not at concentrations below 5 and above 100 parts per million.

The Flow Microcalorimetry technique used offered the opportunity to understand the strength of the bonds existing between the biocide and the minerals after the adsorption process. These bonds were thought to arise as a result of weak Van der Waals forces or electrostatic interactions. Heat and concentration measurements from the FMC were made under flow condition (dynamic), unlike the adsorption isotherm performed in a static condition. These data confirmed one of the findings of the isotherms, which was that low surface area minerals (less than  $50 \text{ m}^2\text{g}^{-1}$ ) were able to adsorb the isothiazoline biocide. Nevertheless, the desorption energies indicated that the minerals held to the biocide with differing levels of strength (from almost irreversible adsorption with the diatomaceous earth celtix to completely reversible with the kaolin NPD-16A).

The isotherms and FMC results indicated that montmorillonite MCBP and silica carplex CS-5 were the best OIT adsorbing minerals in both static and dynamic environments. The

calculated values of the adsorbed biocide were:

- For MCBP: 105 and 205 mg/g for the FMC and isotherm respectively
- For Carplex: 88 and 125 mg/g for the FMC and isotherm respectively

The differences in values between the two methods were probably partly due to the different adsorption processes used (dry adsorption in the high shear mill for the isotherms, and wet adsorption in cyclohexane for the FMC, both causing different amounts of OIT to adsorb to the minerals), and also in part because in the static environment, the adsorbed values included loosely bound biocide molecules. These loosely bound biocide molecules were flushed away in the FMC under flow condition. The two methods also showed that New Zealand Halloysite, NPD-16A, Infilm 939 and Suprex were the worst performing minerals (for biocide adsorption), and consequently were not selected for the bioassay experiment.

The isotherms and FMC results indicated that varying amounts of the isothiazoline biocides adsorbed to the surface of the minerals used. The FMC data also showed the strengths of these attachments. However, the length of time these biocides molecules could remain on the surface of the minerals (hence the minerals controlled release potentials) could not be determined this way, and a desorption experiment was set up to assess this (and is described in chapter six).

# **CHAPTER SIX**

## **OIT DESORPTION STUDIES**

The objective of this chapter is to study the desorption profiles of the minerals that showed the highest adsorption potentials from the FMC work (see Chapter 5), namely MCBP (montmorillonite), Carplex (silica), T-38 (calcium silicate) and Celtix (diatomaceous earth). Supreme clay (the kaolin) was added to this list, as this clay is used in the paint industry as functional filler. The kaolins infilm 939, suprex, NPD-16A and New Zealand halloysite were discarded from this experiment as they showed, from the FMC experiment, the lowest OIT adsorption potential. The experiments were carried out to assess and compare the desorption profiles of OIT-mineral complexes in paint films, and also OIT and minerals freely added to paint films. The CIT/MIT biocide was dropped for the remainder of the study because:

- The adsorption experiment in Chapter 5 showed that the area occupied by this biocide on any of the minerals used was far greater than that of OIT
- CIT/MIT could not be obtained in its pure form (100%), hence it was not also possible to use it for the sorption experiments on the FMC
- OIT is the biocide of interest for paint applications such as interior and domestic coatings

## 6.1 Materials and Methods

The method of OIT adsorption onto the carriers was discussed in section 5.2.3 of the previous chapter. Upon adsorption of the OIT, the biocide-loaded minerals were added to an exterior paint formulation. However, two paint formulations per mineral used were made:

- The first formulation method contained the mineral loaded with the biocide (biocide adsorbed to the mineral prior to use; this is denoted as “mineral / OIT”).
- The second formulation method contained the mineral, together with the independently added biocide (biocide not adsorbed to the mineral prior to use; this is denoted as “mineral + OIT”), and considered the standard in this experiment.

These treatments were made in order to compare the two desorption profiles of the biocide. Paint drawbacks were made on Leneta paint charts obtained from Leneta, New Jersey, USA. The painted Leneta sheets (2 per mineral) were then dried at a temperature of 23<sup>0</sup>C (within 2<sup>0</sup>C) and a relative humidity of 50% (within 5%) for 24 hours. One disc from each sheet was cut out using the hole punch, and weighed. A disc was also cut out of a clean (non painted) Leneta chart, weighed, and its mass subtracted from that of the dried painted sheet. This was done to obtain the mass of the paint on the Leneta sheets, and hence the exact concentration of OIT available for use in the desorption experiment.

### 6.1.1 Typical paint formulation

The paint made was an exterior coating, according to a formulation that is covered by a secrecy agreement. Various modifications of the initial formulation were made to account for those detailed in section 6.1, but cannot be discussed in this thesis.

Ten paint films were made in total, two for each of the minerals used (MCBP (montmorillonite), Carplex (silica), T-38 (calcium silicate) and Celtix (diatomaceous earth). Supreme clay (the kaolin). The first formulation was used as a control, where both the biocide and mineral were added independently to the paint. The second formulation, containing the mineral-biocide complex, was compared to the first. The in-can biocide,

generally designed to protect any paint film from microbial degradation, was removed from the formulations made in order to prevent competition between that biocide and OIT for attachment to the minerals' surfaces. OIT was added to the formulations at the saturation level determined from an experiment aimed at finding the concentration needed to kill the micro-organisms (described in Chapter 7).

Each of the 10 paints needed for the desorption study was made according to a standard paint making procedure:

- The dry components of the paint formulation (all the powders used) were weighed out in a dish
- The wet components (solvents) were also weighed out into a paint tin
- The dry components were then added to the wet component in the paint tin, and mixed at 1500 rpm for 5 minutes using a Dispermat high shear mixer
- The mixer was stopped after that time, the impeller cleaned, and the components mixed again at 4000 rpm for 15 minutes
- After that time, the mixer was turned down to 2000 rpm, the remaining components were weighed and added to the solution. Some of these components were added very slowly to the paint in order to avoid a pH shock and to provide a physical crosslinking in the film, as the hydroxyl groups on the partially hydrolysed titanate interact by H-bonds to the functional groups on the polymer particles.

### **6.1.2 Method of desorption measurement**

The concentration of OIT in the dried paint was then calculated using this equation:

$$\text{OIT in paint (ml/g)} = \left\{ \frac{\text{Total OIT (ml)}}{\text{Total paint (g)}} \right\} \cdot \text{Weight of dried paint (g)} \quad \text{Equation 6.1}$$

The total active OIT in the paint made was 0.9 ml (45% of 2 ml used), and the total weight of the paint made for each of the minerals was 400 g. The exact amounts of active OIT in the painted Leneta discs were tabulated, and are shown in Table 6.1

Table 6.1: Amount of OIT in dried films on Leneta discs

	<b>Total Weight of paint on disc (mg)</b>	<b>OIT concentration in the dried paint (ml/g)</b>
MCBP / OIT (*)	46.3	0.104
MCBP + OIT (**)	52.8	0.119
Carplex / OIT	58.4	0.131
Carplex + OIT	52.6	0.118
Supreme / OIT	45.9	0.103
Supreme + OIT	52.3	0.118
T-38 / OIT	47.2	0.106
T-38 + OIT	45.2	0.102
Celtix / OIT	46.4	0.104
Celtix + OIT	47.4	0.107

(\*): Biocide adsorbed to the mineral, and the complex added to the paint

(\*\*): Biocide and mineral independently added to the paint, with no prior adsorption

The discs obtained from the Leneta sheets (see section 6.1) were added to 200 ml of deionised water in plastic beakers, and the beakers were placed on a laboratory rotator / shaker (Electrolab Rocking Shaker) operating at a constant speed of 10 rpm. The painted discs were submerged in order to simulate wet atmospheric conditions affecting painted

outdoor surfaces, resulting in the loss of biocide from the paint films. The work was undertaken in a static environment, and care was taken to select the amount of water necessary to:

- Submerge the painted Leneta sheets
- Potentially dissolve all the biocide present in the paint film before the water becomes saturated with the biocide.

During the desorption process, aliquots were taken at time interval (30 seconds, 5, 10 and 30 minutes, 1, 2, 4, and 6 hours, 1, 2, 3, 5, 6 and 7 days). The concentrations of OIT in these aliquots were determined experimentally using HPLC. The settings of the HPLC, together with the concentration of acetonitrile (HPLC mobile phase) used for OIT were described in section 3.2.3.1 of Chapter 3.

## **6.2 Results of the desorption experiments**

As there were two treatments per minerals (OIT adsorbed onto the minerals, and OIT independently added to the paint films), the data for each mineral were plotted on a graph, and discussed in order to compare the desorption profiles of the two treatments. The initial OIT concentrations in the dried paint films (see Table 6.1) were converted to percentages (100%, as they were the starting biocide concentrations in the films), together with the amounts of OIT in the aliquots collected. In all the following graphs, mineral / OIT denotes mineral to which OIT is attached, and mineral + OIT denotes mineral free of OIT, prior to its addition to the paint films.



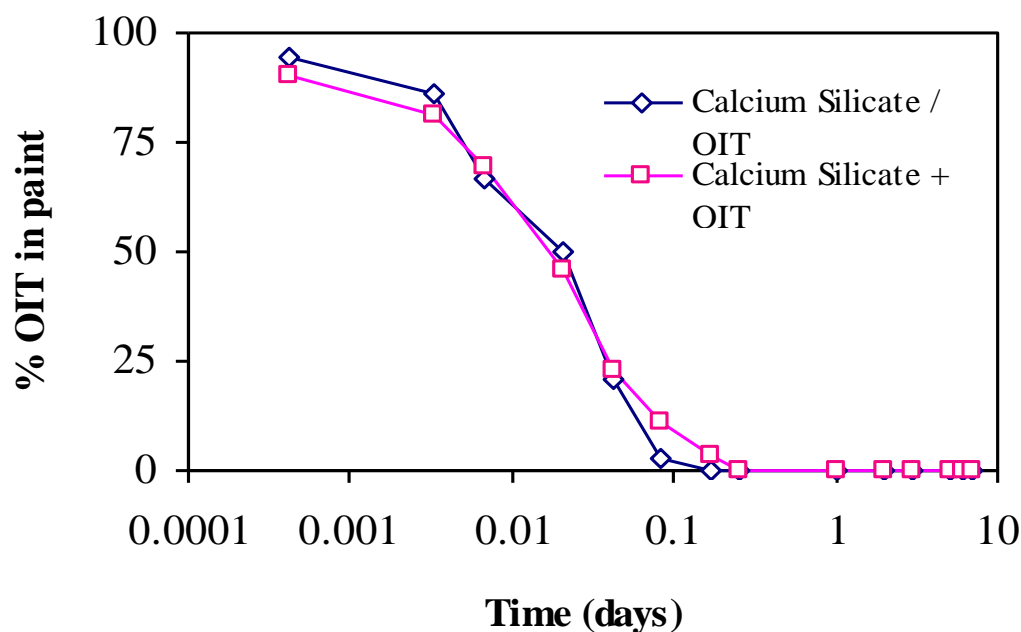


Figure 6.1: OIT release profile from adsorbed (◇) and non-adsorbed (□) OIT to Calcium Silicate T-38

The respective release times of OIT were put on a log scale in order to fully understand the trends from the start of the desorption process up to the end of the first day. Figure 6.1 shows that the release profile of OIT from the calcium silicate T-38 was almost identical for the 2 treatments. It could be seen that half the biocide content of the paint films had already eluted in water just after 30 minutes. The paint films appeared to be totally depleted of their OIT content after just 4 hours of their submersion into the water, indicating the mineral's poor retention of the biocide from paint films. This finding was in sharp contradiction with the results from the experiment on the FMC (see Figure 5.3 of Chapter 5), which indicated that 54 mg/g of OIT adsorbed onto T-38 surface, and 11 mg/g desorbed from the surface under flow condition (20%, over a 3 hour period). This was probably due to components in the

paint films preventing the biocide from fully adsorbing to the surface of the mineral (mineral/OIT), or displacing the biocide from the mineral's surface (mineral + OIT), and hence accelerating its desorption.

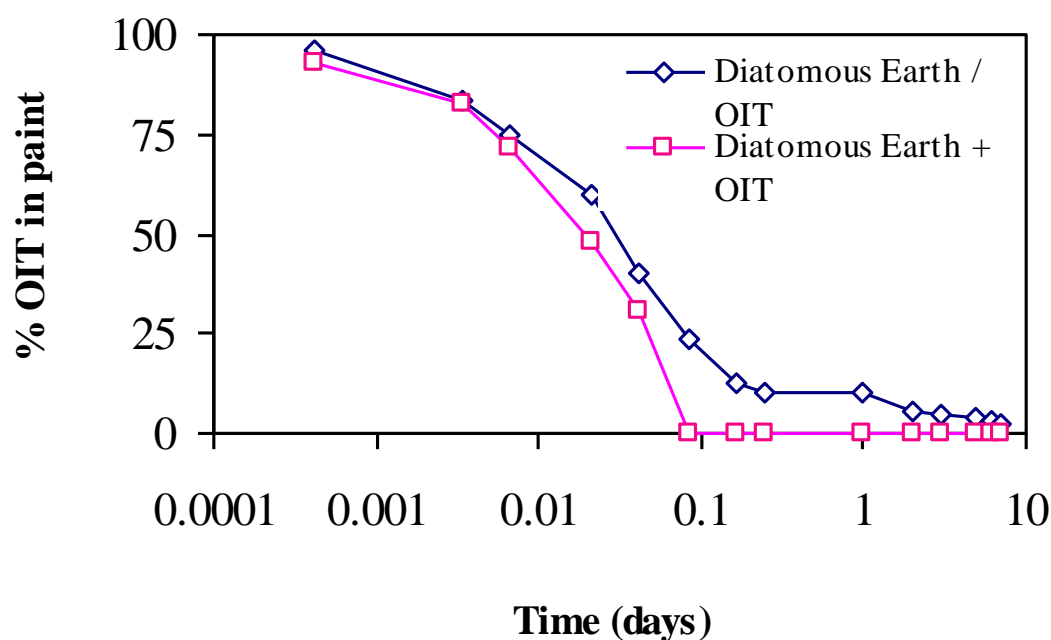


Figure 6.2: OIT release from adsorbed ( $\diamond$ ) and non-adsorbed ( $\square$ ) OIT to diatomaceous earth celtix

Figure 6.2 shows that the release profile of OIT was similar for both paint films containing the diatomaceous earth celtix for the first 10 minutes. However, the film with the independently added biocide (celtix + OIT) lost all its biocide content after 2 hours (the biocide molecules will migrate quickly to the surface of the paint films as there was almost no inhibition from the mineral), whereas the second film appeared to be depleted of its content only after 3 days (some degree of interference from the mineral). The experiment on

the FMC showed that 21.6 mg/g of OIT adsorbed onto this mineral (Figure 5.3), and 3.91 mg/g desorbed under flow condition (18%). Like with the calcium silicate T-38, this was probably due to components in the paint films preventing the biocide from completely adsorbing to the surface of the mineral (or removing it), and hence accelerating its desorption.

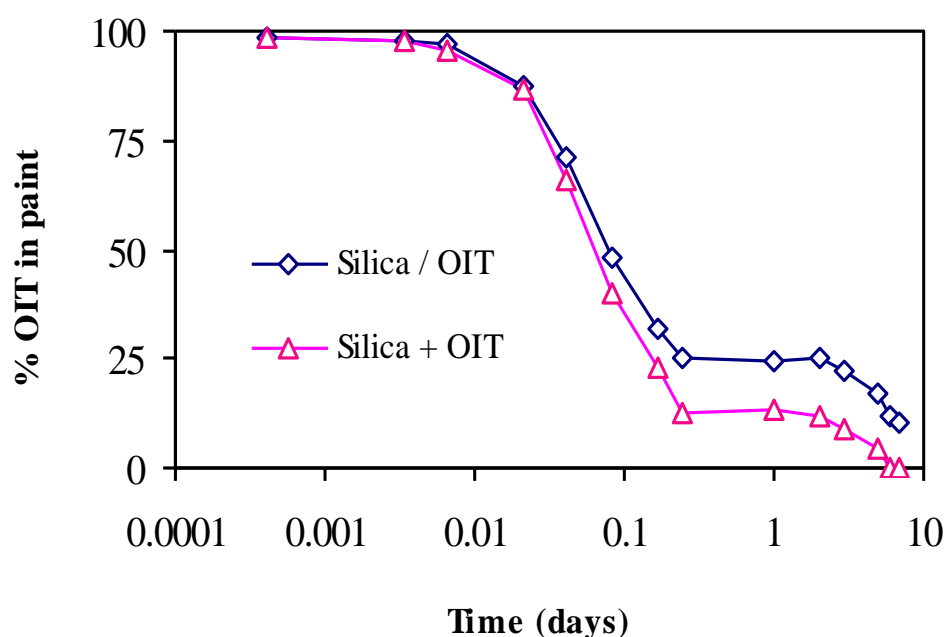


Figure 6.3: OIT release profile from adsorbed ( $\diamond$ ) and non-adsorbed ( $\Delta$ ) OIT to the silica carplex

Figure 6.3 shows the desorption of OIT from paint films containing the silica carplex. The profile appeared to suggest that the silica retained the biocide for a longer period of time than both the calcium silicate and the diatomaceous earth minerals. The biocide release profiles for the 2 paint films were identical for the first 30 minutes (87.5% and 87% of OIT left in the films, respectively for carlex/OIT and carplex+OIT). The paint film containing the

independently added mineral and biocide was totally depleted of its biocide content after 6 days, whereas the second film still retained almost 12% of its OIT content after the same time period, and 10.5% at the end of the experiment.

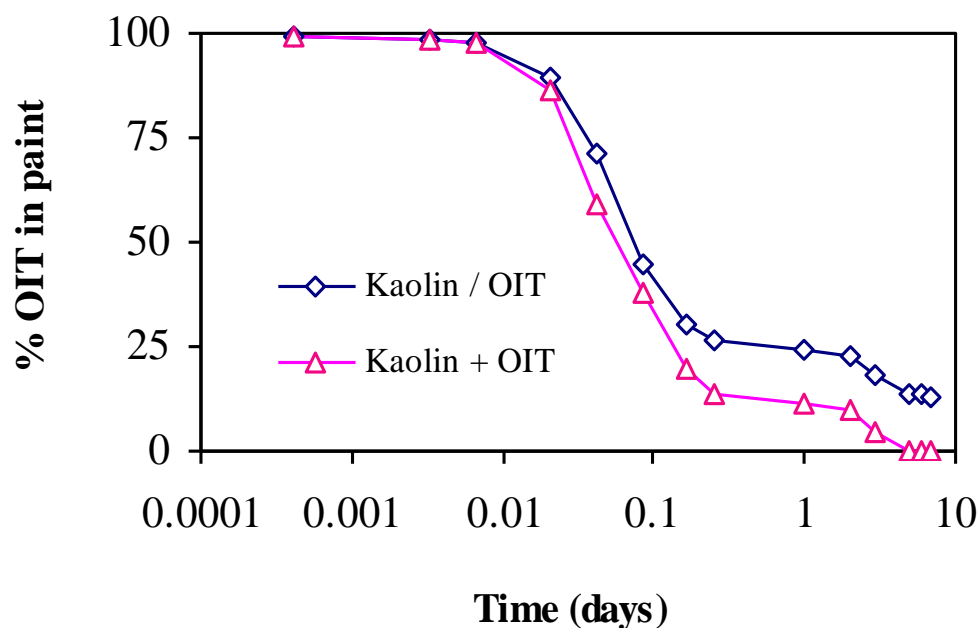


Figure 6.4: OIT release profiles from adsorbed (◇) and non-adsorbed (Δ) OIT to the kaolin clay supreme

Figure 6.4 shows OIT release profile from the supreme kaolin material. The data suggested that all the biocide eluted out of the paint film containing the freely added mineral and OIT within 5 days, whereas the other film still retained 13.6% of its OIT content after the same period, only decreasing to 13.2% after 7 days. The data also suggested there was significant OIT lost within the first 24 hours of the start of the experiments (more than 60%), possibly due in part to loosely bound OIT molecules (those that physisorbed onto the surface of the

mineral) being removed by the water.

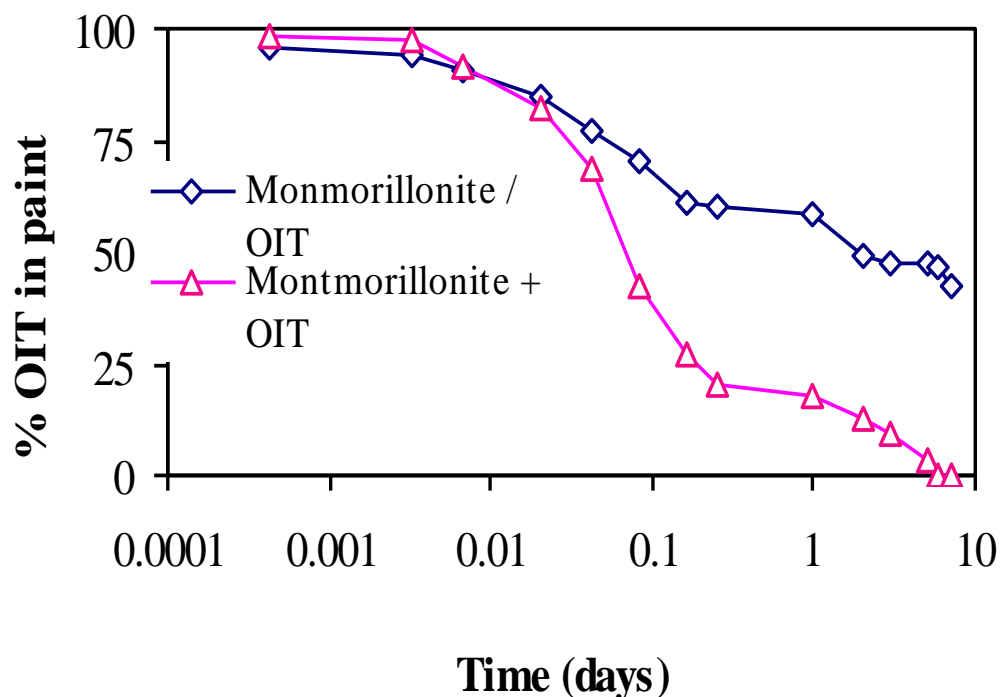


Figure 6.5: OIT desorption profiles from paint films with adsorbed ( $\diamond$ ) and non-adsorbed OIT ( $\Delta$ ) to montmorillonite clay MCBP

Finally, Figure 6.5 shows the release profile of OIT from the montmorillonite MCBP. This mineral shows the best OIT desorption profiles of all the minerals used in this study. The profiles of the two paint films were similar up to the first half hour of the start of the desorption experiment. After the first day of the experiment, almost 60% of OIT still remained in the paint film containing the biocide-Impregnated Montmorillonite, whereas the second film (MCBP + OIT) only still held on to just over 17% of its OIT content. This latter film was eventually depleted of its biocide content after six days, whereas the former film

Table 6.2: Percentages of biocide still remaining in the paint films after the desorption experiment

Time	MCBP/ OIT	MCBP+ OIT	Carplex/ OIT	Carplex +OIT	Supreme /OIT	Supreme+ OIT	T-38/OIT	T-38+OIT	Celtix/OIT	Celtix+OIT
0	100	100	100	100	100	100	100	100	100	100
30s	95.4	97.9	98.4	98.4	99.1	98.9	94.7	90.2	96.1	93.1
5 min	93.8	97.1	97.9	97.5	98.5	98.7	86.4	81.1	83.5	82.7
10 min	90.5	91.2	97.1	95.8	97.6	97.9	66.8	69.1	74.9	71.5
30 min	85.2	82.1	87.5	87	89.4	86.2	49.9	45.6	60.0	47.9
1 h	76.8	68.5	71	65.8	71.2	58.7	20.7	23.2	40.5	31
2 h	70.6	42.2	48	40	44.7	38.1	2.5	11.2	23.4	0
4 h	60.7	26.8	31.7	23	30.4	19.7	0	3.6	12.9	0
6 h	59.8	20.1	25.2	12.5	26.5	13.6	0	0	10.3	0
1 day	58.3	17.4	24.4	13.4	24.1	11.4	0	0	9.9	0
2 days	49	13	25.3	12.2	22.4	9.8	0	0	5.6	0
3 days	47.6	9.4	22.5	8.6	18.3	4.5	0	0	4.4	0
5 days	47.1	3.7	16.8	4.12	13.6	0	0	0	4.2	0
6 days	46.2	0	11.7	0	13.5	0	0	0	3	0
7 days	42.3	0	10.5	0	13.2	0	0	0	2.3	0

(MCBP / OIT) still retained more than 40% of its biocide content after seven days.

### 6.3 Discussion

The experiments described in this chapter were carried out to obtain and compare the desorption profiles of OIT adsorbed (and non-adsorbed) to minerals added to an external paint formulation. The existing paint “in can biocide” was not added to the formulations made in order to prevent competition between that biocide and OIT for attachment to the surfaces of the minerals. The removal of the “in can biocide” did not compromise the integrity of the paints, as there was no bacterial colonisation, possibly due to the presence of OIT (for this study, and the subsequent longer Bioassay work, see in Chapter 7). All the paints were made under the same standard conditions of temperature, humidity, and drying time, and the paint films on the Leneta plates had the same thickness. As desorption was carried out in a static environment (unlike with the Flow Macrocalorimeter under flow condition), a significant amount of water was used (200 ml) in order to submerge the plate and to allow the biocide to elute from the surface area available.

The experiment showed that the paint film with the biocide adsorbed to the kaolin supreme held on to 13.2% of its biocide content after seven days of desorption. The second film, with supreme and OIT freely added, was depleted of its entire OIT content after 5 days of the desorption experiment. This 1:1 platy clay has 13% of structural water, and is believed to entrap the biocide between its alumina and silica plates during the adsorption process. The biocide elutes by way of using the tortuous paths between the plates. There was, however, not a significant difference in the desorption of OIT between the 2 paint films, and a paint manufacturer may not want to go through the intercalation process, as this will add time and

some extra costs to the process.

Calcium silicate (T-38) was the worst performing mineral for the desorption of OIT. Both films (independently added and pre-mixed OIT-mineral) were depleted of their entire biocide content after just six hours. This was possibly due to the structure of the mineral, as XRF data in Table 4-2 showed that it was mainly made of 46.3% silica, 30.9% calcium oxide and 19.2% of structural water. This significant amount of entrapped water molecule could be interfering with the adsorption of OIT. The second worst performing mineral was the diatomaceous earth (Celtix). The first paint film (with independently added OIT) was depleted of its biocide content after 2 hours, whereas the second film still held on to 2.3% of its biocide content after 7 days. The desorption profiles of this mineral showed a slight difference between the two treatments, and a net improvement to T-38. Celtix is composed of 91% silica and had less structural water molecules than T-38 (at just 4.2%), and this could have been a contributing factor in the improved profile compared with T-38. although both minerals performed better in the FMC desorption experiments, their performance could not be reproduced using paint films. Although both irregular shape minerals are currently used for filtration, they could not be used in controlled release systems in paints on the basis of the data presented, unless significant mineral surface modifications were carried out to improve the OIT adsorption. They were therefore discarded for the subsequent Bioassay experiment.

Carplex is a pure silica (99.88%  $\text{SiO}_2$ ), with no structural water within its core. The film with the OIT-adsorbed mineral retained 10.5% of its biocide content after 7 days, whereas the second film was completely depleted after 6 days of experiment. The data for this amorphous mineral were, however, very similar to those of the platy supreme clay. As the pores' size of



the mineral is the only factor affecting the release of the biocide, it is anticipated that their slight narrowing could significantly increase this release time (and amount).

The montmorillonite MCBP was by far the best performing mineral in this desorption study. The paint film with biocide adsorbed to the mineral still retained 42.3% of its OIT content, whereas the second film was completely depleted of its biocide content after 6 days. This clay has shown in all experiments that it was more efficient at adsorbing the biocide than any other mineral used, possibly due to its 2:1 structure. It consists of an octahedral sheet of silicate sandwiched between two tetrahedral sheets, and has a formula  $\text{Na}_{0.2}\text{Ca}_{0.1}\text{Al}_2\text{Si}_4\text{O}_{10}(\text{OH})_2(\text{H}_2\text{O})_{10}$ , and large surface area of  $800 \text{ m}^2\text{g}^{-1}$  when the clay is hydrated. This clay will expand upon hydration, allowing almost all biocide present to move within its plates, where it is believed the various cations present strongly participate in the adsorption process. The data suggested that this mineral could be used as a controlled release clay in paint formulations in order to release the biocide over a longer period of time. As the mineral expands, the amount used in the paint needs to be kept very low in order to preserve the structural integrity of the paint.

All the data showed a prolong release of the OIT when it was adsorbed to the minerals used (with the exception of the calcium silicate T-38). This was due to the fact that the biocide had to navigate within or between the structures of the minerals before being release into the water. It should be noted that these paints are not intended to protect structures that are constantly under water (ship hulls), but are more likely to find uses as paints for damp rooms such as kitchens and bathrooms, where mould growth is a particular problem. The best three performing minerals were chosen for the Bioassay experiment: supreme (kaolin), carplex CS-

5 (silica) and MCBP (montmorillonite).

# **CHAPTER SEVEN**

## **BIOASSAY STUDIES**

This chapter describes the work was carried out to determine the potency of a paint formulation to which biocide-loaded montmorillonite MCBP, silica carplex CS-5 and kaolin supreme carriers were added, in particular the ability of the paint film to significantly lower the level of micro-organisms or inhibit their growth. The time taken by the OIT molecules to elute out of the paint formulation was also estimated. Accelerated weather testing was initially used to simulate the damage caused by UV exposure, atmospheric moisture and precipitation on paint films. This artificial weathering was particularly useful for determining the effectiveness of the OIT controlled release potential of the carriers used. The paint formulation used in this experiment was the same as that in the desorption work described in Chapter 6, and is covered by a secrecy agreement. The three minerals were chosen because:

- They have a reasonably good adsorption potential in the adsorption experiment described in Chapter 5
- They displayed a slower desorption profile (see Chapter 6)

## **7.1 Materials and Methods**

In this section, the materials used and the methods of analysis were described separately. Details of the paint formulation used (various components, quantities used, equipment, time, humidity) cannot be revealed as they are covered by a secrecy agreement.

### **7.1.1 Biocide adsorption onto the minerals**

In this part of the bioassay process, water was first added to each of the dry powders and mixed well in order to form a paste (this process caused the montmorillonite to expand, but not the kaolin and the silica). Secondly, OIT was added to each of the pastes obtained, and

mixed again. The pastes were finally oven-dried at 30°C in order to release the water molecules and entrap the biocide between the carriers' core / plates. The carrier-biocide complexes were then added to the paint formulation. A control experiment was conducted, where identical pastes were made, but with no OIT added to them. The OIT was later freely added to the paint formulation. The amount of each component of the pastes is described in Table 7-1.

Table 7.1: Composition of powder-OIT preparation for use in the paint film.

	<b>Amount used (g)</b>	<b>OIT added (ml)</b>	<b>Water (ml)</b>	<b>Total wet powder (g)</b>	<b>Drying time (at 30°C)</b>	<b>Weight lost (g)</b>	<b>Total dried powder (g)</b>
Kaolin Supreme	20	2	40	62	2 hours	40	22
Silca Carplex	2	2	15	19	2 hours	15	4
Montmorillonite MCBP	2	2	60	64	3 days	60	4

Carplex and MCBP were used in smaller quantity in their respective formulations than supreme because:

- There is a density difference between the 3 clays (a higher quantity would make the formulations more viscous and consequently not useable later)
- The Silica and Montmorillonite based formulations still needed some amount of Supreme in order to maintain the rheology of the paint formulation

The differences in the amount of water used and the time taken to dry the material reflected

the nature of the clays used. MCBP is 2:1 platy and needed more water to fully expand, whereas carplex is amorphous in nature and readily formed a paste with limited amount of water. 40 ml of water were used in the kaolin because of the volume of clay used in the experiment. OIT was used to replace the traditional dry film biocide used in this formulation, because it degrades easily in the environment. The amount of conventional biocide normally used in the paint formulation was 0.6% w/v, exactly 2.4 ml per 400g of paint, and generally corresponds to industry standard. 2 ml of OIT was used in all formulations mentioned in this Chapter, as this was the volume needed to eliminate all organisms in the calibration experiment (Figure 7.1).

### **7.1.2 Paint preparation**

After the paint films were made, a bench paint applicator was used to coat flat hydrophobic Leneta test sheets (300  $\mu\text{m}$  thickness). These coated sheets were allowed to dry in a controlled room environment (where humidity and temperature were kept constant) for two days, and cut in circles of 7 cm diameter using a hole punch. These coated circular sheets were sent to the paint test laboratory for further testing.

### **7.1.3 “Renault”, or paint ageing test**

The “Renault” test consisted of placing the Laneta sheets in a QUV Weatherometer, where they were subjected to constant bombardment by UV light and water. The conditions inside the Weatherometer therefore mimicked the exterior atmospheric conditions that a painted wall can be exposed to. This test is extensively used by the motoring industry to monitor the durability of the paint used on their vehicles, and to assess their level of corrosion. The test consisted of the following steps:

- The circular sheets mentioned above were immobilised on panel holders and placed inside the QUV
- The paint films on the panels were then exposed to a 3500 Watts xenon light for 102 minutes at 70<sup>0</sup>C
- This was followed by exposure of the same surfaces to sprinkling water for 18 minutes, in the dark (to simulate a night time paint exposure)
- The cycle was repeated until the experiment was stopped at 1500 hours. Some panels were removed at time interval (24, 48, 72, 96, 120, 180, 312, 336, 600, 720, 840, 960, 1200 and 1500 hours) for microbiological assessment (biocide potency test). The relative humidity within the QUV was 52% (+/- 5%) outside of sprinkling period.

Data obtained from the ageing “Renault” test can be interpreted as follows: every 100 hours the paint film was aged in the QUV corresponded to 1 month in real time (where a painted wall can be subjected to the same atmospheric conditions outside). The total QUV run time of 1500 hours, therefore represented 15 months in real time.

#### **7.1.4 Bioassay (OIT potency test)**

Culti-Loops containing viable micro-organisms (*Pseudomonas Aeruginosa*) known to affect coated surfaces were purchased from OXOID Microbiology, together with ready-made pseudomonas cetrimide agar plates, tryptone soya broth solution in glass bottles (pH 7.3 ± 0.2) and a maximum recovery buffer (peptone sodium chloride, pH 7). The bacterium used is Gram negative (it does not retain crystal violet in gram staining, due to the nature of its cell membrane), rod-shaped and aerobic in nature. Before use, the microbial loop was diluted:

- The loop containing the organisms was cut, put in a 1 ml tryptone soya broth and incubated at 32°C for 5 minutes. This allowed the activation and dispersion of the organisms in the solution.
- 100 µl of this solution were added to 900 µl of the recovery buffer to obtain a 1 in 10 dilution of the original organisms. Subsequent additions of this latter solution generated a useable solution of 1 in 100,000 dilutions of the original organisms in the soya solution. This high dilution was made in order to facilitate the reading of the cetrimide agar plates after incubation and growth of the organism

The growth of this organism followed a typical bacterial growth curve, except for a longer lag phase (24 hours) observed during incubation at 32°C.

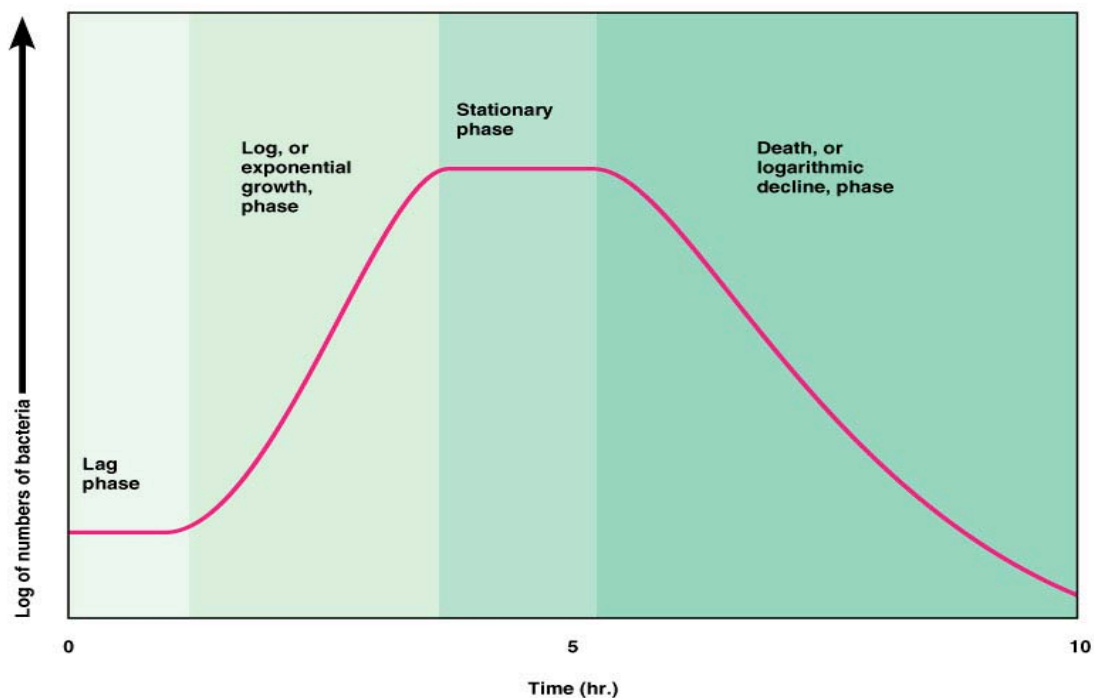


Figure 7.1: A typical bacteria growth curve. The lag phase can be longer for different organisms [98]



Events occurring during the phases of bacterial growth are summarised below:

- Lag phase: production of new enzymes needed for growth
- Log phase: maximum growth of the organism
- Stationary phase: growth equals death; nutrients (limited) or waste products (increased) limiting growth
- Death phase: death greater than growth; lack of nutrients or accumulation of waste products killing cells

The cetrimide agar plates were seeded with the diluted *pseudomonas Aeruginosa* solution. The Leneta sheets containing the paint films were then placed face down on the seeded agar plates, which were in turn put in the fridge for 24 h to allow OIT to diffuse out of the paint films. After 24 h, the sheets were removed, and the cetrimide agars were incubated at 32°C for 48 h (24 h to allow for the lag phase of the organisms and a further 24 h for growth). After that period, the numbers of microbial colony forming units present on the cetrimide agar plates (if any) were counted using a laboratory bench cell counter (see Figures 7.5, 7.6 and 7.7). Three controls were made for each test carried out and they were:

- A seeded cetrimide agar plate (to determine the maximum number of colony forming unit that can be seen after the dilution described above)
- A second seeded agar plate incubated with a circular Leneta sheet with no paint film on it (to determine if the presence of the sheet alone was impeding the growth of the organisms)
- A third seeded agar plate with a panel as described above, with paint film containing no biocide on the panel (to determine if any other component of the paint was killing

the organisms)

### 7.1.5 Determination of OIT loading of paint films

In order to assess the volume of OIT needed to eliminate or reduce to a minimum the presence of micro-organisms in the paint films, an experiment was run where varying amounts of the biocide (0.5, 0.75, 1, 2.5 and 3 ml) were added to seeded agar plates (see Figure 7.4). Three control plates were made (same as those described in section 7.1.4). This experiment was also important for assessing the potential commercial and environmental benefits of this controlled release technology. It was anticipated that the amount of biocide primarily added to paint films in uncontrolled systems could be considerably lowered, leading to a decrease in the environmental discharge of OIT.

## 7.2 Results

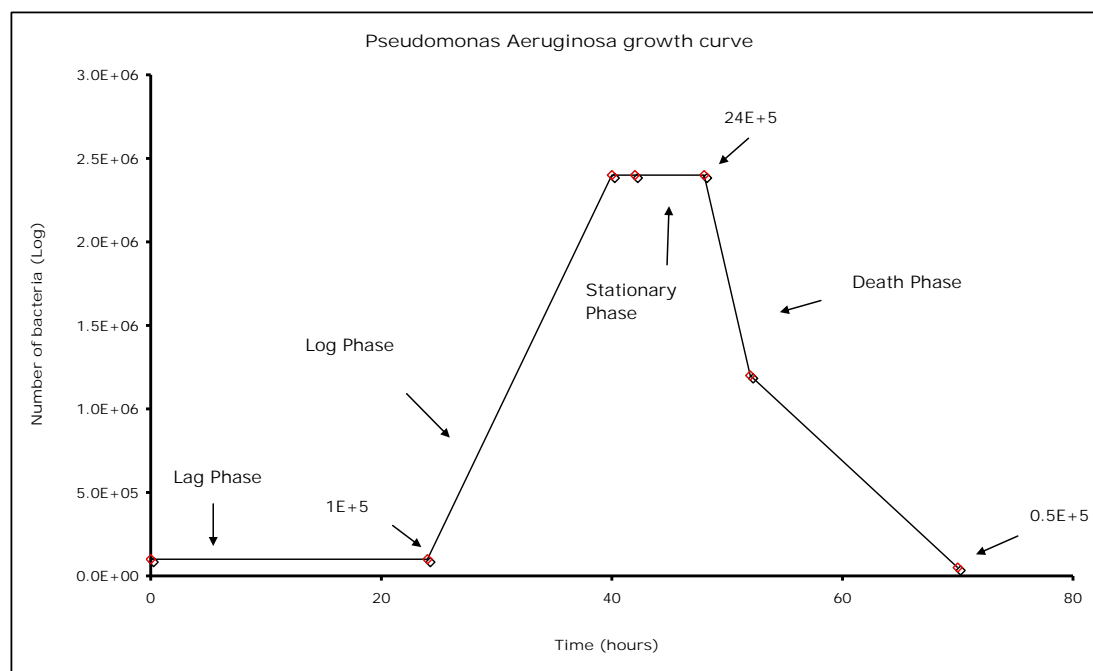


Figure 7.2: *Pseudomonas Aeruginosa* growth curve, as observed in laboratory experiments

Figure 7.2 shows the complete growth curve of *pseudomonas aeruginosa* as observed in the laboratory. The figure also showed that the lag phase of this organism was 24 hours, which was longer than that of most common organisms. This may be due to the length of time it took the organism to make the enzymes needed for its growth.

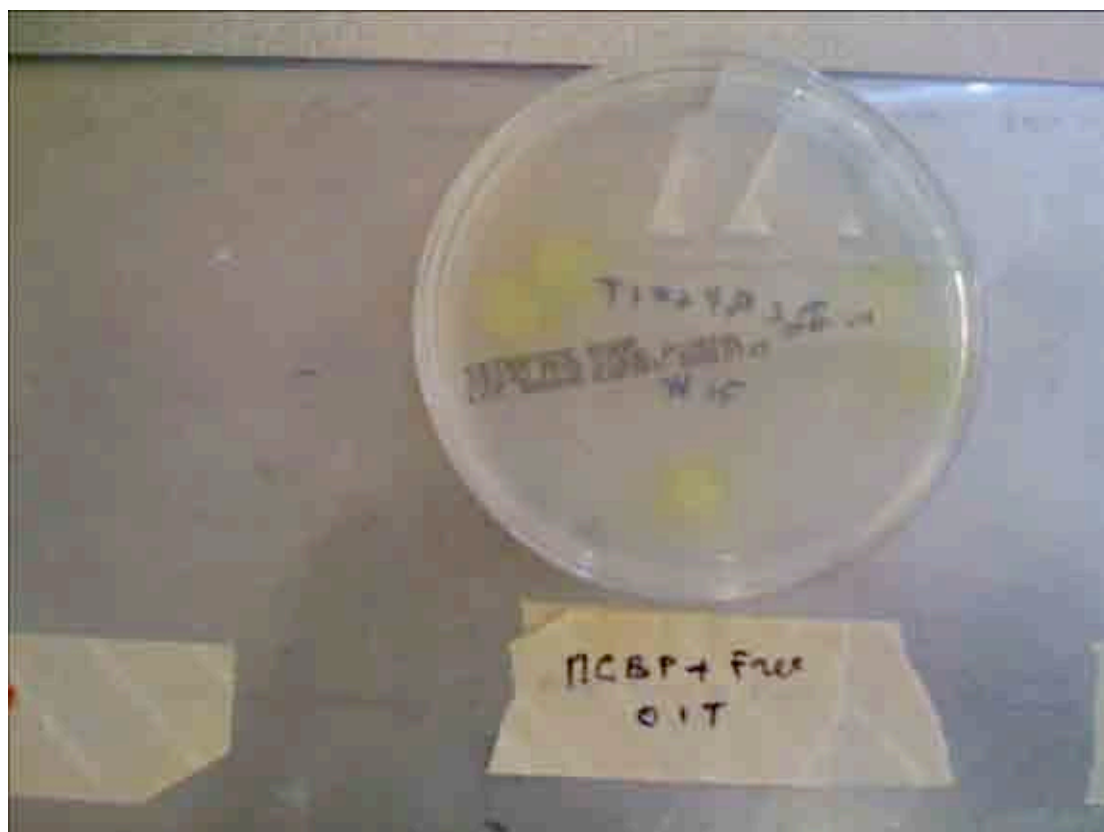


Figure 7.3: Cefrimide agar plate showing *pseudomonas aeruginosa* colony forming units (in green) after 48 hours incubation period

Figure 7.3 shows an agar plate with 5 bacterial colonies formed after 600 hours weathering test in the QUV. The colonies here (green colour) are emerging due to the original paint on the Leneta disc being depleted of its biocide content during the weathering test.

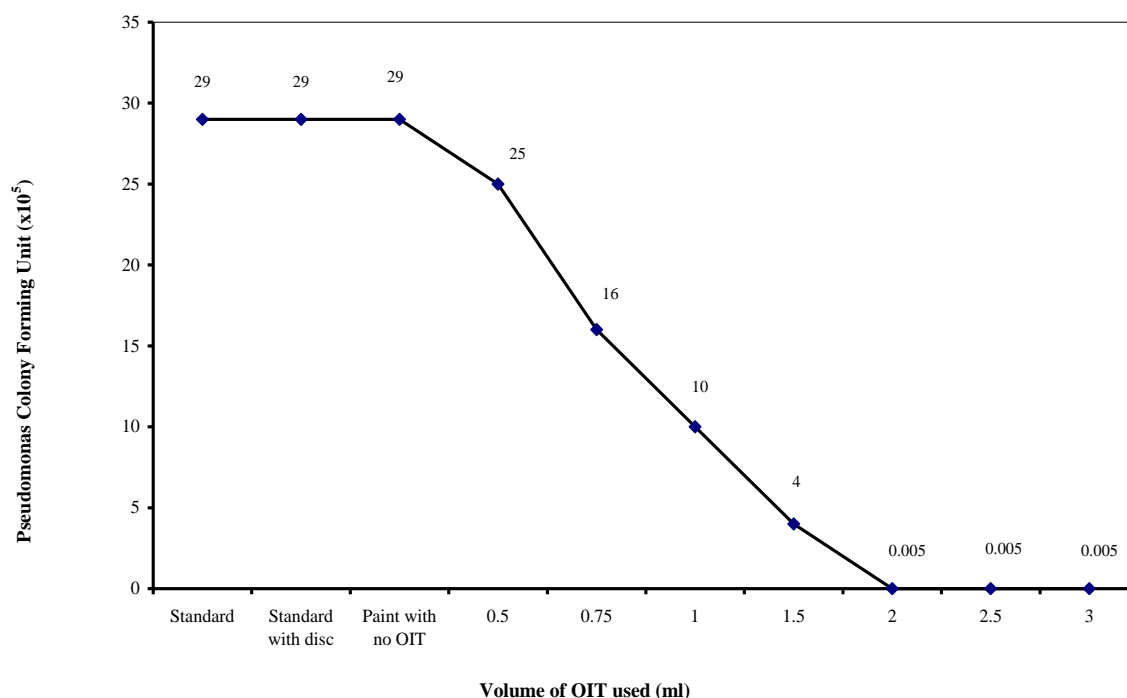


Figure 7.4: OIT calibration to determine the volume of biocide needed to inhibit or limit the growth of the organism

Figure 7.4 demonstrated that the addition of OIT to the paint films decreased or/and inhibited the growth of *pseudomonas aeruginosa*. This finding illustrated the fact that the biocide was inhibiting the normal metabolic pathways of the organism by binding to the enzyme cofactors Nicotinamide Adenine Dinucleotide (NAD) and Flavin Adenine Dinucleotide (FAD). It could be seen that a volume of OIT higher than 2 ml (considered to be the saturation point) did not alter the level of organism in the paint. This level (2 ml) was therefore used to load the paint films for the remainder of the bioassay work. The number of microbial Colony Forming Unit (CFU) at 2 ml OIT, (500), is very negligible in paint.

The number of microbial colony forming units in all three controls remained the same. Each

of these controls showed that there was no inhibition to the growth of the organism. This demonstrated that:

- Neither the panel on which the paints were applied, nor the other components of the paint films were affecting the growth of the organisms
- Only OIT was therefore having a detrimental effect on microbial levels

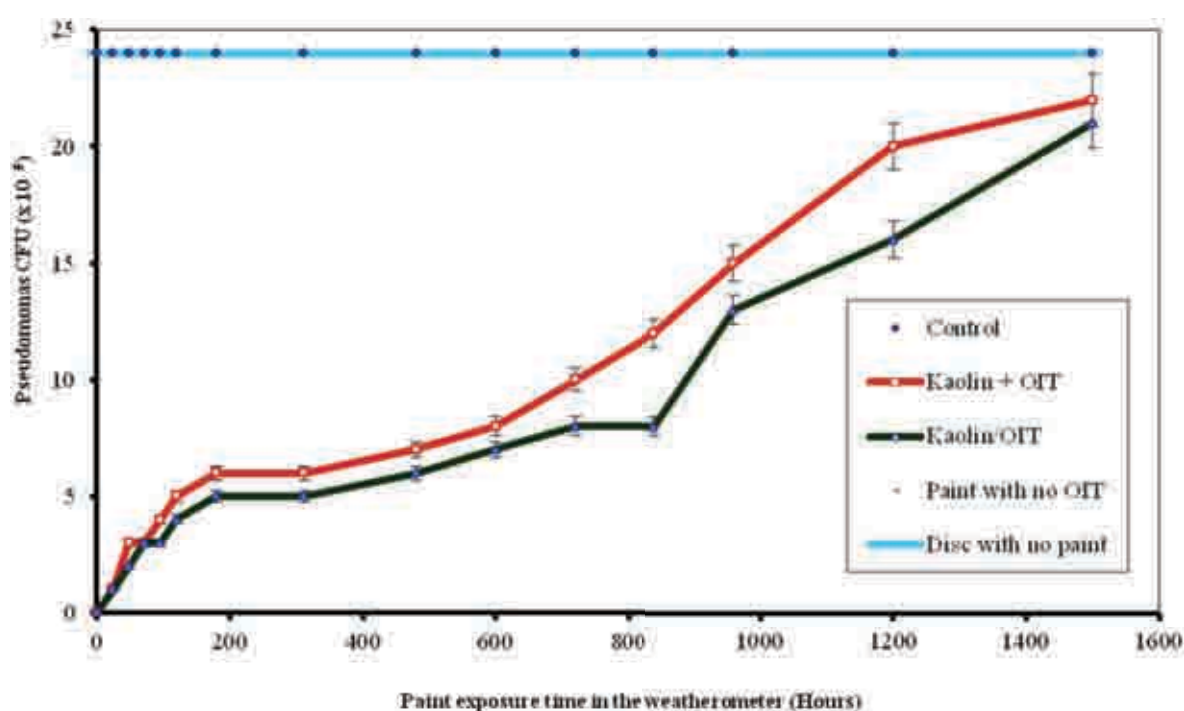


Figure 7.5: *Pseudomonas* colonies formation on paint films containing the kaolin, and subjected to artificial degradation in the QUV over a 1500 hours period

Figure 7.5 shows the formation of bacterial colonies on paint films containing kaolin supreme clay and OIT over a 1500-hour period. It can be seen that there was practically no difference between the 2 paint films for the first 200 hours. The only significant differences between the

2 paint films were:

- At 840 hours, the bacterial colonies were 12 and 8 ( $\times 10^5$ ) respectively for the freely added and the adsorbed OIT
- At 1200 hours, the number of colonies was 20 and 16 ( $\times 10^5$ ) for the same paint films

The controls with the disc with no paint, and the paint with no OIT confirmed that neither the Leneta discs, nor the other components in the paints were killing the organisms, as the numbers of colonies were the same as those of the agar plate. The numbers of colonies at 1500 hours were almost the same at 22 and 21 ( $\times 10^5$ ) respectively for the 2 paints films, and were approaching the controls ( $24 \times 10^5$ , represented by the lines at the top of the graph). This was an indication that the films were being depleted of their biocide content, leading to an increase in the number of bacterial colonies.

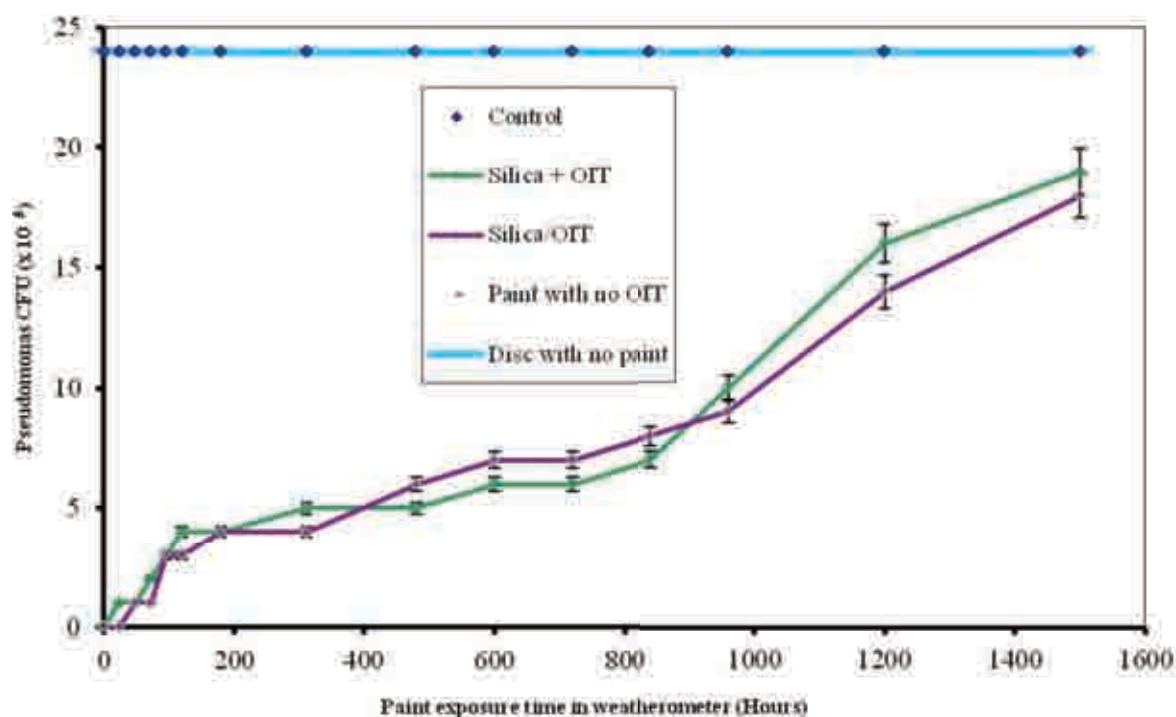


Figure 7.6: *Pseudomonas* colonies formation on paint films with silica carplex, subjected to artificial degradation in the QUV over a 1500 hours period

Figure 7.6 shows the formation of bacterial colonies on paint films containing silica carplex, over a 1500-hour period. The profiles of the 2 bacterial colony formations were almost identical, with the difference for both the adsorbed and non-adsorbed carplex being very negligible. Bacterial colonies at 1500 hours were 18 and 19 ( $\times 10^5$ ) for the encapsulated and independently added Carplex respectively, lower than those of the supreme clay.

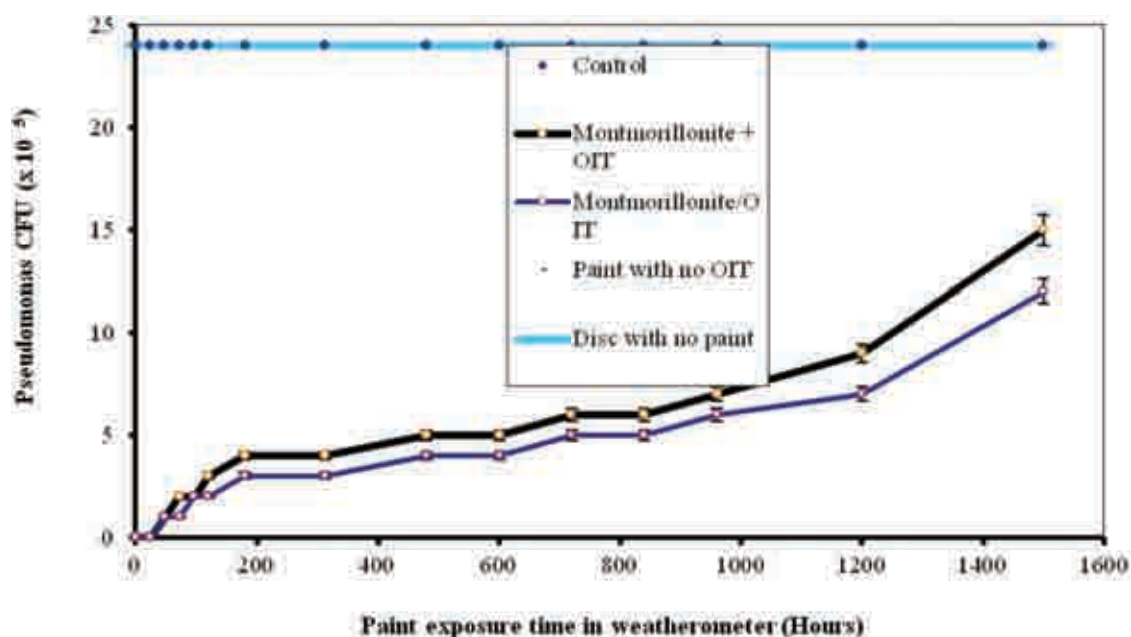


Figure 7.7: Pseudomonas colonies formation on paint films with montmorillonite MCBP, subjected to artificial degradation in the QUV over a 1500 hours period

Figure 7.7 shows the formation of bacterial colonies on paint films containing montmorillonite MCBP, over a 1500-hour period. The profiles for the 2 paint films suggest that bacterial growth on the paint film containing the encapsulated MCBP was at a lower rate than that of the film with freely added mineral and biocide. This was due to the fact that the OIT molecules have been shown to desorb slower from this mineral (see Chapter 6 on desorption experiment), and will need to thereafter migrate onto the surface of the film in order to impede on the growth of the organisms. This could also be due to the fact that only a lower amount of the biocide was released from the montmorillonite at time, but in enough concentration to impede the growth of the organism. The number of bacterial colonies was 12 and 15 ( $\times 10^5$ ) for the adsorbed and freely added OIT to mineral respectively, significantly



lower than those of the silica and the kaolin. All values are presented in Table 7.2

Table 7.2: Number of pseudomonas colony forming units ( $\times 10^5$ ) recorded after paint ageing test in the QUV (at specific times)

Treatment	Time (hours)					% of growth at 1500 hours
	24	312	600	1200	1500	
<b>Supreme / OIT</b>	1	5	7	16	21	87.5
<b>Supreme + OIT</b>	1	6	8	20	22	91.6
<b>Carplex / OIT</b>	0	4	7	14	18	75
<b>Carplex + OIT</b>	1	5	6	16	19	79.2
<b>MCBP / OIT</b>	0	3	4	7	12	50
<b>MCBP + OIT</b>	0	4	5	9	15	62.5
<b>Control</b>	24	24	24	24	24	100
<b>Paint with no OIT</b>	24	24	24	24	24	100
<b>Disk with no Paint</b>	24	24	24	24	24	100

(Percentages of growth were ratios of values at 1500 hours compared to control values)

The data in Table 7-1 indicated that there was a maximum growth of the organisms in all the 3 controls used, confirming that only the presence of the biocide in the paint films inhibited that growth. There was also a difference in bacterial growth profile between the three minerals, with the montmorillonite (MCBP) performing better than the others (with the silica

in second and the kaolin coming last, and was confirmed by the bacterial percentages of growth in Figures 7.8, 7.9 and 7.10). This finding was consistent with that of the biocide desorption profiles in Chapter 6, which also showed that MCBP performed better than any other mineral used. However, the growth profiles also indicated that, with time, the number of colony forming units on all the paint films was approaching the control. This was an indication that the OIT contents of the films were decreasing. Every 100 hours a painted panel spent in the weatherometer was equivalent to 1 month spent in “real” environment outside. The experiment was therefore run (and data collected) for a period of 15 months (1500 hours). New controls were made for each time indicated in the Table because the organism has a short life span (see Figure 7.2 for its growth curve). The controls’ data indicated that only OIT was affecting the growth phase (Log) of the organism.

The biocide content of the paint films throughout the ageing period, together with the total ageing time, were calculated using the information provided above (600 hours in the QUV corresponded to 6 months in real time). The control ( $24 \times 10^5$  CFU) contained no OIT and therefore represented a 0% biocide in this calculation, whereas the paint exposure time at 0 hour represented 100% OIT, since no paint degradation or loss had taken place. This calculation was performed in order to relate the biocide content of the paint films to the bacteria’s growth throughout the ageing process. Data obtained were plotted on 3 different curves and analysed.

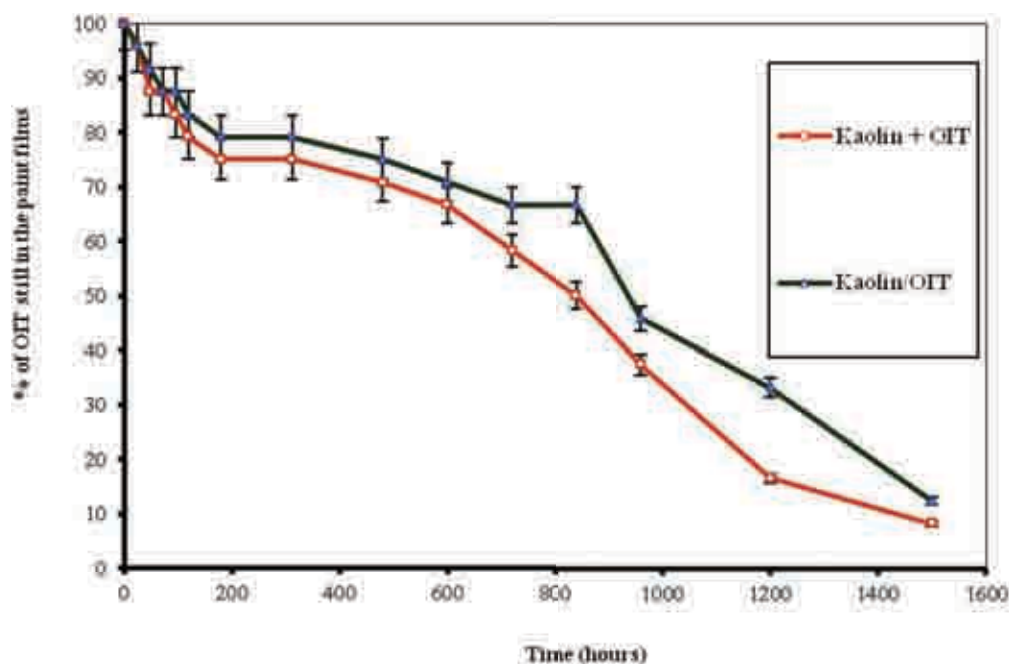


Figure 7.8: Percentage of OIT left in the paint films containing kaolin supreme throughout the ageing process

Figure 7.8 shows a decrease in the films biocide levels as the ageing in the QUV progressed. This finding was in line with the increase in the number of bacterial colonies observed during the same period of time (Figure 7.5), and indicated that the biocide molecules were migrating to the surface of the paint films where:

- They degraded under intense UV light in the QUV (during its first cycle)
- They were washed away during the sprinkling period of the second cycle of the QUV

The amount of OIT left in the 2 films after the ageing process was minimal and fast approaching the zero line, and probably due to the mineral's inability to retain the biocide for

a longer period of time (possibly due to its morphology and surface area, as observed in Chapter 6 of the desorption studies).

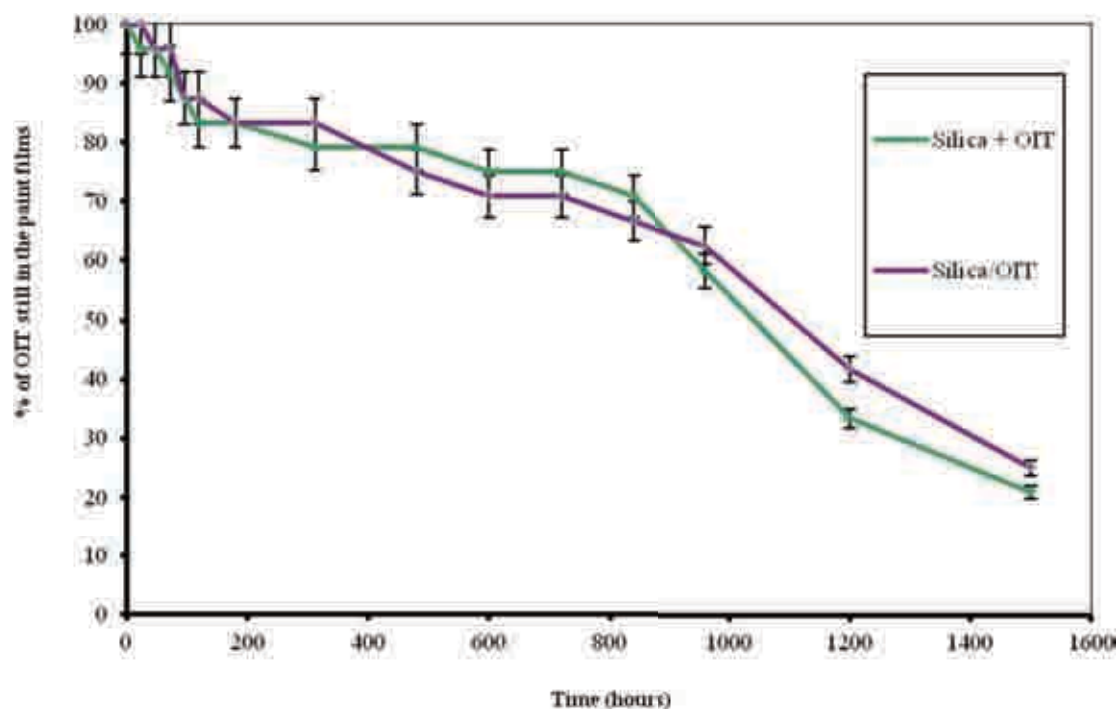


Figure 7.9: Percentage of OIT left in the paint films containing silica carplex throughout the ageing process

Figure 7.9 also shows a decrease in the films biocide levels for the silica carplex system as the ageing in the QUV progressed. This finding was inversely proportional to the increase in the number of bacterial colonies observed during the same period of time (Figure 7.6). It appears from Figure 7.9 that the two films would have been completely depleted of their biocide content in the ageing process proceeded to 2000 hours (20 months period in real time application)

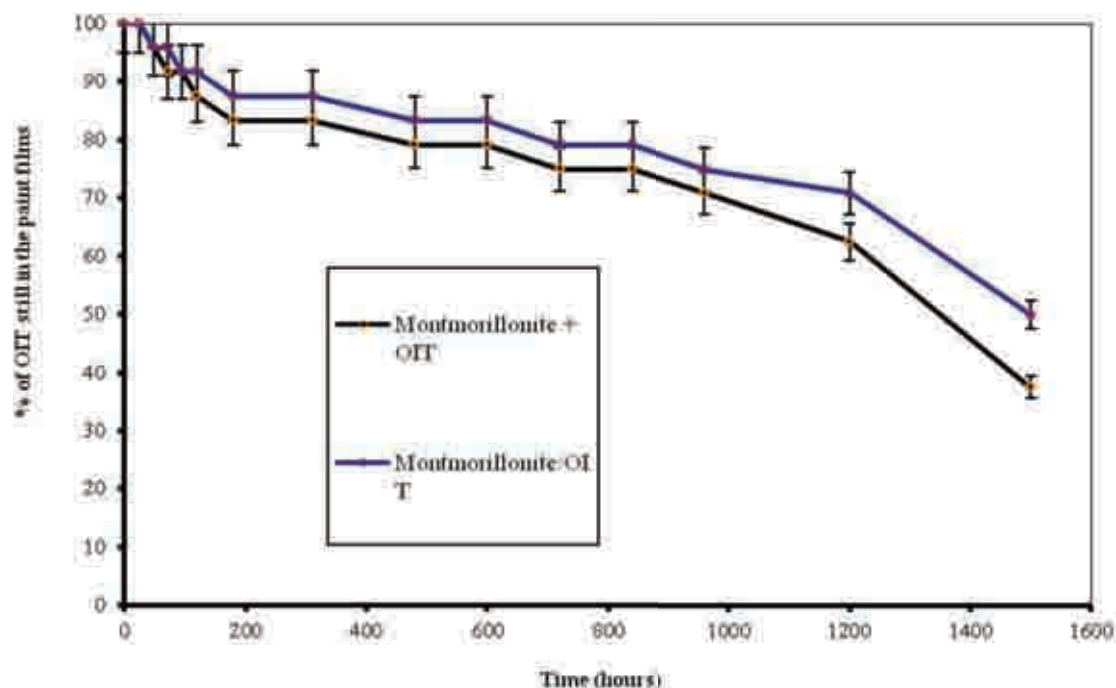


Figure 7.10: Percentage of OIT left in the paint films containing montmorillonite MCBP throughout the ageing process

Like Figure 7.8 and 7.9, Figure 7.10 also shows a decrease in the films biocide levels as the ageing in the QUV progressed. This finding was also inversely proportional to the increase in the number of bacterial colonies observed during the same period of time (Figure 7.7). It appears from the graph that there was a consistent difference between the 2 films, with MCBP appearing to retain a lot more biocide (when OIT is adsorbed to the mineral) than when the mineral and the biocide are freely added to the formulation. All findings were summarised in Table 7.3

Table 7.3: Percentage of OIT left in the paint films after 1500 hours ageing test

<b>Mineral</b>	<b>Adsorbed OIT</b>	<b>Added OIT</b>
Montmorillonite MCBP	50	38
Silica Carplex CS-5	25	22
Kaolin Supreme	13	8

Table 7-3 shows the percentages of OIT remaining in the paint films after the ageing process in the weatherometer. The adsorbed biocide on all minerals was released slower than the freely added OIT. This was probably as a result of the structure of the minerals used, with the adsorbed biocide being trapped between the layers and structure of the platy and amorphous minerals respectively. The tortuosity of OIT's path through the platy minerals, and the pore size restriction of the silica, contributed to the delayed release of the biocide, whereas the freely added OIT could elute out of the films with minimum inhibition.

The montmorillonite MCBP was the best performing mineral used, followed by the silica and the kaolin respectively. This was probably due to the different energies of desorption of OIT from the minerals (see chapter 5 on FMC, Figure 5.1). OIT needed to migrate to the surface of the films in order to kill the organisms (in the bioassay tests) or be broken down during the ageing tests. The energies of desorption obtained from the FMC work were 16, 5.9 and 1.5 mJ/g for the montmorillonite, silica and kaolin respectively, and they indicated that the montmorillonite was twice and four time more efficient at retaining the biocide than the silica and the kaolin respectively.

### 7.3 Discussion

This bioassay work was carried out using an external paint formulation. Supreme clay was used in this experiment because it displayed a very good OIT desorption profile (see Chapter 6). MCBP and carplex were used because they showed the highest adsorption potential in previous studies (see FMC work in Chapter 5), and also possess the highest surface areas of all the minerals used in this study.

The wet adsorption process used allowed the entrapment of OIT within the structures of the minerals. The paint formulations containing the freely added OIT were also made to compare their release profiles with those of the entrapped biocide. It was hoped that a significant difference in these release profiles could lead to future commercial and environmental benefits.

The dilution of the original microbial broth (with a 1 in  $10^5$  dilution factor) was made in order to obtain a more accurate reading of the agar plates after incubation. The cell counter used to evaluate the total number of microbial forming units was a semi quantitative method, and a lower dilution factor would have lead to an over population of the agar plates, rendering them impossible to read. The cetrimide plates used were specifically made for *pseudomonas aeruginosa*, as they contained the right nutrients for its growth.

The bacterial growth data showed the organism had a longer lag phase, possibly due to the time it took to produce the enzymes required for its growth. The three controls used in both the calibration and degradation studies did not inhibit the growth of the bacteria, as they did not contain any biocide. The release profiles of the biocide also showed that as the minerals

were being depleted of their OIT content, more bacterial growth occurred on the plates. These findings lead to the conclusion that no other constituent of the paint film participated in the inhibition process. The molecular basis for the inhibition of the bacteria's growth was due to OIT binding to Nicotinamide Adenine Dinucleotide (NAD) and Flavin Adenine Dinucleotide (FAD), two key enzyme cofactors in the organism Krebs cycle, preventing the bacteria from producing Adenosine Triphosphate (ATP), effectively killing it.

The bioassay data showed that the biocide was not permanently trapped within the structures of the minerals used, and thus confirmed the results obtained from the Flow Microcalorimeter (see Chapter 5). The released of the biocide from paint films containing montmorillonite MCBP was twice and four times slower than the films containing the silica carplex CS-5 and the kaolin supreme respectively for both treatments. This was possibly due to the higher energy needed to remove it from the montmorillonite clay as a result of stronger bonds between OIT and the mineral. MCBP expands upon hydration (all 2:1 clays do), unlike the other 2 minerals used (supreme is a 1:1 clay, and the silica is amorphous). This property of the MCBP is thought to be very useful in the biocide entrapment process, with the biocide being entrapped into the core upon drying, and released at a lower rate. The freely added biocide was released faster in all the minerals used, compared to the “adsorbed” biocide. As OIT was not physically attached to the minerals, it could therefore move freely between and around the plates of the montmorillonite and the kaolin, and was also not inhibited by the pore size effect of the Silica.

The entrapment of OIT into the minerals produced very good release profiles, compared with the profiles of the more traditional technique of adding the biocide to the paint films. But



there was almost no benefit in impregnating the kaolin with OIT, because the profiles of the 2 films were very similar throughout the ageing process. Paint manufacturers may consider using montmorillonite as a controlled release mineral in their systems, as this clay has displayed a better release profile than the other two minerals tested in this study.

# **CHAPTER EIGHT**

## **INDUSTRIAL PERSPECTIVE OF THE PROJECT**

In this chapter, the importance of this project to Imerys Minerals was reviewed. As cost is an important part of project management in any company, the viability of any technology used in this controlled release work is also assessed. The project aim, the biocide sorption technologies used, together with the importance of the results obtained were also discussed. The paint characterisation data (optical and mechanical properties) were also presented in order to assess how they differ to those of the standard paint formulation.

### **8.1 Industrial aims of the project**

According to the Biocides Directives (98/8/EU), “biocidal products are those that are intended to destroy, render harmless, prevent the action of, or otherwise exert a controlling effect on any harmful organism by chemical or biological means”. As such, biocides have been used for years to control the growth of micro-organisms in many different applications. In the Food industry, iron is used as an antimicrobial agent to extend the shelf life of many products, and in the paint industry, lead, copper, mercury and others have been extensively used in decorative paints, and to protect marine vessels from biofouling. In recent years, many countries have introduced legislation to either reduce the amount of biocide released in the environment, or to replace the traditional transition metals-based biocides by more environmentally “friendly” ones. This legislation was brought in as a result of:

- The toxic nature of these biocides (the traditional biocides can destroy both the target and non-target organisms and plants)
- Their impact on the environment (heavy metals like Hg,  $\text{Cu}^{2+}$ ,  $\text{Zn}^{2+}$  stay in the environment for a long time)

- The cost to the paint manufacturer (as the release is not controlled, a lot more biocide is loaded into paints than is actually needed, causing the costs to soar).

Imerys supplies various grades Kaolin and Calcium Carbonate to paper and paint manufacturers around the world. This project was set up to examine ways by which some of these minerals could be used as carriers of the biocides. The main focus was primarily to adsorb isothiazoline biocides onto minerals of diverse morphologies and surface areas. These biocides were selected because they are subject to degradation by micro-organisms, and as such do not stay in the environment for long. It was hoped that the success of this project could

- Help the company provide a new generation of minerals for controlled release purposes
- Reduce the cost of biocide to the paint companies
- Reduce the environmental damage associated biocides release

## **8.2 Technology used**

The technologies used for the various parts of this work are assessed in this chapter in order to predict their potential costings to either Imerys or any interested paint manufacturer. Companies are always looking at ways to reduce their manufacturing costs and improve their products, and any new technology will need to be aligned with this philosophy in order to be accepted and introduced in the company's portfolio.

### **8.2.1 Mineral “impregnation” of biocide**

As discussed in Chapters 3 and 4, the minerals used for this work were of different surface

areas and morphologies. The initial hypothesis was to exploit the different morphologies and surface areas of the clays for the adsorption and controlled delivery of the biocide. Section 5.2.3 explained that the initial adsorption of the biocides onto the clays was achieved by using a laboratory bench high shear mill (with the exception of New Zealand halloysite). Milling causes platy minerals to delaminate, thus offering a way to intercalate them with different compounds. The 1:1 clays used have one of each sheet of silica tetrahedron and aluminium octahedron, whereas 2:1 clays have two tetrahedral sheets on either side of an aluminium octahedron sheet. These tetrahedral and octahedral sheets are variously arranged and modified during mineral formation to create several types of clay minerals.

The amorphous silica, irregular shape calcium silicate T-38, and diatomaceous earth celitx were impregnated in the same way. The technique of milling is extensively used in the mineral industry, and has the advantage of breaking down large particles into small one, thus increasing their surface area per gram of mineral. Adsorption of the biocides onto the minerals in this way therefore does not add to the manufacturing costs because of the widespread use of milling technology in the mineral processing industry.

The impregnation of the halloysite tubes was achieved by mixing, in a beaker, the mineral in a dilute solution of the biocide. The biocide-halloysite solutions were then placed in a vacuum oven for two hours in order to displace air trapped within the halloysite tubes and allow the biocides to penetrate the tubes. The technique is time consuming, and could add some extra manufacturing costs to the process due to the use of the vacuum oven.

### 8.2.2 Paint making and ageing test

The paints made in this work followed a protocol that is covered by a secrecy agreement. In this work, only three minor modifications of this protocol were made, namely:

- The use of the silica and the montmorillonite clays in separate paint films
- The adsorption of the biocide to the minerals before use in some of the paint formulations.
- The removal of the in-can biocide, to prevent competitive adsorption between that biocide and the OIT used

The paint-ageing test used is an industry standard test to study the effects of environmental factors such as ultra violet light and moisture on the degradation of paint films (see Chapter 7).

The paint making and ageing tests are industry standard and have been tried and tested. They do not add any further cost to the paint manufacturers or the Minerals processing industries.

### 8.2.3 Bioassay measurements

The bioassay tests carried out (assessment of the potency of the biocide in the paint films, using *pseudomonas aeruginosa* as target micro-organisms) was a standard microbiological assessment for paint films. Micro-organisms naturally grow on minerals, clay slurries, and on painted surfaces. This test was a useful tool to determine how that growth was affected by the biocides used.

### **8.3 Paint mechanical and optical test measurements**

Kaolin supreme, silica carplex and montmorillonite MCBP were used in this study due to their potential to adsorb substantial amounts of OIT biocide (see section 4.2 on the Flow Microcalorimeter), and, as seen in Chapter 7, they have displayed a slower desorption of the biocide from the paint ageing tests. In order to obtain a full understanding of the effectiveness of the kaolin, silica and the montmorillonite in the paint, optical and mechanical tests were carried out on the paint films containing the three minerals (with 2 different treatments per mineral, as described in Chapter 7), and the results compared.

#### **8.3.1 Colour measurement (The CIE “Lab” and XYZ Colour Space)**

Whiteness/brightness values are very important for kaolin and other minerals, as their possible usage in paint formulations is highly dependent on these values. How a colour is described makes a big difference in the ability to gauge how a consumer will perceive it. Some standard colour spaces, such as the RGB description, are good for specifying how a camera should detect a colour but provide no insight into how a human will perceive it. The Commission Internationale d’Eclairage (CIE) (Vienna, Austria) created a set of colour spaces that specify colour in terms of human perception. It then developed algorithms to derive three imaginary primary constituents of colour (X, Y, and Z) that can be combined at different levels to produce the entire colour range that the human eye can perceive. The resulting colour model, CIEXYZ, and other CIE colour models, form the basis for all colour management systems. The goal of this standard is for a given CIE-based colour specification to produce consistent results on different devices, up to the limitations of each device [99].

### 8.3.1.1 XYZ space

There are several CIE-based colour spaces, but all are derived from the fundamental XYZ space. The XYZ space allows colours to be expressed as a mixture of the three tristimulus values X, Y, and Z. The term tristimulus is derived from the fact that colour perception results from a retinal response to three types of stimuli. After experimentation, the CIE set up a hypothetical set of primaries, XYZ, that correspond to the way the retina behaves [99].

The CIE defined these primaries so that all visible light maps into a positive mixture of X, Y, and Z, and so that Y correlates approximately to the apparent lightness of a colour. Generally, the mixtures of X, Y, and Z components used to describe a colour are expressed as percentages ranging from 0 percent up to, in some cases, 100 percent [99].

Yxy space expresses the XYZ values in terms of x and y chromaticity co-ordinates using the following set of equations:

$$\begin{aligned} Y &= Y \\ x &= \frac{X}{(X + Y + Z)} \\ y &= \frac{Y}{(X + Y + Z)} \end{aligned} \quad \text{Equation 8.1}$$

The Z tristimulus value is incorporated into the new co-ordinates and does not appear by itself. This allows colour variation in Yxy space to be plotted on a two-dimensional diagram. Figure 8.1 shows the layout of colours in the x and y plane of Yxy space [99].



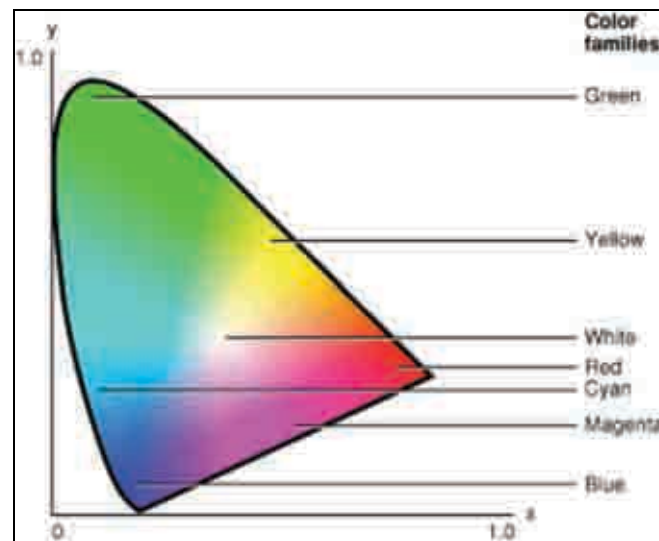


Figure 8.1: Yxy chromaticities in the CIE colour space [99]

One problem with representing colours using the XYZ and Yxy colour spaces is that they are perceptually non-linear. It is not possible to accurately evaluate the perceptual closeness of colours based on their relative positions in XYZ or Yxy space. Colours that are close together in Yxy space may seem very different to observers, and colours that seem very similar to observers may be widely separated in Yxy space [99].

#### 8.3.1.2 $L^*a^*b^*$ space

$L^*a^*b^*$  space (Figure 8.2) is a non-linear transformation of the XYZ tristimulus space. These spaces are designed to have a more uniform correspondence between geometric distances and perceptual distances between colours that are seen under the same reference illuminant [99]. The values are worked out using the following set of equations:

$$\begin{aligned}
 L^* &= 116 \cdot \left( \frac{Y}{Y_0} \right) \cdot \frac{1}{3} - 16 \\
 a^* &= 500 \left[ \left( \frac{X}{X_0} \right) \cdot \frac{1}{3} - \left( \frac{Y}{Y_0} \right) \cdot \frac{1}{3} \right] L^* \\
 b^* &= 200 \left[ \left( \frac{Y}{Y_0} \right) \cdot \frac{1}{3} - \left( \frac{Z}{Z_0} \right) \cdot \frac{1}{3} \right]
 \end{aligned}
 \tag{Equation 8.2}$$

Where X,Y and Z are tristimulus values and  $X_0$ ,  $Y_0$  and  $Z_0$  are tristimulus values for a perfect diffuser for the illuminant used [100]

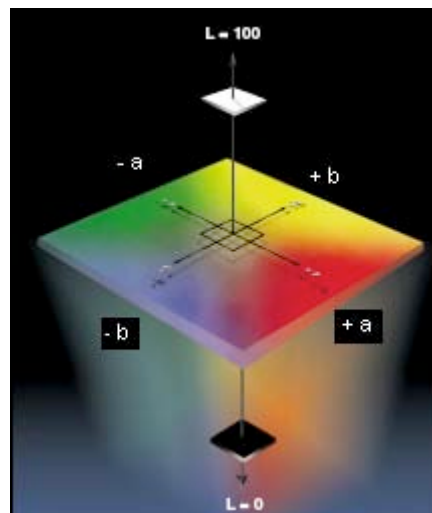


Figure 8.2:  $L^*a^*b^*$  colour space [100]

The  $a^*$  value from the  $L^*a^*b^*$  results show how red/green the sample is. A positive  $a^*$  value means a red colouration of the sample (and a probable iron contamination in the mineral samples), whilst a negative  $a^*$  value indicates a green colouring of the sample. The  $L^*$  value is the grey-scale. The closer the value for the sample is to 100, the whiter the substance will be. A positive  $b^*$  value means the sample colour is slightly yellow, while a negative  $b^*$  value indicates a blue colouring of the sample. However, when  $a^*$  or  $b^*$  is zero, the colour of the

sample is on the grey scale.

### 8.3.1.3 Materials and Methods

100  $\mu\text{m}$  film of the paints made were drawn down on labelled Melanex (clear plastic) sheets pre-cleaned with acetone, using the automatic paint applicator. Samples were stirred prior to application and a clean bar used each time. The painted Melanex sheets were then dried at a temperature of 23<sup>0</sup>C (within 2<sup>0</sup>C) and a relative humidity of 50% (within 5%) for 24 hours. 5 discs from each sheet were cut out using the hole punch. L\*a\*b\* measurements were carried out using the Minolta spectrophotometer CM-3610d, which was linked to a computer for data acquisition. The Minolta was calibrated using the zero calibration metal, consisting of a black Minolta tube with open end. Then, a white Minolta calibration plate was also placed under the analyser, and measured. The five discs were stacked on top of each other under the analyser and measured by changing over the top one each time. The final results were saved as a SpectraMagic (.wsv) file, which was in turn saved as a spreadsheet (.txt) file. From Excel, this file was finally saved as an Excel file for future analysis.

### 8.3.2 Gloss Measurement

Paints come in a variety of finish gloss levels, which correspond to different levels of specular reflection. These are not standardised, but normally run: Flat, matt, eggshell, satin, semi gloss and high gloss. Specular reflection is the mirror like reflection of light (or other kinds of wave) from a surface, in which light from a single incoming direction (a ray) is reflected into a single outgoing direction. Such behaviour is described by the law of reflection, which states that the direction of incoming light (the incident ray), and the direction of outgoing light reflected (the reflected ray) make the same angle with respect to

the surface normal, thus the angle of incidence ( $\theta_i$ ) equals the angle of reflection ( $\theta_r$ ).

This is in contrast to diffusion reflection, where incoming light is reflected in a broad range of directions. The most familiar example of the distinction between specular and diffuse reflection would be glossy and matt paints. While both exhibit a combination of specular and diffuse reflection, matt paints have a higher proportion of diffuse reflection and glossy paints have a greater proportion of specular reflection.

ISO 2813 (1994) defines specular gloss as 'the ratio of luminous flux reflected from an object in a specular direction for a specified source and receptor angle, to the luminous flux reflected from glass with a refractive index of 1.567 in a specular direction'. Thus, a measure of the glossiness of a surface is the quantity of light reflected from a test surface at a specified angle, compared with that of a standard surface, which is a black glass. The specified angle is that measured from the normal to the test surface. It is important to specify this angle, since the gloss may vary greatly as the viewing angle is changed. For example, a sheet of paper on a desk appears to have a matt finish, but the same sheet of paper looks shiny when held up to the light and viewed from a very low angle.

The three main geometries are 20, 60 and 85 degrees, with two more specialist angles of 45 and 75 degrees. Therefore, depending on the material, surface texture and gloss levels required, different angles are specified for different materials. For example, a 20 degrees angle, which gives the best resolution, is applicable to high gloss paint finishes such as cars, plastics, varnishes and polished metals. A 60 degrees angle is probably the most universal, and is usually specified for normal paints and varnishes. The 85 degrees angle is applicable to

low gloss finishes such as matt paints, plastic car interior parts or even textiles. Of the specialist angles, the 45 degrees angle is sometimes used for measuring the gloss of plastic films and some types of ceramics, while the 75 degrees is specific to the paper industry.

Different manufacturers group these reflection levels differently, and some consider flat and matt to be synonymous. Manufacturers describe finish by percent gloss, where 0% gloss is a dull unreflective surface and 100% gloss is mirror-like. Values for percent gloss vary, as do the terms. One manufacturer measures gloss as percentages (at an unspecified angle) and gives:

- Flat (1 to 9% gloss)
- Matt (10 to 25% gloss)
- Eggshell (26 to 40% gloss)
- Semi Gloss (41 to 69% gloss)
- Gloss (70 to 89% gloss)

Another manufacturer interprets these values as such:

- Relative durability of finishes: Since the material they use to create gloss is dense and glassy, gloss paints will be more resistant to damage than flat paints.
- Ease of cleaning: Glossy surfaces do not trap dirt like flat finishes, and generally are easier to clean. High-gloss paint is also more resistant to staining.
- Ease of repair/touchup: Flat can be touched up locally without repainting the entire surface.

Other considerations may include the preparation time for high gloss surfaces, which is

considerably more than for flat. The gloss finish will also reveal surface imperfections such as sanding marks and fingerprints. In the automotive and marine industry, this is a major consideration. In traditional household interiors, walls are usually painted in flat or eggshell gloss, wooden trim (including doors and window sash) in high gloss, and ceilings almost invariably in flat. Similarly, exterior trim is usually painted with gloss paint, while the body of the house is painted in a lower gloss.

#### 8.3.2.1 Materials and Methods

100  $\mu\text{m}$  films of the paints made were drawn down manually on labelled glass sheets pre-cleaned with acetone using the applicator. Samples were stirred prior to application and a clean bar used each time. The samples were then dried at a temperature of 23<sup>0</sup>C (within 2<sup>0</sup>C) and a relative humidity of 50% (within 5%) for 24 hours. Gloss measurements were carried out using the Gardner Haze-Gloss meter (see Figure 8.3), which was calibrated using the BYK Gardner High-Gloss standard and the BYK Gardner Haze-Gloss standard respectively.

The paint drawdowns were not stacked prior to measuring as this could affect the results. Three measurements along the film were taken at two different angles of incidence, 60<sup>0</sup> and 85<sup>0</sup>, and the average readings were taken.

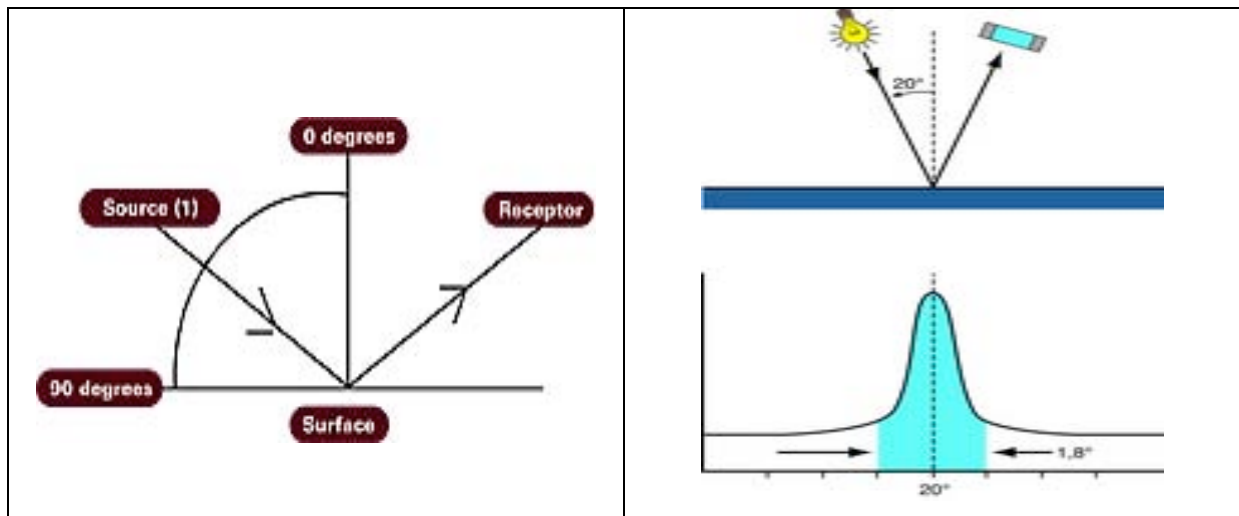


Figure 8.3: 45 and 20 degrees gloss measurements by the Gardner Gloss meter [101]

### 8.3.3 Contrast Ratio (Opacity) Measurement

Opacity / Contrast ratio is the measure of impenetrability to electromagnetic or other kinds of radiation, especially visible light. It is a measure of a display system, defined as the ratio of the luminance of the brightest colour (white) to that of the darkest colour (black) that the system is capable of producing. A high contrast ratio is a desired aspect of any display, but with the various methods of measurement for a system or its part, remarkably different measured values can sometimes produce similar results.

#### 8.3.3.1 Materials and Methods

100  $\mu\text{m}$  films of the paints made were drawn on labelled Morest charts (with black and white bands) not pre-cleaned with acetone. For side-by-side Drawdowns, half of the drawdown was of standard sample, the other of the test sample. Samples were stirred prior to application and a clean bar used each time. Samples were dried at a temperature of 23<sup>0</sup>C (within 2<sup>0</sup>C) and a relative humidity of 50% (within 5%) for 24 hours.

Measurements were carried out using the Minolta spectrophotometer CM-3610d, linked to a computer for data acquisition. The spectrophotometer was calibrated as follow:

- A “zero calibration” black Minolta tube with open end upwards, and the label facing the user, was placed under the analyser and the measurement was taken
- A white Minolta calibration plate was thereafter also placed under the analyser and measurement was also taken

In order to measure the samples, the “Opacity/Reflectivity” option was selected on the Minolta first. Then the black area of an unused Morest chart (see Figure 8.4) was measured at three different points, followed by the white Morest chart (also at three different points). The “% Opacity” results obtained were recorded, and the remaining painted Morest charts were also measured. Data obtained were saved as an Excel file. During measurements, each Morest chart was supported to ensure that it was flat and up against the base of the instrument.



Figure 8.4: A Morest black and white chart



## 8.3.3.2 Results of all optical measurements

Table 8.1: Summary of L\*A\*B\*, Gloss and Opacity data of the paint films made

	L*A*B* tests				Gloss on glass (Accurate method)					% Opacity
	L*	A*	B*	Ry	60°	Stddev	85°	Stddev	N	
<b>Supreme</b>	96.0938	- 0.4706	2.4848	90.23	3.9	0.3	12.5	0	3	95.92
<b>Carplex</b>	96.1206	- 0.4726	2.4987	90.3	3.9	0.2	11	0.2	3	95.84
<b>MCBP</b>	96.0122	- 0.4562	2.592	90.04	4.2	0.4	12.3	0	3	95.73

The high L\* values for the three paints (very close to 100) indicated that these paints were white on this grey scale. The values of a\* (redness and greenness), and b\* (yellowness and blueness), were negative and positive respectively for all samples and very close to zero, also indicating the colour on these scales were closer to the grey scale (see Figure 8.2). This was confirmed by the very high Ry values of more than 90% for all samples. The Ry value is an overall indicator of luminescence reflectance used for white and neutral colours, and is equal to Y brightness. The L\*A\*B\* and Ry values for the three minerals were very similar, indicating there was practically no loss of brightness when supreme was replaced with carplex and MCBP.

The low percentages of gloss at 60° angle (3.9% for both the silica and the kaolin, and 4.2% for the montmorillonite) suggested that the paints were “flat”, whereas the values at 85° angle (12.5%, 11% and 12.3% for the kaolin, silica and montmorillonite respectively) were

synonymous of “matt” paints. Both “flat” and “matt” paints displayed a higher proportion of diffuse reflection than of specular reflection, and are considered by many to be synonymous in the paint industry. They do not tend to reveal surface imperfections, and require little preparation time.

The very high percentage opacity of the paints (95.92%, 95.84% and 95.73% for the kaolin, silica and montmorillonite respectively) denoted the level of light transmitted by these fluids. An opaque object is neither transparent (allowing all light to pass through) nor translucent (allowing some light to pass through). When light strikes an interface between two substances, in general some may be reflected, absorbed, or scattered, and the rest transmitted. An opaque substance transmits very little light, and therefore reflects, scatters, or absorbs most of it. The paints containing silica carplex and montmorillonite MCBP displayed slightly higher contrast ratios than the paint with kaolin supreme. This may be due to the fact that the silica and MCBP contain slightly less iron than the kaolin.

### **8.3.4 Scrub Resistance**

Scrub resistance is the ability of the surface of a composite material to resist being worn away or to maintain its original appearance when rubbed with a brush, sponge or cloth and an abrasive soap. Paints often become soiled, especially near doorways, windows, and in work and play areas. The test method described here covers the determination of the relative resistance of different paints to erosion when repeatedly scrubbed during the life of the paint.

#### **8.3.4.1 Materials and Methods**

400  $\mu\text{m}$  films of the paints made were drawn down on a labelled black Leneta sheet not pre-cleaned with acetone, using the automatic applicator. The paints were stirred prior to

application, and a clean bar used each time. The painted Leneta sheets were dried at a temperature of  $23^{\circ}\text{C}$  (within  $2^{\circ}\text{C}$ ) and a relative humidity of 50% (within 5%) for 7 days prior to use. Two DIN (German ISO standard) brushes were soaked in a metal dish of 0.25wt% caflon NAS-25 solution overnight prior to measurement, ensuring that they were labelled “A” and “B”, both of these having a scrub factor of 0.82. The double brush holder was attached between the two scrub wires, each on the bottom of the screw thread on the brush holder (so the wires are horizontal which avoids a rocking motion). Each black Leneta sheet was cut into 3 equal widths of film, ensuring each was appropriately labelled. For loss-in-weight measurements after 200 DIN cycles (British Standard), the films were wiped with a dry Kimwipe and each film secured with a paper clip, and weighed to 4 decimal places (with the weight of the paper clip tared). Weighing was carried out just before testing as the coalescing solvent evaporates very slowly and continually affects the film weight as a result.

With the matt surface of the glass sheet uppermost, the first two sheets of Leneta were placed onto the glass sheet side-by-side. They were then held in position using the left hand clamp only. The brushes were rinsed and dried (by shaking them). Each brush was placed into the brush holder with the words “DIN 53 778” facing the user. Each of the two pump reservoirs was filled with 0.25wt% caflon NAS-25 and switched on, ensuring that each one drips onto the centre of each brush path at  $1\text{ cm}^3\text{ min}^{-1}$ . The scrub machine was then switched on, and the number of cycles recorded (200 cycles in total, at 37 cycles a 1 minute).

## 8.3.4.2 Results

Table 8.2: Weight loss after 200 scrub cycles

	Drying Time (Days)	BS <sup>(*)</sup> cycles	Initial weight (g)	Final weight (g)	Weight difference (g)	Weight loss (mgcm <sup>-2</sup> ) <sup>(**)</sup>	Average
<b>Kaolin</b>	7	200	19.9926	19.9134	0.0792	0.56	0.58
			17.8918	17.8092	0.0826	0.58	
			17.2921	17.2070	0.0851	0.60	
<b>Silica</b>	7	200	18.5857	18.5010	0.0847	0.60	0.55
			19.4606	19.3848	0.0758	0.53	
			16.6112	16.5352	0.0760	0.53	
<b>Montmorillonite</b>	7	200	18.4463	18.3467	0.0996	0.70	0.65
			18.5430	18.4438	0.0992	0.70	
			17.4630	17.3825	0.0805	0.57	

(\*): British Standard

(\*\*): Weight lost (mgcm<sup>-2</sup>) = [weight difference (g) x 1000] / 142.35 cm<sup>2</sup> (surface area of the Laneta sheet)

Table 8.2 shows the weights of the paint films before and after scrubbing. The average weight loss values indicated that:

- 5% less paint was lost from the paint containing the silica (Carplex) than from the kaolin (Supreme) containing paint
- 12% more paint was lost from the paint containing the montmorillonite (MCBP) than from the same Supreme paint

The data suggested that the silica-based paint offered an improved scrub resistance to both the kaolin and the montmorillonite-based paints. Montmorillonite is a 2:1 clay and has been shown in previous studies to be very abrasive when used in polymer nanocomposites, hence paints loaded with this clay will be more prone to erosion when repeatedly scrubbed during the life of the paint.

### **8.3.5 Stain Resistance**

Stain resistance is the capability of a painted surface to resist retention of household or commercial dirt and stains. These stain resistant paints make it possible for most types of stains, dirt and grime to be simply washed off with soap and water. These paints may provide the benefits of a flat paint (the ability to hide surface imperfections and give walls a smooth rich-looking finish), as well as the durability and ease of cleaning typically found in semi-gloss paints.

#### **8.3.5.1 Materials and Methods**

200  $\mu\text{m}$  films of the paints made were drawn on labelled glass sheets pre-cleaned with acetone using the applicator (mechanical drawdown). Samples were dried at 23<sup>0</sup>C (within 2<sup>0</sup>C) and a relative humidity of 50% (within 5%) for 24 hours, and stirred prior to application. A clean bar was used each time during the application process.

The staining of each sheet was carried out under the fume hood using 10% gilsonite, which was regularly stirred to dissolve any sediment (gilsonite is a form of natural asphalt found only in the Uintah basin, Utah, USA, and primarily used in dark-coloured printing ink). Each film was brushed down and left to stand in an upright position for exactly 1 minute. Enough stain was applied so that it does not start to dry out within that period. The stained sheets

were then washed, as quickly as possible, in the upright position using a “push-down pump” wash bottle of white spirit, left for exactly 1 further minute after washing, and then washed again as before. After the second wash, they were placed onto kimwipe and the surplus white spirit wiped off, and left to dry for approximately 2 hours before starting the stain measurements.

Stain resistance sheets can be stacked prior to measurement. The unstained/stained results (Ry values) were measured three times along each film sheet, using the Elrepho Data Colour spectrophotometer set on filter 10, and the average data calculated. Ry (often used as Ry luminous factor) is expressed as a ratio, and primarily used for white or neutral colours as an overall indicator of reflectance. The stain resistance was determined using the following equation:

$$\text{Stain Resistance (\%)} = \frac{\text{Stained Result}}{\text{Unstained Result}} \times 100 \quad \text{Equation 8.3}$$

#### 8.3.5.2 Results

Stain resistance data obtained from the tests are summarised in Table 8.3

Table 8.3: Stain resistance of the paints made

Paint containing	Mean stained “Ry” values	Mean unstained “Ry” values	Stain Resistance (%)
<b>Supreme</b>	86.19	86.19	100
<b>Carplex</b>	85.89	86.47	99.32
<b>MCBP</b>	85.89	86.21	99.62

The unstained data showed that the both the silica and the montmorillonite-based paints had a better colour reflectance than the supreme-based paint. Nevertheless, the stain resistance data in Table 8.3 showed the supreme-based paint did not retain any of the stain applied, compared with the Silica and montmorillonite based paints. The level of stain retention by the latter two paints was, however, very negligible, hence their high percentages of reflectance.

### 8.3.6 Rheology tests

For high solids paints, flow control is vital because it determines important properties like sagging and leveling. The rheology of the uncured paint is determined by interactions of all the solid particles (pigment, extender, matting agent, rheology modifiers) with the binders and solvents in the system. Understanding these relationships is required if control of the properties is to be achieved. Standard test methods for the rheological properties of this Non-Newtonian fluid were carried out to determine its apparent viscosity, shear thinning, and/or thixotropic properties at various shear rates. The distinction between a thixotropic fluid and a shear thinning fluid is as follow:

- A thixotropic fluid displays a decrease in viscosity over time at a constant shear rate.
- A shear thinning fluid displays decreasing viscosity with increasing shear rate.

A classic example of a thixotropic material is the non-drip paint. This is due to flocculated particles being sheared apart and then re aggregating.

#### 8.3.6.1 Viscosity measurements by the Digital Brookfield Viscometer

In this test, the non-Newtonian properties of the paints were investigated. The paints were stored at 23<sup>0</sup>C (within 2<sup>0</sup>C) for 24 hours prior to testing, and the rotational (Brookfield)

Viscometer ASTM D2196 was used, in the shear rate range  $0.1$  to  $30\text{ s}^{-1}$ . The Brookfield viscometer is standard equipment at Imerys for the measurement of paint viscosity. The experiment was set up as follow:

- The Brookfield Viscometer was warmed up for approximately 10 minutes before use.
- The viscometer was then zeroed at 10 rpm without a spindle. Spindle 6 was then inserted, lowered down into the side of the paint tin and slide across to the centre of the tin, and finally left for exactly 1 minute.
- A shear rate of  $0.3\text{ s}^{-1}$  was then selected (at 1 rpm) for exactly 1 minute, and the viscosity recorded (times by 100 for Spindle 6). This was repeated at 10 rpm ( $3\text{ s}^{-1}$ ) then 100 rpm ( $30\text{ s}^{-1}$ ) (times by 10 then 1 respectively for Spindle 6).

The speed was always reduced after final reading at 100 rpm to 1 rpm for the next sample. This was carried out whilst the motor was running to prevent gear damage. The spindle was washed by removing it (unscrewing). The process was repeated for all paints made.

#### 8.3.6.2 Results of the rheology measurements of the paints made by the Brookfield viscometer

The results of the viscosity measurements of the non-Newtonian paints made are presented in Table 8.4.



Table 8.4: Viscosity data of the paint (Viscosity readings in Poise)

<b>Paint containing</b>	<b>Shear rate (<math>\text{s}^{-1}</math>)</b>		
	<b>0.3</b>	<b>3</b>	<b>30</b>
Kaolin Supreme	770	128	27
Silica Carplex	930	148	32
<b>Montmorillonite MCBP</b>	900	132	26

The data in Table 8.4 showed a decreasing viscosity as the shear rate increased, demonstrating that the paints were all shear thinning. The kaolin, silica and montmorillonite-based paints have all displayed a similar shear thinning behaviour.

The Brookfield viscometer is generally not considered the most reliable equipment for the measurement of fluid viscosity; therefore three other measurements were made to confirm its findings.

#### 8.3.6.3 Viscosity measurements by the Sheen 480 Stormer Krebs Viscometer

Viscometers are used to define the viscous properties of a fluid at ambient or defined temperatures. This viscometer employs a paddle to measure the viscosity of a non-Newtonian fluid (most paints) based on the resistance to flow while stirring. The experiment was set up as follow:

- The viscometer was set to stir the paints at 200 rpm ( $60 \text{ s}^{-1}$ )
- The spindle was lowered fully using the lever and started

- The final reading appeared after approximately 1 minute.

After taking the reading, the spindle was washed by raising a tin of warm water underneath, brushed and then wiped dry. These steps were repeated for each of the paints measured.

#### 8.3.6.4 Viscosity measurements by Sheen Roto-Thinner Viscometer (150 s<sup>-1</sup>)

The Rotothinner instrument uses a disc or ball shaped rotor to determine the viscosity of the sample under test at 150 s<sup>-1</sup> shear rate. The results are displayed on the LCD screen in Poise (P) units (1 P = 1 g.cm<sup>-1</sup>.s<sup>-1</sup>, or 1 P = 0.1 Pa.s). The experiment was set up as follow:

- The viscometer's spindle was fully lowered into the paint tin, and then removed. This was done a couple of times to prevent it sticking.
- The spindle was fully lowered again, and then left to stir for exactly 1 minute, and the reading was recorded.

After the experiment, the spindle was washed by lowering it into a tin of warm water. The experiment was repeated for each of the paint made.

#### 8.3.6.5 Viscosity measurements by Sheen Cone and Plate Viscometer (10,000 s<sup>-1</sup>)

This Cone/Plate viscometer/rheometer is a sophisticated instrument for routinely determining absolute viscosity of fluids in small sample volumes. Its cone and plate geometry provides the precision necessary for development of complete rheological data. This viscometer has a precise torque meter that can be driven at discrete rotational speeds. The torque measuring system, which consists of a calibrated beryllium-copper spring connecting the drive mechanism to a rotating cone, senses the resistance to rotation caused by the presence of sample fluid between the cone and a stationary flat plate. The resistance to the rotation of the

cone produces a torque that is proportional to the shear stress in the fluid. The amount of torque is indicated on a digital display. This reading can easily be converted to absolute centipoise units ( $\text{mPa}\cdot\text{s}$ ) from pre-calculated range charts. The instrument was operated as follow:

- The Cone & Plate viscometer was calibrated using the standard oil “Dow Corning 200/100cs” (silicone oil).
- A small blob of stirred sample was placed onto the plate using a spatula (the plate must not be tapped with the spatula, as this is likely to cause damage).
- The handle was lowered in order to lower the cone onto the plate, and left for exactly 40 seconds to allow the temperature of the cone and plate to stabilise.
- The “Read” button was pressed until it bleeps and the cone started to spin. After approximately 10 seconds a viscosity reading was displayed temporarily (the standard oil should be 1.1) and the cone stopped spinning. The handle was lifted to raise the cone and the sample was wiped off from the cone and plate using Kimwipe. This step was repeated using clean kimwipe and acetone. The underneath and sides of the cone and plate were thoroughly checked for cleanliness.
- The temperature was kept at  $25^{\circ}\text{C}$ , the speed of the cone at 750 rpm, and the viscosity at 10 Poise. A repeat run was performed for each of the paint samples

### 8.3.6.6 Results of the Shear-thinning properties of the paints made

Table 8.5: Viscosity measurement data of the paints made, using the Stormer Krebs, the Roto-Thinner and the Sheen and Cone viscometers (Viscosity readings in Poise)

Paint containing	Shear rate ( $\text{s}^{-1}$ )		
	<b>60</b>	<b>150</b>	<b>10,000</b>
Kaolin Supreme	101	6.1	0.9
Silica Carplex	105	6.8	1.0
Montmorillonite MCBP	99.4	5.8	1.1

The data in Table 8-5 showed a decrease in viscosity of the paints with an increase in shear rate, a typical characteristic of shear thinning non-Newtonian fluids. The data nonetheless confirm the findings of the Brookfield, as all 3 paints were remarkably similar in their shear thinning ability

## 8.4 Conclusion

The industrial importance of this project was explored in this chapter. The project fitted in with the company's philosophy of giving its products increased (or new) functionality, in order to maximise the company's revenues.

As milling is already extensively used by Imerys, the impregnation of minerals by the biocides using the bench high shear mill does not add to the manufacturing costs. In the paint optical test, the  $L^*A^*B^*$  and  $R_y$  values for the three minerals were very similar, indicating there was practically no loss of brightness when the kaolin, the silica or the montmorillonite

was used in the paint formulation. The gloss and opacity characteristics of the paints made were very similar for the three minerals used. These paints were characterised as “flat” (due to their low percentages of gloss at  $60^0$  angle) and “matt” (because of the high gloss percentages at  $80^0$  angle). The very high percentage opacity of these paints suggested they transmitted a lot of light. The paints containing montmorillonite MCBP and the silica carplex displayed slightly higher contrast ratios than the kaolin supreme paint. This may be due to the fact that the carplex and MCBP contain slightly less iron than the kaolin.

The scrub resistance data indicated that the Silica-based paint was less prone to erosion than both the kaolin and the MCBP-based paints, probably due to the fact that the platy clays are in general more abrasive than the amorphous silica. The staining data indicated that the silica and the MCBP-based paints had a better colour reflectance than the supreme-based paint. Nevertheless, the supreme-based paint did not retain any of the stain applied, compared with the silica and MCBP based paints. The level of stain retention by the latter two paints was, however, very negligible, and did not affect their colour reflectance. The rheology measurements confirmed that all the paints made were very similar in their shear thinning ability.

# **CHAPTER NINE**

## **CONCLUSION AND FUTURE WORK**

Nine minerals were initially chosen for this controlled release study, based on differences of their surface area and morphology. The silica (Carplex) was chosen as the initial control mineral because it has a very high adsorption potential, being already used in the brewing industry to remove unwanted chemicals from beer purification. The New Zealand halloysite, calcium silicate (T-38), diatomaceous earth (Celtix), and the montmorillonite (MCBP) were all selected because they have been used in controlled release experiments with varying degree of success. The four kaolins, NPD-16A, infilm 939, suprex and supreme were chosen because they are produced by Imerys, and could offer an alternative to the silica and montmorillonite in a controlled release system.

Two different biocides, OIT and CIT/MIT, based on the isothiazoline chemistry, were chosen because they were both biodegradable when release and cause very minimal environmental damage.

These nine minerals were then carefully characterised to identify their individual surface area (B.E.T nitrogen analysis), chemical compositions (XRF), crystal structures (XRD), morphologies (SEM) and particle size distributions (Malvern Mastersizer). The particle size distribution using the Malvern Mastersizer revealed that the silica (Carplex), the kaolinite (Supreme) and the montmorillonite (MCBP) were the finest three clays of the group of minerals studied, with a better size distribution and “Top Cut”  $d_{98}$  values. This constituted one of the reasons these clays were selected for the paint and bioassay work. Scanning Electron Microscopy uncovered the shapes of the minerals used. Using this technique, it was possible to establish the platy nature of the kaolins and montmorillonite (suprex, supreme, NPD-16A, infilm 939 and MCBP), the rod-shape of the halloysite, the amorphous nature of

the silica (Carplex CS-5), and the irregular shape of the diatomaceous earth and the calcium silicate (T-38 and Celtix). These morphologies helped to identify methods to entrap the biocide (using vacuum pump for Halloysite, and wet and/or dry method for the other minerals).

It was important to know how much biocide could be adsorbed onto these minerals. Initial experiments were therefore set up to determine the adsorption isotherms using Flow Microcalorimetry (FMC) and High Performance Liquid Chromatography (HPLC) techniques to calculate the optimum biocide loading of the minerals, so that a system could be developed that could deliver a level of biocide above the minimum inhibitory concentration of the biocide. The adsorption isotherms (in both static and dynamic environments) identified how much biocide was adsorbed, and how strongly it adsorbed/desorbed to and from the minerals. The low surface area minerals were able to carry the isothiazoline biocides, contrary to what was stated in the open literature [86]. The ratios of the footprint data between the two biocide molecules indicated that the thermodynamics favour OIT in the adsorption process of minerals. This could be due to the orientation of the biocide molecules as they adsorb onto the minerals, with the more hydrophobic octyl side chain on OIT away from the minerals' surfaces, whereas the hydrophilic methyl on CIT/MIT was participating in the adsorption process. The Flow Microcalorimetry data confirmed OIT was adsorbed to all the minerals, but the desorption energies indicated that these minerals held to the biocide with differing levels of strength (from almost irreversible adsorption with the diatomaceous earth celtix to completely reversible with the kaolin NPD-16A). The isotherms and FMC results indicated that:



- Montmorillonite MCBP and silica carplex CS-5 were the best OIT adsorbing minerals in both static and dynamic environments.
- New Zealand halloysite, the kaolins NPD-16A, infilm 939 and suprex were the worst performing minerals (for biocide adsorption), and consequently were not selected for the bioassay experiment.

The montmorillonite MCBP used is a 2:1 clay mineral with larger interlayer spaces, giving it the capacity to hold biocide molecules and a variety of cations. The larger interlayer spaces allow the clay to shrink/swell. This clay was reported to look like a sponge in previous analysis [102], just like the silica used. This property made MCBP and the silica the ideal minerals for use in adsorption experiments.

The amount of biocide that actually desorbs from a paint film containing the minerals and the biocide was investigated using the FMC and HPLC. From the results it was clear that the calcium silicate T-38 and the diatomaceous earth celtix were unsuitable for future controlled release experiments because they were both depleted of their biocide content after four hours (Celtix) and 7 days (T-38). Both irregular shape minerals could therefore not be used in the paint formulation and were discarded.

The montmorillonite (MCBP), the silica (Carplex) and the kaolin (Supreme) were, however, promising candidates because they held on to the biocide for a longer period of time. The montmorillonite has shown in all experiments that it was more efficient at adsorbing the biocide than any other mineral used, possibly due to its 2:1 structure. The data suggested that this mineral could be used in a paint formulation to release the biocide over a longer period of time. As the mineral expands upon hydration, the amount used in the paint needs to be kept

very low in order to preserve the structural integrity of the paint.

The desorption experiments also uncovered a prolong release of the OIT when it was encapsulated within the minerals used (with the exception of the calcium silicate T-38). This was probably due to the fact that the biocide had to navigate within or between the structures of the minerals to the surface of the paint films before being release into the water.

Next, bioassay experiments were carried out using the best performing minerals in the adsorption and desorption work, the montmorillonite, silica and kaolin. The work was done, after extensive paint ageing tests, to confirm that the biocide desorbed from the paint film and inhibited the growth of the bacteria. Data obtained first showed the organism had a longer lag phase, possibly due to the time it took to produce the enzymes required for its growth. The bioassay also confirmed that the biocide was not permanently trapped within the structures of the minerals and the paints (absence of bacteria colonies on the agar plates in the first 24 hours), and thus confirming the OIT desorption results. All three minerals used showed depletion in their biocide content as the ageing test progressed (with the appearance of bacterial colonies). Nevertheless, the montmorillonite MCBP was again the best performing mineral with half its initial biocide concentration still in the paint after 1500 hours experiment, followed by the silica and the kaolin.

Further tests were carried out to ensure that the properties of the montmorillonite, silica, and kaolin did not affect the paint rheology, colour, gloss, opacity, stain and scrub resistance. The rheology tests showed that all the paints made were shear thinning. Data obtained from the scrub resistance suggested that the Silica-based paint offered an improved scrub resistance to

both the kaolin and the montmorillonite-based paints. Montmorillonite has been shown in previous studies to be very abrasive when used in polymer nanocomposites, hence paints loaded with this clay will be more prone to erosion when repeatedly scrubbed during the life of the paint. The stain resistance data of the paints were almost identical for the three minerals. The gloss, opacity and colour measurements of the paints were also very similar, and the use of the Kaolin, the Silica and the Montmorillonite in the paint formulation did not alter the optical property of the paints made.

There is a recommendation for future work that could expand upon the findings of this work for industrial application. In order to increase the release time of the biocide from the paint films, the biocide impregnated minerals may be encapsulated within a secondary carrier (a protective framework, like a sphere). This secondary carrier should be chosen so as it does not compromise the structural integrity of the paint (no interference with the paint mechanical and optical properties). This carrier could then be a rate-limiting step for the release of the biocide used.

A second aspect of the future work would be to undertake a surface treatment of the minerals used before their impregnation with the biocide and consequent addition to the paint films. This can take the shape of adding carboxyl (COOH) groups to the surface of the minerals. These groups are known to have a strong affinity to hydroxyl groups (OH) present on the biocides, and can help entrap the biocide onto the surface of the carriers. However, the strengths of these attachments and the conditions under which the biocide molecules will desorb from the minerals will need to be investigated.

A third and final aspect of the future work could involve ion exchange within the mineral framework. The minor elements (mainly cations like  $\text{Mg}^{2+}$ ,  $\text{Na}^+$ ,  $\text{K}^+$ , and  $\text{Fe}^{2+}$ ) found during the XRF analysis of the minerals, are thought to participate in the biocide impregnation process of the minerals via ion exchange processes<sup>[82]</sup>. An example is shown in Figure 9.1, where chlorine ions are replaced by a different compound.

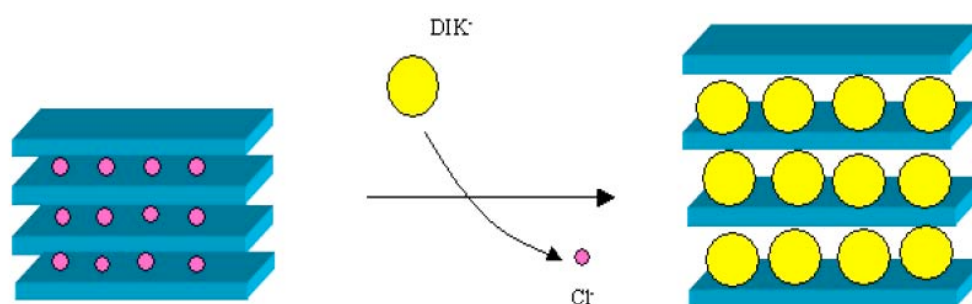


Figure 9.7: Proposed intercalation of compounds into a platy clay (done here via an anion exchange [82]).

In order for the ion exchange process to be successful, care needs to be taken regarding the choice of biocides used. These biocides need to have a strong affinity to the mineral in order to dislodge the cations present on its surface. This form of attachment of the biocide to the mineral needs not be permanent, as the biocide will still need to migrate out of the mineral's plates to be an effective antimicrobial agent.

# REFERENCES

1. Levis S.R., Deasy P.B. Use of coated microtubular halloysite for the sustained release of diltiazem hydrochloride and propranolol hydrochloride, *International Journal of Pharmaceutics* 253 (2003) 145–157
2. Kelly H.M., Deasy P.B., Ziaka E., Claffey N. Formulation and preliminary in vivo dog studies of a novel drug delivery system for the treatment of periodontitis, *International Journal of Pharmaceutics* 274 (2004) 167–183
3. Advanced Nanostructured Surfaces for Control of Biofouling, [www.ambio.bham.ac.uk](http://www.ambio.bham.ac.uk)
4. Qu, F., Zhu, G., Lin, H., Zhang, W., Sun, J., and Qiu, S., A controlled release of ibuprofen by systematically tailoring the morphology of mesoporous silica materials, *Journal of Solid State Chemistry* 179 (2006) 2027–2035
5. Uhrich, K.E., Cannizzaro, S.M., Langer, R.S., and Shakesheff, K.M., *Chem. Rev.* 99 (1999) 3181.
6. Qiu, X.P., Leporatti, S., Donath, E., H. Mohwald, and Langmuir 17 (2001) 5375.
7. Borquist, P., Korner, A., Piculell, L., Larsson, A., and Axelsson, A., A model for the drug release from a polymer matrix tablet – effects of swelling and dissolution, *Journal of Controlled Release* 113 (2006) 216–225
8. Langer, R., and Peppas, N.A., Chemical and physical structure of polymers as carriers for controlled release of bioactive agents: A review, *J. Macromol. Sci., Rev. Macromol. Chem.* C23 (1) (1983) 61–126.
9. Narasimhan, B., Mallapragada, S.K., and Peppas, N.A., in: E. Mathiowitz (Ed.), *Encyclopedia of Controlled Drug Delivery*, John Wiley and Sons, New York, 1999, pp. 921–935
10. Langer, R., Polymeric delivery systems for controlled drug release, *Chem. Eng. Commun.* 6 (1980) 1–48.
11. Higuchi, T., Mechanism of sustained-action medication—theoretical analysis of rate of release of solid drugs dispersed in solid matrices, *J. Pharm. Sci.* 52 (12) (1963) 1145–1149
12. Higuchi, T., Rate of release of medicaments from ointment bases containing drugs in suspension, *J. Pharm. Sci.* 50 (10) (1961) 874–875.
13. Gandhi, R., Kaul, C.L., Panchagnula, R., 1999. Extrusion and spheronization in the development of oral controlled-release dosage forms. *Pharm. Sci. Technol. Today* 2, 160–170.

14. Peppas, N.A., *Hydrogels in Medicine*, CRS Press, Boca Raton, FL, 1986.
15. Alhaique, F., Santucci, E., Carafa, M., Coviello, T., Murtas, E., Ricciari, F.M., and Gellan in sustained release formulations: preparation of gel capsules and release studies, *Biomaterials* 17 (1996) 1981–1986.
16. Risbud, M.V., and Bhonde, R.R., Polyacrylamide-chitosan hydrogels: in vitro biocompatibility and sustained antibiotic release studies, *Drug Deliv.* 7 (2000) 69-75.
17. Soppimath, K.S., Aminabhavi, T.M., Dave A.M., Kumbar S.G., and Rudzinski W.E. , Stimulus-responsive smart hydrogels as novel drug delivery systems, *Drug Dev. Ind. Pharm.* 28 (2002) 957–974.
18. Chen G., and Hoffman, A.S., Graft copolymers that exhibit temperature-induced phase transitions over a wide range of pH, *Nature* 373 (1995) 49–52.
19. Jeong, B., Bae, Y.H., Lee, D.S., and Kim, S.W., Biodegradable block copolymers injectable drug-delivery systems, *Nature* 388 (1997) 860–862.
20. Jeong, B., and Gutowska, A., Lessons from nature: stimuli-responsive polymers and their biomedical applications, *Trends Biotechnol.* 20 (2002) 305–311.
21. Durand, D., and Hourdet, Synthesis and thermoassociative properties in aqueous solution of graft copolymers containing poly(N-isopropylacrylamide) side chains, *Polymer* 40 (1999) 4941–4951
22. Lin, H.H., and Cheng, Y.L., In situ thermoreversible gelation of block and star copolymers of poly(ethylene glycol) and poly(N-isopropylacrylamide) of varying architectures, *Macromolecules* 34 (2001) 3710–3715.
23. Rassing, J., and Attwood, D., Ultrasound velocity and light scattering studies on the polyoxyethylene–polyoxypropylene copolymer Pluronic F127 in aqueous solution, *Int. J. Pharm.* 13 (1983) 47–55.
24. Fuchs, M., Turchiuli, C., Bohin, M., Cuvelier, M.E., Ordonnaud, C. Peyrat-Maillard, M.N., and Dumoulin, E. Encapsulation of oil in powder using spray drying and fluidised bed agglomeration, *Journal of Food Engineering* 75 (2006) 27-35
25. Langer, R., 1990. New methods of drug delivery. *Science*, 24, 1527-1533.
26. Park, K., Shalaby, W. S. W. and Park, H., 1993, *Biodegradable hydrogels for drug delivery*, Technomic Publishing company Inc., Lancaster, USA.
27. Nitsch, M. J. and Banakar, U. V., 1994. Implantable drug delivery. *J. Biomater. Appl.*, 8, 247-284.
28. Göpferich, A. and Langer, R. S., 1995. Predicting drug release from cylindrical polyanhydride matrix discs. *Eur. J. Pharmacol.*, 41, 81-87.

29. Baker, R. W. and Lonsdale, H. K., 1974. In Controlled release of biologically active agents (Eds, Tanquary, A. C. and Lacey, R. C.). Plenum Press, New York, pp. 15-71.
30. Baker, R., 1987. Controlled release of biologically active agents, Wiley Interscience Publications, New York.
31. Langer, R., 1980. Polymeric delivery systems for controlled drug release. *Chem. Eng. Commun.*, 6, 1-48.
32. Langer, R. S. and Peppas, N. A., 1981. Present and future applications of biomaterials in controlled drug delivery systems. *Biomaterials*, 2, 201-214.
33. Leong, K. W. and Langer, R., 1987. Polymeric controlled drug delivery. *Adv. Drug Del. Rev.*, 1, 199- 233.
34. Siepmann, J. and Göpferich, A., 2001. Mathematical modeling of bioerodible polymeric drug delivery systems. *Adv. Drug. Del. Rev.*, 48, 229-247.
35. Göpferich, A., 1997. In Handbook of biodegradable polymers (Eds, A., D., Kost, J. and Wiseman, D.) Harwood Academic Publishers, pp. 458-460.
36. Pitt, G., Gratzl, G. L., Kimmel, G. L., Surles, J. and Schindler, A., 1981. Aliphatic polyesters II: The degradation of poly(DL-lactide), poly( $\epsilon$ -caprolactone), and their copolymers in vivo. *Biomaterials*, 2, 215-220.
37. Tamada, J. A. and Langer, R., 1993. Erosion kinetics of hydrolytically degradable polymers. *Proc. Natl. Acad. Sci. USA*, 90, 552-556.
38. Grizzi, I., Garreau, H., Li, S. and Vert, M., 1995. Hydrolytic degradation of devices based on poly(DL- lactic acid) size-dependence. *Biomaterials*, 16, 305-311.
39. Heller, J. 1997. In Handbook of biodegradable polymers (Eds, Domb, A. J., Kost, J. and Wiseman, D. M.). Harwood academic publishers, Amsterdam, The Netherlands, pp. 99-118.
40. Ahola, M., Rich, J., Kortesus, P., Kiesvaara, J., Seppälä, J. and Yli-Urpo, A., 1999b. In vitro evaluation of biodegradable  $\epsilon$  -caprolactone-co-D,L-lactide/silica xerogel composites containing toremifene citrate. *Int. J. Pharm.*, 181, 191-191.
41. Rich, J., Kortesus, P., Ahola, M., Yli-Urpo, A., Kiesvaara, J. and Seppälä, J., 2000. Effect of the molecular weight of poly( $\epsilon$ -caprolactone-co-DL-lactide) on toremifene citrate release from copolymer/silica xerogel composites. *Int. J. Pharm.*, 212, 121-130.
42. Katzhendler, I., Hoffmann, A., Goldberger, A. and Friedman, M., 1997. Modeling of drug release from erodible matrices. *J. Pharm. Sci.*, 86, 110-115.
43. Akbari, H., D'Emanuele, A. and Attwood, D., 1998. Effect of geometry on the erosion characteristics of polyanhydride matrices. *Int. J. Pharm.*, 160, 83-89.



44. Hopfenberg, H. B., 1976. In Controlled release polymeric formulations (Eds, Paul, D. R. and Harris, F. N.). ACS Symposium Series 33, Washington, DC, pp. 33-52.
45. Karasulu, H. Y., Ertan, G. and Köse, T., 2000. Modeling of theophylline release from different geometrical erodible tablets. *Eur. J. Pharm. Biopharm.*, 49, 177-182.
46. Urtti, A., 1985. Deliverial and pharmacokinetic aspects of ocular pilocarpine administration. Doctoral Thesis, University of Kuopio, Finland.
47. Ritger, P. and Peppas, N., 1987a. A simple equation for description of solute release. II. Fickian and anomalous release from swellable devices. *J. Control. Release*, 5, 37-42.
48. Yebra, D.M., Kiil, S., and Dam-Johansen, K., Antifouling technology-past, present and future steps towards efficient and environmentally friendly antifouling coatings, *Progress in Organic Coatings* 50 (2004) 75-104
49. Callow, M.E., Callow, J.A., Marine biofouling: a sticky problem, *Biologist* 49 (1) (2002)
50. Wahl, M., Marine epibiosis. I. Fouling: some basic aspects, *Marine Ecology progress Series* 58 (1989) 175-189
51. Callow, M.E., Fletcher, R.L., Int. Biodeter. *Biodeg.* 34 (1994) 333-348
52. Abarzua, S., Jakubowsky, S., Mar. Ecol. Prog. Ser. 123 (1995) 301-312
53. Clare, A.S., Rittschof, D., Gerhart, D.J., Maki, J.S., Invertebrate Reproduction Dev. 22 (1-3) (1992) 67-76
54. Davies, A., NERC News (1995)
55. Bentley, M.G., Clare, A.S., Marine invertebrate chemical signals, *Biological Sciences Review* 13 (2001) 7-9
56. Karlsson, J., and Eklund, B., New biocide-free antifouling paints are toxic, *Marine Pollution Bulletin* 49 (2004) 456-464
57. Townsin, R.L., Development in the calculation of rough underwater surface power penalties. Celena 25<sup>th</sup> anniversary Symposium, Genoa (1987)
58. Liu, D., Maguire, R.J., Lau, Y.I., Pacepavicius, G.J., Okamura, H., Aoyama, I., Transformation of the new antifouling compound Irganol 1051 by phanerochaete chrysosporium, *Wat. Res.* 31 (1997) 2363-2369
59. Haak, P.W., Antifouling systems, current status and developments. In: *The Present Status of TBT-copolymer Antifouling paint. Proceedings of the International Symposium on Antifouling paints for Ocean-going Vessels*, The Hague, Feb. 21 (1996)

60. Reincke, H., Krinitz, J., Stachel, B., [www.arge-elbe.de](http://www.arge-elbe.de) (1999)
61. Edge, M., Allen, N.S., Turner, D., Robinson, J., and Seal, K., The enhanced performance of biocidal additives in paints and coatings, *Progress in Organic Coatings* 43 (2001) 10-17
62. Woods Hole Oceanographic Institution (WHOI), US Naval Institute, Annapolis, Iselin, COD, 1952
63. Callow, M., *Chem. Ind.* 5 (1990) 123-127
64. Lunn, I., Antifouling: A brief Introduction to the Origins and Development of the marine antifouling industry, BCA Publications, Thame, UK (1974)
65. Gitlitz, M.H., *Journal of Coating Technology* 53 (678) (1981) 46-52
66. Kiil, S., Weinell, C.E., Pedersen, M.S., Dam-Johansen, K., Arias-Codolar, S., *Journal of Coating Technology* 74 (932) (2002) 45-54
67. Gerigk, U., Scheider, U., Stewen, U., Prepr. Ext. Abstr. *ACS Natl. Meet.* 38 (1) (1998) 91-94
68. Champ, M.A., Published in the proceedings of 24<sup>th</sup> UJNR (US/Japan) Marine Facilities Panel Meeting in Hawaii, November 7-8 (2001)
69. Champ, M.A., *Sci. Total Envir.* 258 (2000) 21-71
70. Abbot, A., Abel, P.D., Arnold, D.W., Milne, A., *Sci. Total Envir.* 258 (2000) 5-19
71. De Mora, S.J., Tributyltin: Case study of an environmental contaminant. *Cambridge University Press, Cambridge* (1996)
72. Thomas, K.V., The environmental behaviour of antifouling paint booster biocides: a review, *Biofouling* 17 (2001) 73-86
73. Thomas, K.V., McHugh, M., Waldock, M., Antifouling paints booster biocides in UK coastal waters: inputs, occurrence and environmental fate, *Science of the Total Environment* 293 (1-3) (2002) 117-127
74. Andersson, S., Kaustsky, L., Copper effects on reproductive stages of Baltic Sea *Fucus vesiculosus*, *Marine Biology* 125 (1996) 171-176
75. Andersson, S., The influence of salinity and antifouling agents on Baltic Sea *Fucus vesiculosus* with emphasis on reproduction, PhD thesis in Marine Ecotoxicology, Stockholm University, Sweden (1996)
76. Christen, K., IMO will ban the use of a popular biocide, *Environ. Sci. Technol.* 33 (1999) A11
77. Gillatt, J., *Polym. Paint Colour J.*, 12 (1993) 183

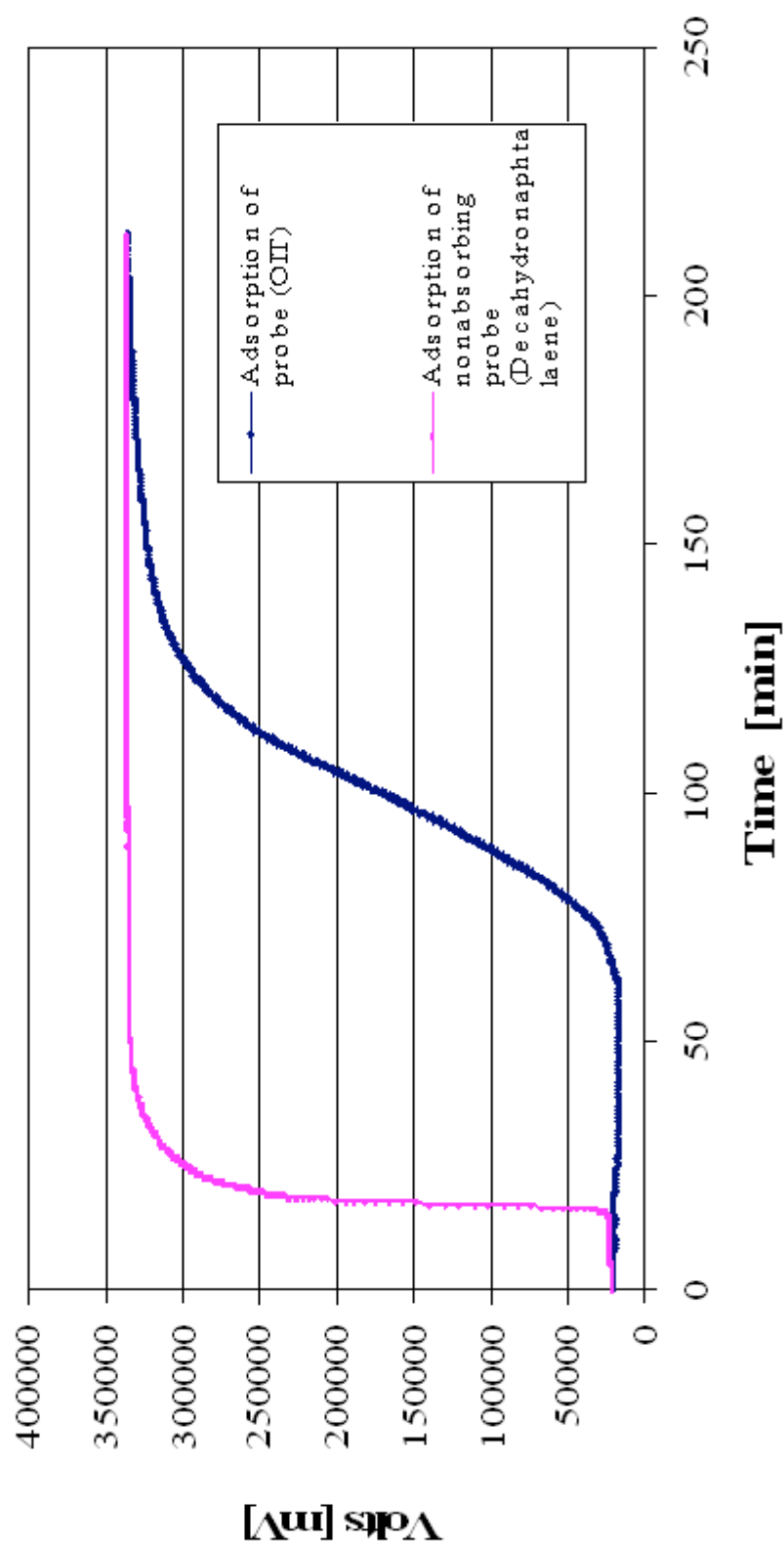
78. Seidel, U., Koch, M., Brunner, E., Staudte, B., and Pfeifer, H., NMR and IR studies on the adsorption of methane and trimethylgallium on zeolite HY, *Microporous and Mesoporous Materials* 35-36 (2000) 341-347
79. Celis, R., Hermosin, M.C., Carrizosa, M.J., Cornejo, J., Inorganic and organic clays as carriers for controlled release of the herbicide hexazinone, *J Agric. Food Chem.* 50 (8) (Apr10 2002) 2324-2330
80. Polubesova, T., Nir, S., Rabinivitz, O., Borisover, M., Rubin, B., Sulfentrazone adsorbed on micelle-montmorillonite complexes for slow release in soil, *J Agric. Food Chem.* 51 (11) (May21 2003) 3410-3414
81. Undabeytia, T., Mishael, Y.G., Nir, S., Papahadjopoulos-Sternberg, B., Rubin, B., Morillo, E., Maqueda, C., A novel system for reducing leaching from formulations of anionic herbicides: clay-liposomes, *Environ. Sci Technol.* 37 (19) (Oct 1 2003) 4475-4480
82. Ambroggi, V., Fardella, G., Grandolini, G., Perioli, L., Tiralti, M.C., Intercalation compounds of hydrotalcite-like anionic clays with ant-inflammatory agents, II: Uptake of Diclofenac for a controlled release formulation, *AAPS PharmSciTech* 3 (3), article 26 (2002)
83. R.K. Iler, *The Chemistry of Silica*, Wiley, New York, 1979.
84. L.T. Zhuravlev, *Pure Appl. Chem.* 61 (1989) 1969.
85. L.T. Zhuravlev, *Langmuir* 3 (1987) 316.
86. M. Edge a,\* , N.S. Allen a , D. Turner a , J. Robinson a , Ken Seal b., The enhanced performance of biocidal additives in paints and coatings, *Progress in Organic Coatings* 43 (2001) 10–17.
87. Seville JPK, Tüzün U and Clift R, *Processing of Particulate solids*, Powder Technology Series, Blakie Academic and Professional, London, 1997, Chapter 1, pages 1 to 52.
88. Malvern Instruments Ltd, innovative solutions in materials characterisation, Process solutions, Technology focus, laser diffraction technology focus, accessed 10<sup>th</sup> January 2006, [http://www.malvern.co.uk/ProcessEng/systems/laser\\_diffraction/technology/technology.htm](http://www.malvern.co.uk/ProcessEng/systems/laser_diffraction/technology/technology.htm)
89. Arner, E.,C., Pratta, M.A., Freimark, B., Lischwe, M., Trzaskos, J.M., Magolda, R.L., Wright, S.W., Isothiazolinones interfere with normal matrix metalloproteinase activation and inhibit cartilage proteoglycan degradation, *Biochem. J.* (1996) 319, 417-424
90. <http://www.chem.vt.edu/chem-ed/spec/beerslaw.html> (accessed 17th July 2007)

91. <http://www.cem.msu.edu/resch/VirtualText/Spectrpy/UV-Vis/spectrum.htm> (accessed 4th April 2007)
92. Grim, R.E., Clay Mineralogy Second Edition, Chapter 4, pages 51 to 125, McGraw-Hill Book Company, America, 1968
93. US Geology Survey – US Department of the Interior, maintained by Eastern Publications Group, last modified 10<sup>th</sup> October 2001, assessed 7<sup>th</sup> December 2005, <http://pubs.usgs.gov/of01-041/html/docs/clays>, modified from Grim, 1962
94. Price, R., Gaber, B.P., and Lvov, Y., In-vitro characteristics of tetracycline HCL, khelin and nicotinamide adenine dinucleotide from halloysite; a cylindrical mineral, *Microencapsulation*, 2002, vol 18 (6) 713-722
95. Bates, T.F., Hildebrand, F.A., and Swinford, A., Morphology and structure of endellite and halloysite, *American Mineralogist*, 1950 (35) 463-484
96. Giles, C.H., Smith, D., A general Treatment and Classification of the Solute Adsorption Isotherm, I. Theoretical, *Journal of Colloid and Interface Science*, Vol. 47, No. 3, June 1974
97. Giles, C.H., D'silva, A.P., Easton, I.A., A general Treatment and Classification of the Solute Adsorption Isotherm, Part II. Experimental Interpretation, *Journal of Colloid and Interface Science*, Vol. 47, No. 3, June 1974
98. [http://microvet.arizona.edu/courses/Mic205/exams/05exams/06-14\\_BacteriaGrowth\\_1.jpg](http://microvet.arizona.edu/courses/Mic205/exams/05exams/06-14_BacteriaGrowth_1.jpg), accessed 7<sup>th</sup> March 2008
99. Apple Developer connection, Device-Independent Color Spaces, accessed 10<sup>th</sup> May 2006, [http://developer.apple.com/documentation/GraphicsImaging/Conceptual/csintro/csintro\\_colorspace/chapter\\_3\\_section\\_5.html](http://developer.apple.com/documentation/GraphicsImaging/Conceptual/csintro/csintro_colorspace/chapter_3_section_5.html).
100. Technidyne corporation, technical information, optical properties, L\*a\*b\* poster, accessed 11<sup>th</sup> May 2006 <http://www.technidyne.com/frameset.htm?Physical.HTM>
101. [www.coleparmer.ca/techinfo/techinfo.asp?htmlf](http://www.coleparmer.ca/techinfo/techinfo.asp?htmlf), accessed 15<sup>th</sup> June 2010
102. Donga, Y., Feng, S.S., Poly(D,L-lactide-co-glycolide)/montmorillonite nanoparticles for oral delivery of an anticancer drug, *Biomaterials* 26 (2005) 6068-6076

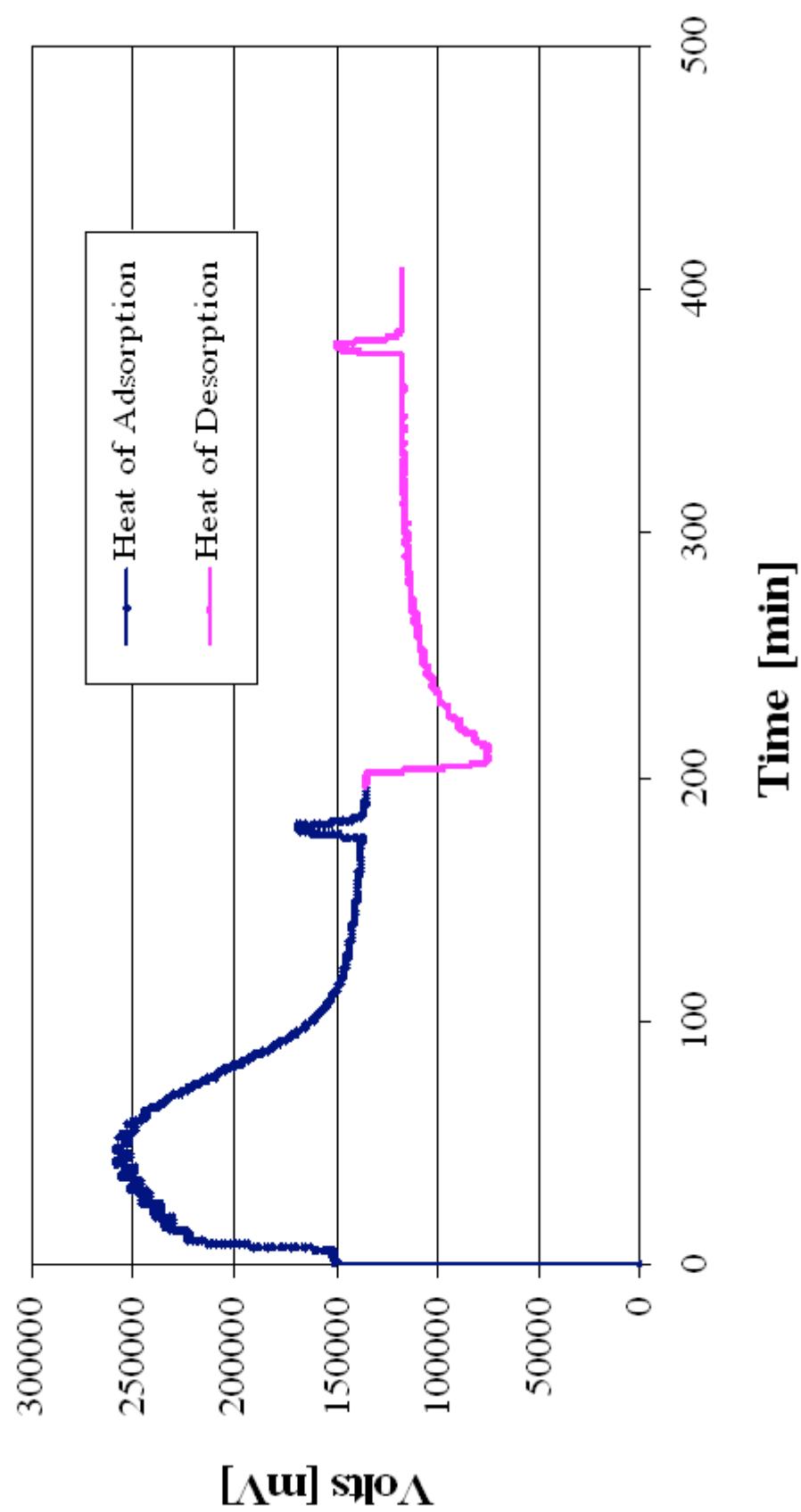
# **APPENDICES**

## APPENDIX 1

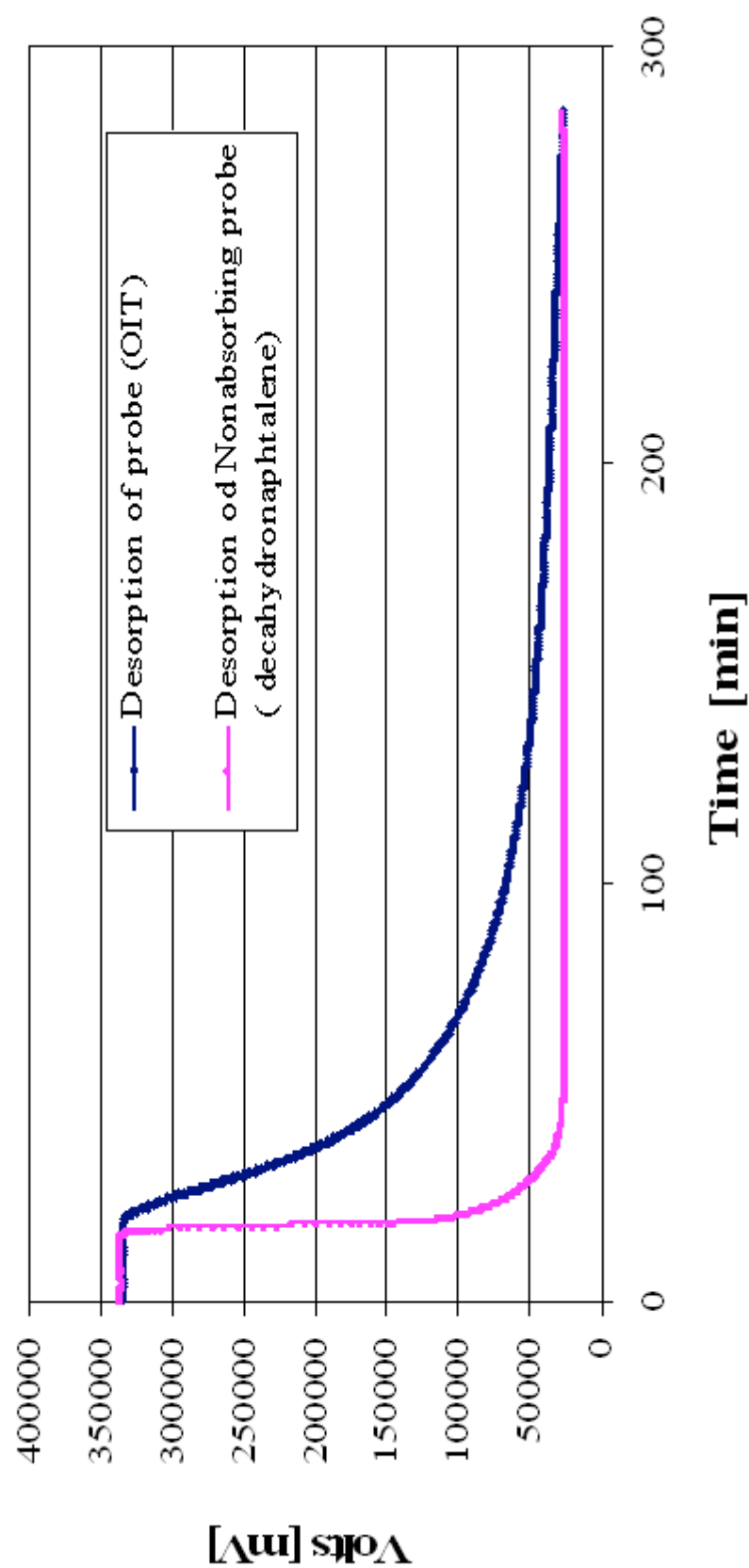
1.A: Calculation of amount of OIT adsorbed onto each of the minerals from FMC experiments



1.B: Measurement of the heat of adsorption and desorption of OIT within the FMC cell



1.C: Calculation of amount of OIT desorbed onto each of the minerals from FMC experiments





1 D: Data obtained from FMC experiment for the first 5 minerals

Sample	MCBP			NPD-16A		Supreme		T-38		Cetix	
Probe	n=1	OIT	Average	n=1	OIT	n=1	Average	n=1	OIT	n=1	Average
Date	240708	280708		210708		290708	210708	210708		220708	
Probe Mineral	0.1277	0.0936		0.072		0.0920	0.0371	0.0371		0.0416	
Calorimeter Adsorption Area	4.54E+08	3.47E+08		2.88E+07		3.23E+07	6.02E+07	6.02E+07		3.11E+07	
Calibration Area	9.89E+06	9.87E+06		9.79E+06		8.29E+06	9.79E+06	9.79E+06		9.63E+06	
Calibration Area	1.01E+07	9.38E+06		9.61E+06		8.29E+06	9.62E+06	9.62E+06		9.67E+06	
Energy	4.09	3.24		0.27		0.35	0.56	0.56		0.29	
	32.03	34.7	33.4	3.71	3.7	3.81	15.04	15.0	6.98	7.0	
Description Area	2.16E+08	1.63E+08		1.48E+07		1.41E+07	2.14E+07	2.14E+07		2.64E+06	
Calibration Area	9.89E+06	9.60E+06		9.79E+06		9.72E+06	9.79E+06	9.79E+06		9.63E+06	
Calibration Area	9.83E+06	9.38E+06		8.86E+06		8.29E+06	8.86E+06	8.86E+06		9.30E+06	
Energy	1.97	1.55		0.14		0.14	0.21	0.21		0.03	
	15.44	16.52	16.0	1.98	2.0	1.5	5.55	5.6	0.60	0.6	
OIT	6.70E+06	6.81E+06		7.34E+06		6.76E+06	7.34E+06	7.34E+06		6.75E+06	
Weight of	0.076	0.0800		0.0874		0.0606	0.0874	0.0874		0.0801	
Area/Weight	8.82E+07	8.51E+07	8.67E+07	8.40E+07	8.40E+07	1.12E+08	8.40E+07	8.40E+07		8.43E+07	8.43E+07
Adsorption Area	1.49E+09	1.04E+09		4.71E+07		1.94E+08	2.10E+08	2.10E+08		9.46E+07	
Weight	1.35E-02	9.78E-03		4.49E-04		1.39E-03	2.00E-03	2.00E-03		8.98E-04	
	105.8	104.5	105.13	6.2	6.24	15.1	53.9	53.94	21.6	21.59	
Description Area	4.77E+08	3.74E+08		4.13E+07		5.55E+07	4.31E+07	4.31E+07		1.57E+07	
Weight	4.33E-03	3.52E-03		3.94E-04		3.98E-04	4.10E-04	4.10E-04		1.49E-04	
	33.87	37.56	35.72	5.47	5.47	4.32	11.06	11.06	3.59	3.59	
Molar heat Mw	213.34	213.34	213.34	213.34	213.34	213.34	213.34	213.34		213.34	
Adsorption	64.6	70.8	67.7	127.0		53.7	59.5	59.5		69.0	
Description	97.2	93.8	95.4	77.2		75.4	107.1	107.1		36.0	
Adsorption	0.13	0.04	0.13	0.27		0.88	0.44	0.44		0.89	
Description	1.19	1.19	1.19	0.24		0.25	0.09	0.09		0.15	

1 E: FMC data of the remaining minerals

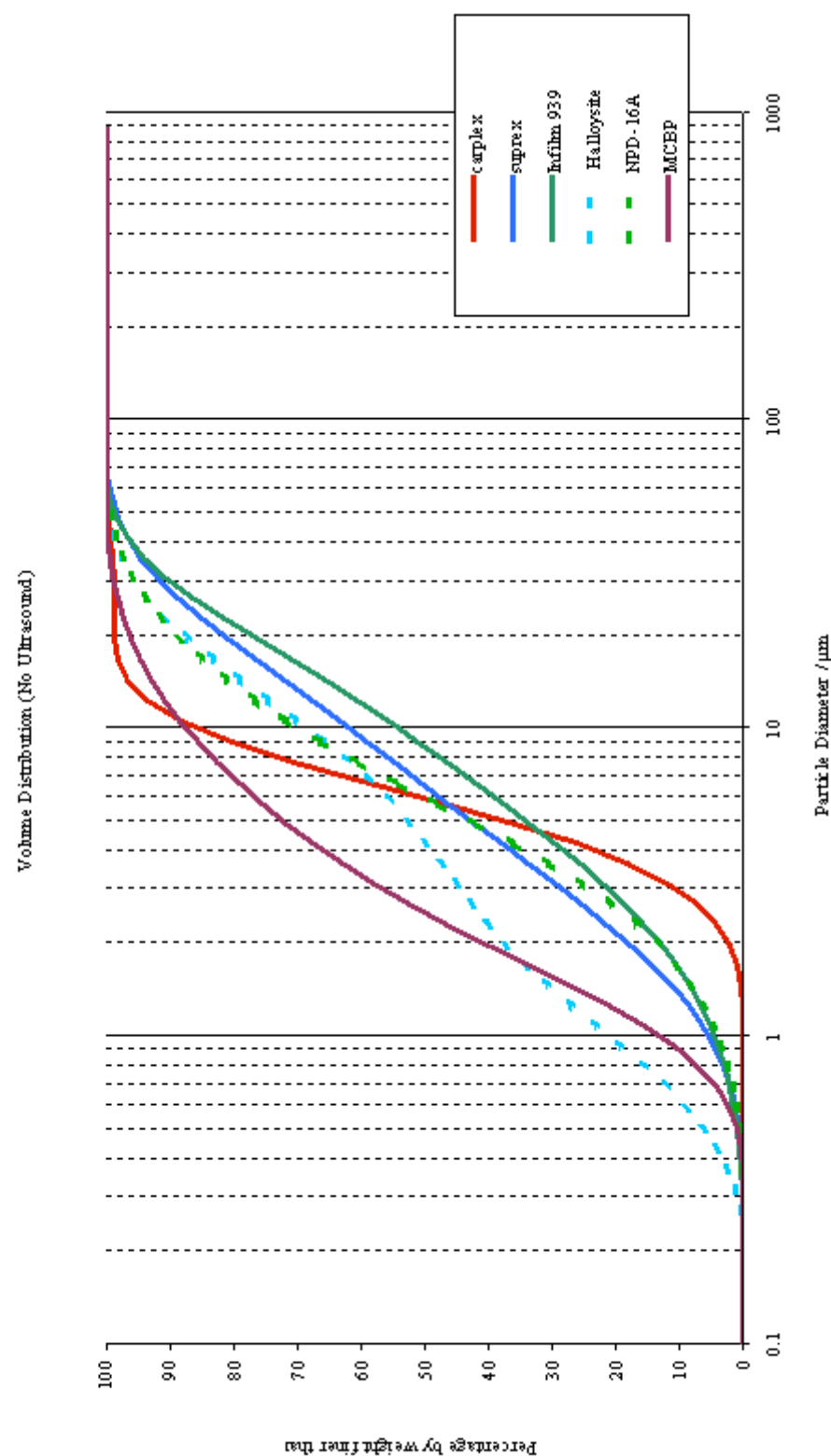
Sample		Infilm939			Suprex		Caplex CS-5			New Zealand	
Probe		OIT			OIT		OIT		Average	OIT	
		n=1	n=2	Average	n=1	Average	n=1	n=2		n=1	Average
Date		150708	180708	170708	170708		290708	300708		230708	
Probe Mineral	[g]	0.1267	0.1437	0.1212	0.1111		0.0203	0.0206		0.102	
Calorimeter											
Adsorption Area	[μv•s]	7.10E+07	6.91E+07	5.90E+07	5.44E+07		3.72E+07	4.35E+07		5.88E+07	
Calibration Area	[μv•s]	1.03E+07	9.48E+06	1.03E+07	1.04E+07		8.45E+06	9.55E+06		9.62E+06	
Calibration Area		1.03E+07	9.85E+06	1.04E+07	9.78E+05		8.29E+06	9.54E+06		9.47E+06	
Energy	[J]	0.62	0.64	0.51	0.86		0.40	0.41		0.55	
	[J/g]	4.90	4.48	4.22	7.74	7.7	19.73	19.9	19.8	5.44	5.4
Desorption Area	[μv•s]	3.36E+07	3.81E+07	2.99E+07	2.41E+07		1.01E+07	1.42E+07		2.53E+07	
Calibration Area	[μv•s]	8.53E+06	9.48E+06	1.07E+07	1.04E+07		8.63E+06	9.58E+06		9.62E+06	
Calibration Area		8.74E+06	9.86E+06	1.04E+07	9.90E+06		8.29E+06	9.54E+06		9.55E+06	
Energy	[J]	0.35	0.35	0.25	0.21		0.11	0.13		0.24	
	[J/g]	2.76	2.46	2.10	1.92	1.9	5.29	6.51	5.9	2.33	2.3
Refractome											
OIT		7.67E+06	7.16E+06	6.58E+06	6.58E+06		6.76E+06	6.28E+06		6.77E+06	
CalibArea		0.0764	0.0894	0.084	0.084		0.081	0.0840		0.076	
Weight of f	[g]										
Area/Weight	[μv•s/g]	1.00E+08	8.01E+07	7.84E+07	7.84E+07	7.84E+07	8.35E+07	7.47E+07	7.91E+07	8.90E+07	8.90E+07
Adsorption Area	[μv•s]	2.80E+08	2.28E+08	2.17E+08	1.61E+08		1.88E+08	1.67E+08		2.20E+08	
Weight	[g]	2.23E-03	2.28E-03	2.21E-03	1.64E-03		1.80E-03	1.79E-03		1.98E-03	
	[mg/g]	17.6	15.8	18.3	14.8	14.79	88.7	86.8	87.78	19.4	19.38
Desorption Area	[μv•s]	1.02E+08	9.52E+07	7.53E+07	7.66E+07		5.30E+07	4.21E+07		5.79E+07	
Weight	[g]	8.13E-04	9.51E-04	7.68E-04	7.82E-04		5.08E-04	4.50E-04		5.20E-04	
	[mg/g]	6.42	6.62	6.34	7.04	7.04	25.01	21.86	23.44	5.10	5.10
Molar heat Mw											
	[g/mol]			213.34		213.34	213.34	213.34	213.34		213.34
Adsorption	[kJ/mol]	59.4	60.3	49.3		111.7	47.4	49.0	48.2		59.8
Desorption	[kJ/mol]	91.8	79.5	70.8		58.3	45.1	63.5	53.7		97.4
Adsorption	[mg/m2]			0.78		0.59			0.59		0.39
Desorption	[mg/m2]			0.29		0.28			0.16		0.10

### APPENDIX 3

#### 3.A Complete Particle Size Distribution (PSD) of platy, tubular and amorphous minerals

	carplex	suprex	Infilm 939	Halloysite	NPD-16A	MCBP
<b>10</b>	2.91	1.36	1.64	0.62	1.66	0.90
<b>20</b>	3.74	2.16	2.83	0.95	2.60	1.22
<b>30</b>	4.46	3.15	4.27	1.42	3.56	1.56
<b>50</b>	5.93	6.51	8.71	4.34	5.94	2.50
<b>70</b>	7.69	13.30	16.22	10.46	10.00	4.60
<b>80</b>	8.95	18.81	21.64	14.87	13.80	6.93
<b>90</b>	11.10	28.04	29.89	22.14	21.41	11.67
<b>98</b>	16.21	47.51	46.11	39.08	40.07	25.15
	7.722	4.192	19.306	1.060	6.628	1.953
	1.763	1.085	0.282	4.721	0.990	4.151
<b>st1</b>	0.411	0.794	0.769	0.880	0.683	0.702
<b>d70/d30</b>	<b>1.724</b>	<b>4.229</b>	<b>3.800</b>	<b>7.391</b>	<b>2.806</b>	<b>2.958</b>
<b>-1um</b>	0.1	6.0	4.9	22.8	4.2	14.6
<b>-2um</b>	3.4	21.1	15.2	39.9	16.0	46.5

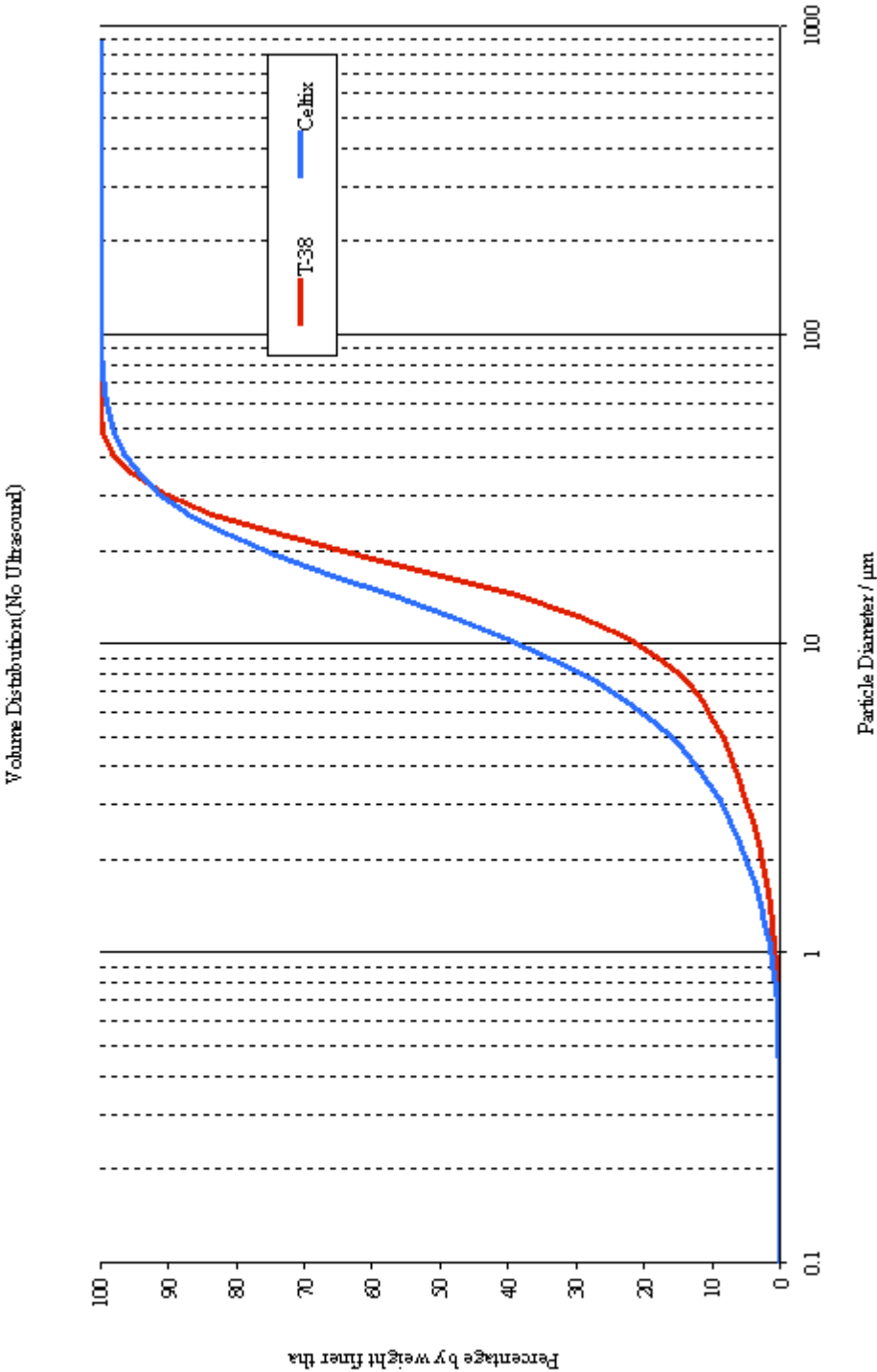
### 3.B: Volume distribution of the platy, tubular and amorphous minerals



### 3.C: Complete PSD of irregular shape minerals

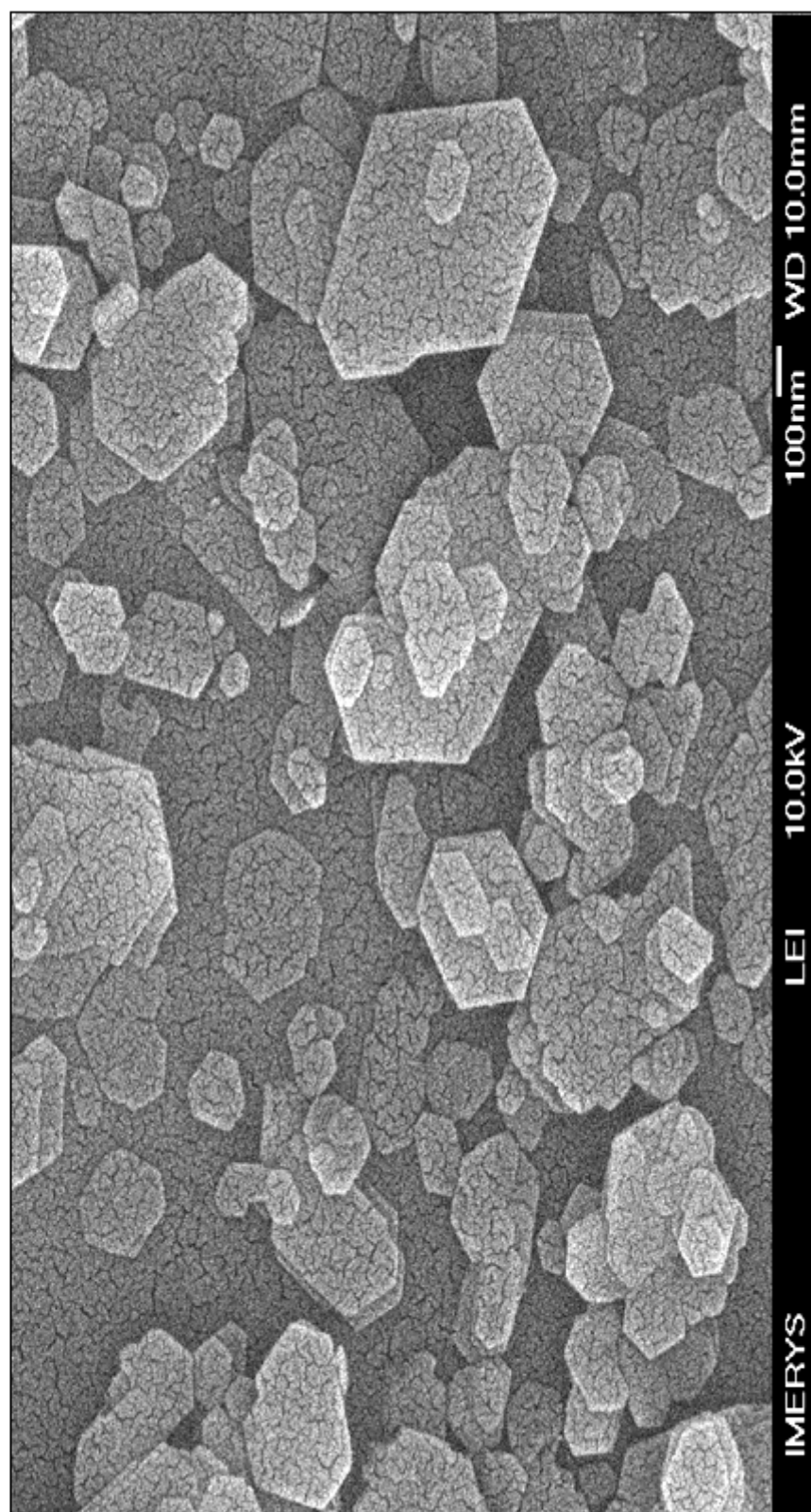
	<b>T-38</b>	<b>Celtix</b>
<b>10</b>	5.82	3.40
<b>20</b>	9.67	5.93
<b>30</b>	12.31	8.16
<b>50</b>	16.65	12.56
<b>70</b>	21.46	17.95
<b>80</b>	24.89	21.93
<b>90</b>	30.19	29.19
<b>98</b>	41.07	49.80
	19.306	16.571
	0.664	0.551
<b>st1</b>	0.440	0.574
<b>d70/d30</b>	<b>1.744</b>	<b>2.199</b>
<b>-1um</b>	0.7	1.5
<b>-2um</b>	3.0	5.8

3.D: Volume distribution of the irregular shape minerals



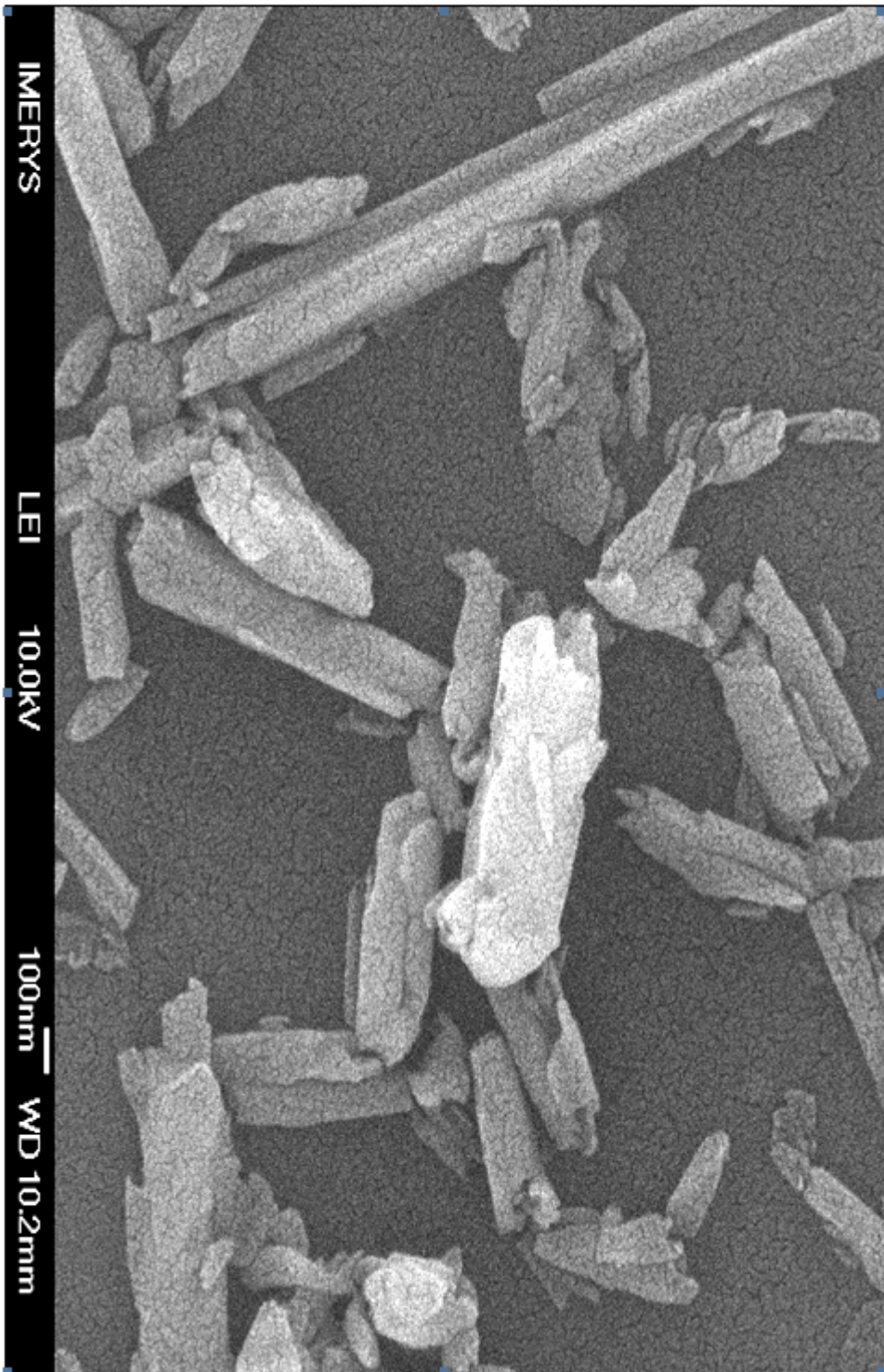
#### APPENDIX 4

4.A: Scanning Electron Microscopy (SEM) of Infilm 939 to 200 nm magnification, clearly showing the plates



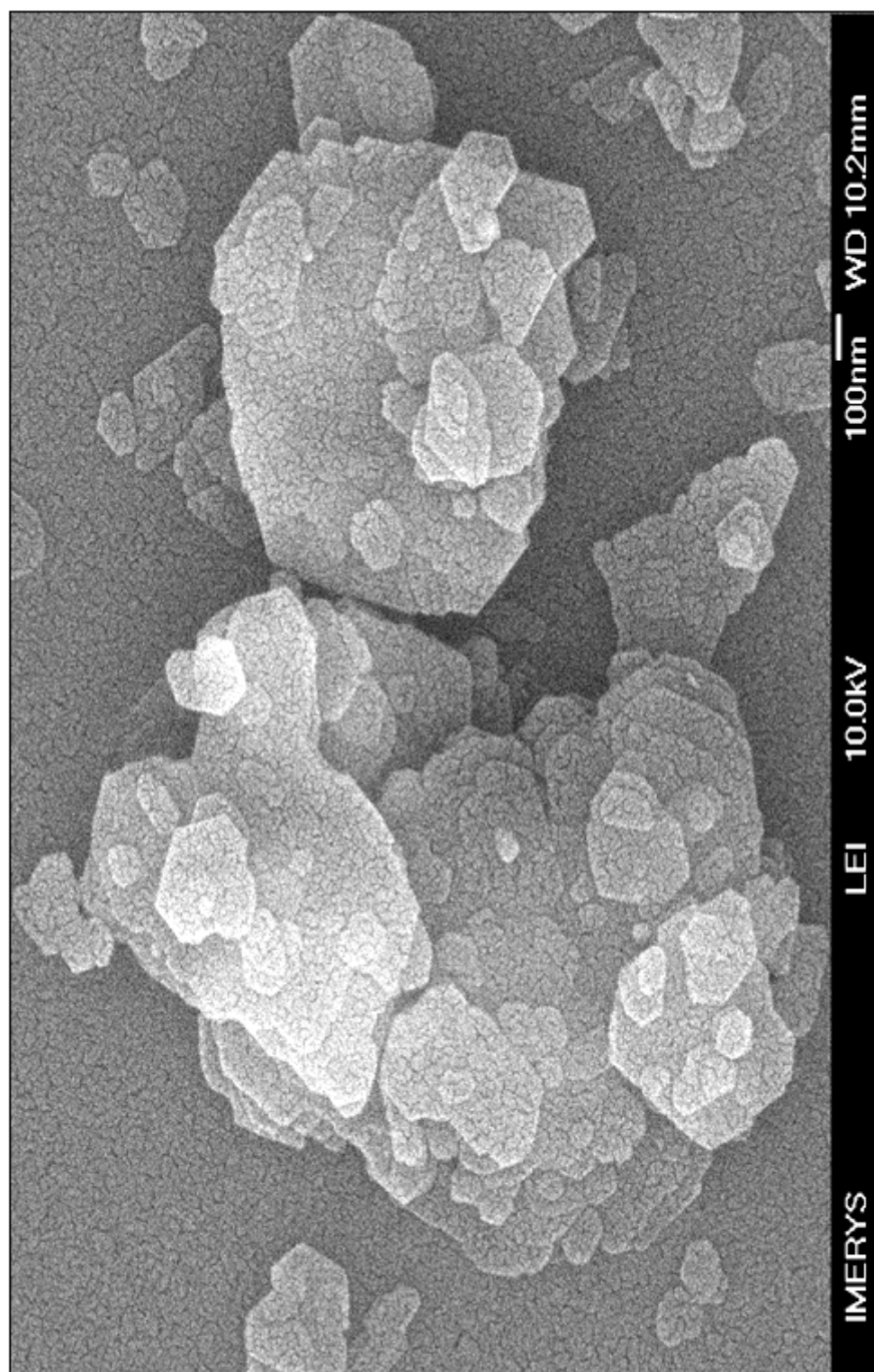


4.B: SEM of New Zealand Halloysite to 200 nm magnification, showing the tubes





4.C: SEM of the dispersant-free Suprex also to 200 nm magnification, clearly showing the plates



## APPENDIX 5

### 5.A: Paints stain resistance data (for both stained and unstained paint films)

Parameters:

Target Status: CRBELL

Color Mode L\*a\*b\*

Observer 10°

Primary Illuminant D65

Sample#	Name	Status	Ry
TARGET	<b>Supreme stained</b>		
		SCE/100	86.19 100
1	<b>Supreme unstained</b>		
		SCE/100	86.19
2	<b>Carplex stained</b>		
		SCE/100	85.89 99.3292
3	<b>Carplex unstained</b>		
		SCE/100	86.47
4	<b>MCBP stained</b>		
		SCE/100	85.89 99.6288
5	<b>MCBP unstained</b>		
		SCE/100	86.21

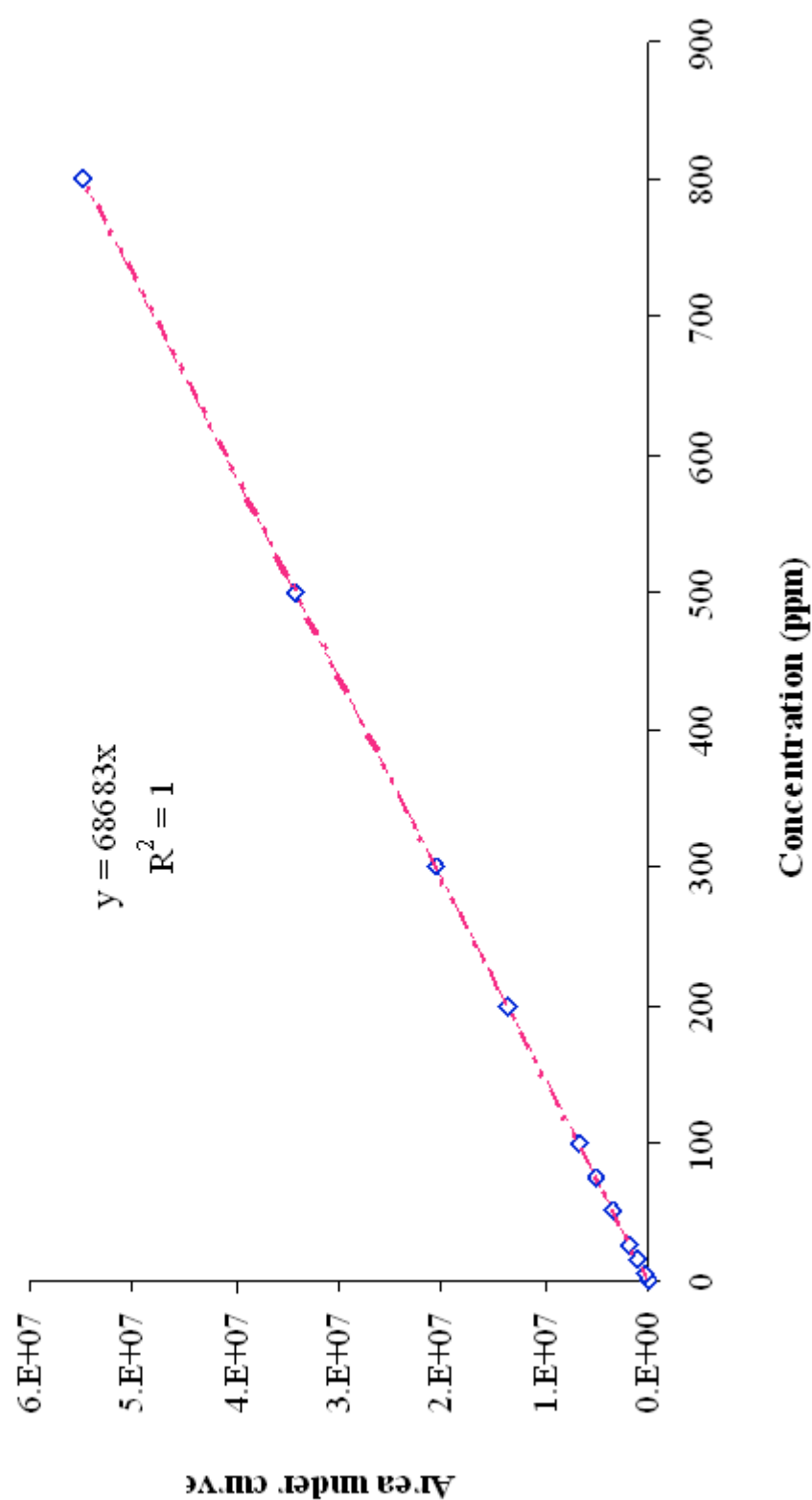
**5.B:** Paint opacity measurement data (5 measurements per minerals)

Parameters:  
 Target Status: CRBELL  
 Color Mode L\*a\*b\*  
 Observer 10°  
 Primary Illuminant D65

Sample#	Name	Status	Ry	
TARGET	sup/1			<b>Supreme</b>
1	/2	SCE/100	82.13	
2	/3	SCE/100	82.05	
3	/4	SCE/100	82.3	
4	/5	SCE/100	82.79	
6	car/1	SCE/100	82.76	<b>Carplex</b>
7	/2	SCE/100	81.19	
8	c/3	SCE/100	82.35	
9	c/4	SCE/100	82.14	
10	c/5	SCE/100	82	
14	m/1	SCE/100	76.11	<b>MCBP</b>
15	m/2	SCE/100	83.33	
16	m/3	SCE/100	83.73	
17	m/4	SCE/100	83.34	
18	m/5	SCE/100	83.68	
		SCE/100	83.4	

# APPENDIX 6

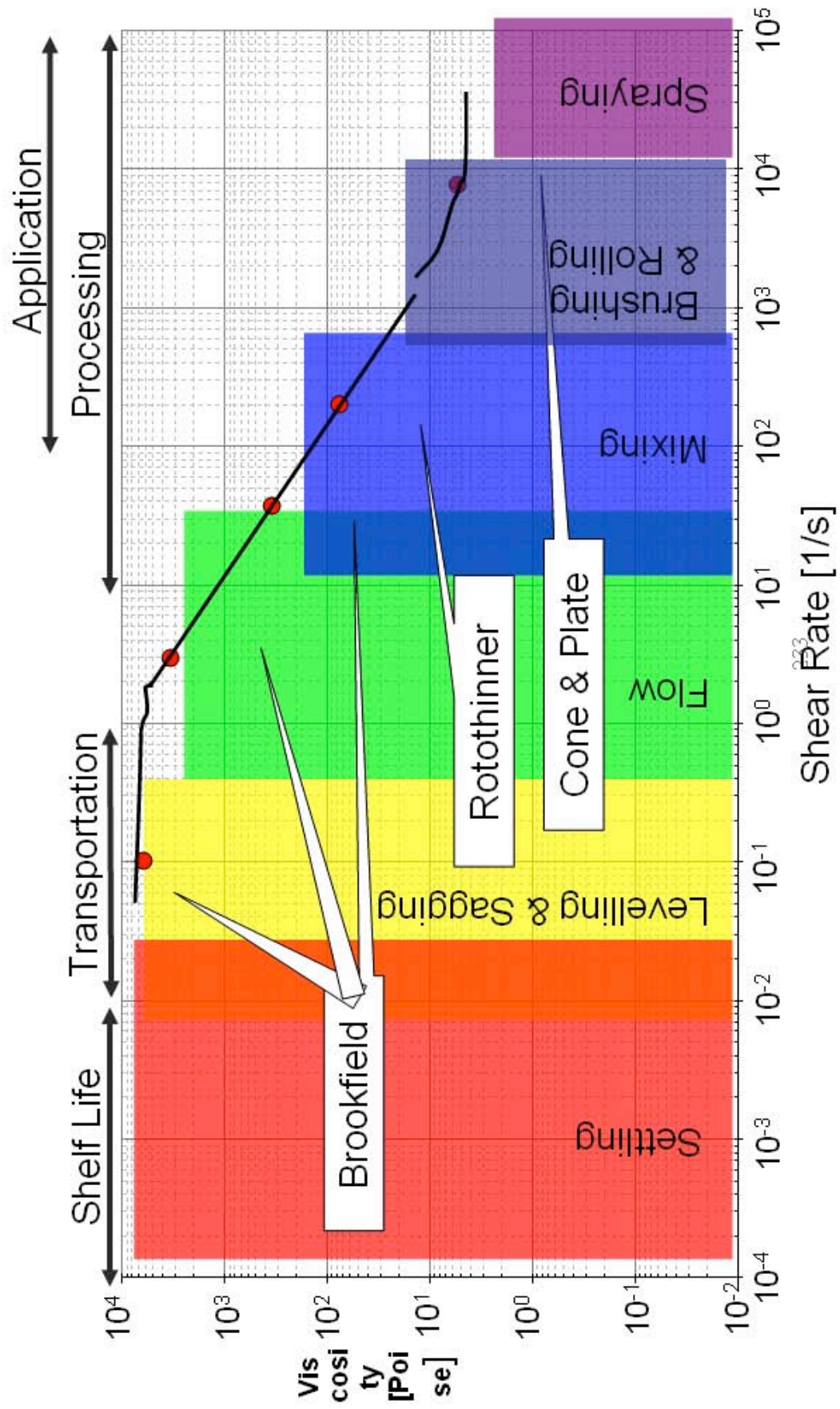
CIT/MIT calibration used to determine the concentrations of the unknown solutions



# APPENDIX 7

Data obtained from the OIT desorption from the paint films experiment

Time (d)	MCBP			Carplex			Supreme			T-38			Celtix		
	Adsorb	Added	Added	Adsorb	Added	Added	Adsorb	Added	Added	Adsorb	Added	Added	Adsorb	Added	Added
0	100	100	100	100	100	100	100	100	100	100	100	100	100	100	100
0.0004	95.4	97.9	97.9	98.4	98.4	98.4	99.1	98.9	98.9	94.7	90.2	90.2	96.1	93.1	93.1
0.003	93.8	97.1	97.1	97.9	97.5	97.5	98.5	98.7	98.7	86.4	81.1	81.1	83.5	82.7	82.7
0.007	90.5	91.2	91.2	97.1	95.8	95.8	97.6	97.9	97.9	66.8	69.1	69.1	74.9	71.5	71.5
0.021	85.2	82.1	82.1	87.5	87	87	89.4	86.2	86.2	49.9	45.6	45.6	60	47.9	47.9
0.042	76.8	68.5	68.5	71	65.8	65.8	71.2	58.7	58.7	20.7	23.2	23.2	40.5	31.0	31.0
0.083	70.6	42.2	42.2	48	40	40	44.7	38.1	38.1	2.5	11.2	11.2	23.4	0	0
0.167	60.7	26.8	26.8	31.7	23	23	30.4	19.7	19.7	0	3.6	3.6	12.9	0	0
0.25	59.8	20.1	20.1	25.2	12.5	12.5	26.5	13.6	13.6	0	0	0	10.3	0	0
1	58.3	17.4	17.4	24.4	13.4	13.4	24.1	11.4	11.4	0	0	0	9.9	0	0
2	49	13	13	25.3	12.2	12.2	22.4	9.8	9.8	0	0	0	5.6	0	0
3	47.6	9.42	9.42	22.5	8.64	8.64	18.27	4.5	4.5	0	0	0	4.4	0	0
5	47.1	3.7	3.7	16.81	4.12	4.12	13.63	0	0	0	0	0	4.2	0	0
6	46.23	0	0	11.69	0	0	13.52	0	0	0	0	0	3	0	0
7	42.3	0	0	10.49	0	0	13.19	0	0	0	0	0	2.3	0	0



# **Conferences Attended and Papers Published**

- PARTEC conference in March 2007, Nuremberg, Germany (oral presentation, and a paper published as part of the conference proceedings)
- Mining Engineering conference in 2007 at Imperial College (Abstract)
- Particle Technology conference in Orlando, USA, in May 2008 (oral presentation, and an extended abstract produced as part of the conference proceedings)
- Yearly Engineering Doctorate conferences at Birmingham University (April 2006-2008, oral presentations)